# SYSTEMATIC ANALYSIS OF RNAI COMPONENTS IN MOUSE SPERMATOGENESIS

A Dissertation
Presented to the Faculty of the Graduate School
of Cornell University
In Partial Fulfillment of the Requirements for the Degree of
Doctor of Philosophy

**by**

**Andrew Modzelewski**

**January 2014**

SYSTEMATIC ANALYSIS OF RNAI COMPONENTS IN MOUSE SPERMATOGENESIS

Andrew Modzelewski

Cornell University 2014

The four mammalian Argonautes (AGO1-4) are highly conserved small RNA binding proteins, only one of which, AGO2, is capable of cleaving RNA for canonical RNA interference (RNAi). The remaining AGOs are thought to be involved in miRNA silencing however their precise functions have not been demonstrated in mammals. While the Argonautes share over 80% identity at the amino acid level, any small differences in sequence or structure likely confer distinct biological functions in specific cellular contexts.

Most eukaryotes utilize the RNA Induced Silencing Complex (RISC) to silence genes by AGO-associated RNA processing. Another RNAi mechanism, the RNA Induced Transcriptional Silencing (RITS) complex, induces and maintains heterochromatinization in *S. pombe* and *D. melanogaster*, but has yet to be demonstrated in mammals.

*Ago4* is expressed most highly during pachynema of prophase I in male germ cells. AGO4 localizes to spermatocyte nuclei during meiotic prophase I, specifically at sites of asynapsis and the transcriptionally silenced XY domain, the sex body (SB), suggesting a role for AGO4 in silencing at regions of unsynapsed DNA. To elucidate the role of *Ago4 in mouse spermatogenesis*, we generated an *Ago4*$^{-/-}$ mouse line and discovered its involvement in at least two major stages of

meiotic progression, initiation of meiosis in spermatogonia and silencing in spermatocytes.

*Ago4*$^{-/-}$ animals are subfertile, with males showing significantly reduced testes size and epididymal sperm numbers. Spermatogonia initiate meiosis early, resulting from premature induction of retinoic acid-response genes. At the cellular level, prophase I spermatocytes from Ago4$^{-/-}$ males exhibit errors in proper sex body assembly, accompanied by misloading of RNA polymerase II within this domain. Quantitative Reverse Transcription PCR (qRT-PCR) revealed the increase of *Ago3* expression specifically in the *Ago4*$^{-/-}$ testis, suggesting some level of functional redundancy among the Argonaute subfamily. Expression of *Ago1* and *Ago2* remain unchanged in the absence of *Ago4.*

mRNAseq demonstrated altered silencing patterns during pachynema, leading to disrupted meiotic sex chromosome inactivation (MSCI) while small RNA cloning from isolated pachytene cells reveals significantly diminished populations of miRNAs in *Ago4*$^{-/-}$ males compared to wildtype. Greater than 20% of these losses originate from the X-chromosome and potentially misregulate various meiotic processes. The localization of specific differentially expressed miRNAs was investigated through hybridization of Locked Nucleic Acid (LNA) probes for miRNA-FISH on spermatocytes. These miRNAs display distinct localization patterns throughout the pachytene nuclei, particularly the SB, and are depleted in altered pachytene cells. Given the identical localization of AGO4, this finding provides some insight into the mechanism behind meiotic silencing initiation and/or maintenance. Taken together, I hypothesize that specific non-

slicing AGO proteins may function in RITS-like pathway in mammalian spermatogenesis.

Recent reports describe the global suppression of miRNA function in mouse oocytes, which rely solely on endogenous small interfering RNAs (endo-siRNAs) for proper development. Whether both miRNA and endo-siRNA are required for spermatogenesis, and what their potential roles are is unclear. To ascertain whether each small RNA population is dispensable for male meiosis, as well as what their overall roles may be, we have generated two mutant mouse lines that allow for the genetic dissection of miRNA and siRNA function in the proper regulation of germline maintenance and development. DGCR8 is part of the microprocessor that initially processes primary miRNA (pri-miRNA) transcripts in the nucleus into the characteristic ~70nt hairpins. Therefore, the *Dgcr8* deficient testis will be depleted of all canonical miRNAs. DICER recognizes these hairpins and processes them in the cytoplasm into the mature miRNAs that are then loaded into an Argonaute protein and used for small RNA mediated regulation. DICER can recognize various forms of double stranded RNA (dsRNA), and is therefore able to also generate endo-siRNAs that guide canonical RNAi. Thus, the *Dicer* deficient testis will lack all miRNA and endo-siRNAs. Both testes specific conditional knockout (cKO) animals are infertile and display very similar phenotypical abnormalities. However, upon close examination it is revealed that subtle differences in the observed defects clearly distinguish the *Dicer* and *Dgcr8* defects.

The *Dicer* cKO phenotype is more severe than the *Dgcr8* defect. *Dicer* depletion has a more drastic decrease in testes weight and produces no mature spermatozoa, while in the *Dgcr8* deficient animal, low levels of mature spermatozoa are recovered. Chromosome spread preparation show severe XY chromosome structural abnormalities from both animals. However the frequency and abundance of these distinct structural defects are distinct in the *Dicer* and *Dgcr8* cKO testes, implying that the associated small RNAs participate in largely non-overlapping regulatory events. Therefore, I hypothesize that not only are both miRNAs and endo-siRNAs functional in spermatogenesis, but that they have unique regulatory responsibilities to maintain proper meiotic progression.

Taken together, these studies have provide vast insight into small RNA biology in the mammalian germline and promise to reveal a more comprehensive understanding of processes that govern meiotic progression. These results point to exciting roles for AGO4, miRNAs and endo-siRNAs in the nucleus of mammalian germ cells. Here, I have provided the first evidence for small RNA regulated meiotic entry, a functional consequence to endo-siRNA loss and a functional role for AGOs in meiotic cells in the initiation or maintenance of silencing at asynapsed chromosomes in the germline, perhaps via a RITS-like complex, or novel RNAi mechanism.

## BIOGRAPHICAL SKETCH

Andrew Modzelewski was born in Perth Amboy, New Jersey and lived in the town of Carteret until the age of 18. He is the third and final son of polish immigrants Helen and Waldemar Modzelewski to which he owes his motivation and dedication. His parents put education above all other pursuits and thus sent him to private Catholic Elementary and High Schools. Science and lab classes immediately captured his interest at an early age and it was clear that he had a life of scientific research ahead of him.

High school years came and went and while he was involved in wrestling, football and other activities, these years mainly nurtured Andrew's passion for learning. Knowing that attending college would be the only reasonable method of continuing his education, the pressures of the looming financial burden were obvious. To this end, together with the irresponsible lenders of the early 2000's, his cautiously optimistic mother co-signed his first house with him, just a few weeks after his 18th birthday. This three story, six bedroom, *one bathroom* house served as both income and home to Andrew for most of his time at the Pennsylvania State University. While there, he shared a roof with nearly twenty fellow undergraduates and remains in close communication with just a few, who still affectionately refer to him as "Slumlord Drew". Perhaps the greatest impact on Andrew's outlook on life and science was Dr. Ivan "Ike" Shibley, who somehow had the patience to deal with him for two Organic Chemistry and four Philosophy courses. If not for Ike, Andrew would be a very different person, whatever that means.

While still enrolled at Penn State, managing the house, working at the nearby home improvement store, and running molecular dynamics simulations of copper-magnesium alloys phase transitions in the lab of Lorena Tribe, he met his partner in life's adventure, Crystal Conn in the class of Dr. Alice Shaparenko, who taught him everything he knew and forgot about calculus, but never forgot her lessons on diligence. Together, Andrew and Crystal took an academic Co-op position at Johnson & Johnson's McNeil Pharmaceuticals (Tylenol) for a semester to gain industry experience. Here, they learned firsthand how many doors a well-earned PhD can open. After this, they spent another year at Penn State while both doing biochemistry and biophysics research in the lab of Dr. John Golbeck studying iron-sulfur reaction centers in anaerobic heliobacteria with the eventual goal of better understanding the water-splitting reaction of this organism. Soon after, their time at Penn State was at an end and Andrew received his major in Biochemistry and Molecular Biology, with minors in Chemistry and Love of Wisdom (a.k.a. Philosophy).

Crystal and Andrew continued their adventure to graduate school together at Cornell University. With lenders across the country realizing the mess they put us all in, Andrew and Crystal first used their contacts at Johnson & Johnson to get a temporary, over-paid, position at the newly merged Pfizer manufacturing plant in Lititz PA in order to finance a down payment before buying Andrew's second house. In spite of crushing student loan debt, and a graduate student's salary, Andrew and Crystal found themselves tax paying Ithacans in the summer of 2008 and new additions to the Genetics and Development graduate student directory at Cornell University.

After exciting and educational rotations in the Schimenti and Vogt labs, Andrew was given the opportunity to study the role of small RNAs in the

regulation of meiotic silencing in the lab of Dr. Paula E. Cohen in May of 2009. Although his first two rotations had promising projects, Andrew could not ignore the challenge presented to him by Paula: a mutant mouse with no phenotype. He spent the next 4 years convincing himself and his reviewers that this was not the case, which will serve as the majority of this thesis. His remaining time in lab was spent further dissecting the overall contribution of small RNAs in the germline while also building the materials needed to elucidate the mechanism behind their actions. Although he will not be able to see this research through to its completion, he is overjoyed at the idea that others will take on the same challenge presented to him by Paula over four years ago and uncover the exciting new mechanisms waiting to be discovered in the mammalian germline.

Although the project was perhaps too risky for a graduate student, in the end it turned out to be exactly the graduate training Andrew hoped for and needed. Even though every single step felt like a step backwards, the entire Cohen lab and members of BMS and MBG departments were always there to help guide Andrew and provide priceless advice. Particular thanks must be given to Dr. Andrew Grimson and his student Stephanie Hilz for helping take this research to the *next generation*.

Equipped with excellent training and a passion for seeking out what's next, Andrew will continue his adventure in California where he accepted a postdoctoral position at the University of California, Berkeley. Andrew will be bringing his experience with the incredibly difficult to work with meiotic system and confidence provided to him from a Cornell PhD program to study the role of miRNAs in malignant transformation in the lab of Dr. Lin He.

# ACKNOWLEDGMENTS

I would like to thank Paula Cohen for giving me the chance to work in her lab and mentor me to become what I hope is a good scientist and person. From day one, I knew she made a decision that she would have to live with for the next half decade based on just a few weeks of me trying not to burn her lab down. Each day forward, I worked hard to make sure she never regretted that decision and I would like to think she never has.

I would also like to thank my committee members John Schimenti, Andrew Grimson and Alex Travis, who contributed immensely to my progression as a graduate student. Some committee members find their involvement to a graduate student minimal and restricted to the annual departmental seminar. This committee, on the other hand, was not so lucky. This did not dawn on them until my A-exam, where it was clear from the look in their eyes, the look of prisoners, and the fact that during hour three of my examination they would not allow me to discuss even a moment of aim three for fear of having somehow found themselves in purgatory, they were going to heavily be involved in this graduate student's story. Thank you and I promise my B-Exam will be shorter.

The Cohen lab, past and present, has truly shaped my development as a researcher. Rebecca Holmes built the foundation for this research with her original interest in small RNAs and meiosis and was passionate enough to generate the *Ago4* knockout mouse that this entire body of work is centered on. Kim Holloway taught me everything I know about mice and meiosis. She has been there since I joined and has advised me through every difficult experiment that shouldn't have worked, but after *delicately* explaining to me what a fool I was, everything always turned around. Xianfei Sun was the senior lab student at the

time I joined and never once displayed the slightest bit of impatience when dealing with me on a daily basis and even trusted me enough to teach me cell culture when I barely knew how to run a PCR. She gave me the confidence to attempt generating a transgenic triple knockout that will hopefully be the basis of the next student's journey in the Cohen lab. Ewelina Bolcun-Filas was not even a week into her post-doc when she was charged with babysitting me during my first rotation. Even after her sentence had ended, she continued to be a fountain of knowledge and advice for me and has been a significant part of every step of my PhD.

Peter Borst is the Cohen lab manager and works tirelessly to make things run as smoothly as possible but his role is really to keep everyone sane and remain close friends with one another. I am not sure how the lab managed before he arrived but I can't imagine it without him. Swapna Mohan has spent the last three years sitting dangerously close to me and my papasan chair, braving both fire and biohazard to pursue her own PhD. With my curious choice of lab chair impinging in her personal space, I always had someone close by to complain about the most recent failure before moving onto the next failure, but always first giving me a piece of advice on how to proceed and telling when my desperate attempts at what must have looked like real science from far away, was never actually going to work. Kadeine Campbell-Peterson joined the lab around the time when I felt like I was finally able to positively contribute to the development of a fellow student. She brought with her a definite style that has forever changed the way the lab operates. She has clear goals and the ambition to reach them. Melissa Toledo has just recently joined the Cohen lab and is beginning to develop as an excellent researcher and has the pleasure to do so in the best possible environment I can imagine.

The MBG department has provided an unmatched support network and made this graduate experience exceptionally pleasant. Dr. Alani genuinely cares about each and every student and is a shining example of what makes a graduate program stand out. Vicki Schaff and Diane Colfe made a trip to the office last ten times longer than it needed to be and ten times more enjoyable than you could imagine and never gave me a hard time about handing in important documents weeks late, knowing how hard it is to descend from the "tower". Although I was something of an orphan in BMS, I was treated as a full-fledged member and was even allowed to be president of G.R.A.P.E.S. (Graduates, Residents And Professionals Experiencing Synergy) for two full years. Amy Pelligrino and Elena Cestero entertained too many of my bizarre requests and let me operate under their all-seeing administrative eyes without ever alerting the proper authorities. I most likely would have starved if not for Amy and Vicki over these past years. I would particularly like to thank Dr. Mark Roberson for continuously seeing potential in me that I was not aware of. As the second busiest man in the building, he still found the time to routinely monitor the well-being and progress of students throughout the department, which was coincidentally when I would corner him to extract every bit of wisdom he had to offer. In a gesture that either meant he trusted me as a researcher, or was punishing his son in some way, he facilitated the opportunity for me to mentor his son Connor in the spring of 2013.

I also want to acknowledge the custodial staff for their friendship at all times, as well as the veterinarians and technicians at the East Campus Research Facility for their hard work that tends to go unnoticed.

Crystal Conn has influenced the biggest part in my life these past five years. Not only has she supported my development as a scientist, but at the same time made me a better person. Thank you for keeping me sane. *Ja cię kocham*.

Finally, I would like to thank my family for setting me on this path. This short section could not possibly express my gratitude, as the details of my appreciation would fill this entire thesis. Thank you.

TABLE OF CONTENTS

**BIOGRAPHICAL SKETCH** ..... **viii**

**ACKNOWLEDGMENTS** ..... **xi**

**TABLE OF CONTENTS** ..... **xv**

**LIST OF FIGURES** ..... **xvii**

**LIST OF TABLES** ..... **xix**

**LIST OF ABBREVIATIONS** ..... **xx**

**PREFACE** ..... **xxii**

**CHAPTER 1** ..... **23**

**Small RNA Sexual Dimorphism during Mouse Meiosis** ..... **23**

1.1 Introduction ..... 23

1.2 Overview of small RNA biogenesis pathways ..... 24

1.3 Mammalian Gametogenesis and Sexual Dimoprhism ..... 27

1.4 Why are germ cells unique in terms of the Small RNA pathways? ..... 30

1.5 Small RNA pathways in male germ cells ..... 32

1.6 Small RNA pathways in female germ cell ..... 36

1.7 Perspectives and looking to the future ..... 38

**CHAPTER 2** ..... **41**

**AGO4 REGULATES ENTRY INTO MEIOSIS AND INFLUENCES SILENCING OF SEX CHROMOSOMES IN THE MALE MOUSE GERMLINE**

2.1 Abstract ..... 41

2.2 Introduction ..... 42

2.3 Results and Discussion ..... 44

2.4 Conclusion ..... 78

2.5 Materials & Methods ..... 81

2.6 Acknowledgements ..... 89

**CHAPTER 3** ..... **90**

**Prophase I-specific Deletion of *Dgcr8* and *Dicer* result in altered Meiotic Sex Chromosome Inactivation, XY chromatin compaction and integrity.** ..... **90**

3.1 Abstract ..... 90

3.2 Introduction ..... 91

3.3 Materials & Methods....94
3.4 Results....95
3.5 Discussion....114
3.6 Acknowledgements....117

**CHAPTER 4....118**

**Concluding Remarks & Future Endeavors....118**

**APPENDIX I....127**

**Generation of Ago3-1-4 Mutant Mice....127**
Summary....127

**APPENDIX II....133**

**Investigating miRNA localization using Locked Nucleic Acid FISH....133**
Summary....133

**APPENDIX III....144**

**Laser Capture Microdissection of Pachytene Stage Sex Bodies....144**
Summary....144

**APPENDIX IV....148**

**Cytological and Small RNA Analysis of Chromosome 16:17 Translocation on mouse spermatogenesis.....148**
Summary....148

**REFERENCES....154**

LIST OF FIGURES

Figure 2-1. AGO4 Localization and Phenotypic Analysis of *Ago4*$^{-/-}$ males.....45
Figure 2-S1. Related to Figure 1: Generation of *Ago4*$^{-/-}$ mouse via targeted deletion of *Ago4* exons 3-17. .....46
Figure 2-2. Upregulation of *Ago3* mRNA and Protein in the Testis of *Ago4*$^{-/-}$ Males. .....51
Figure 2-S2. Related to Figure 2: *Ago1* and *Ago2* are not up-regulated in *Ago4* null testes. .....52
Figure 2-3. Loss of AGO4 Disrupts Localization of SB-Associated Proteins and RNAP II during Pachynema .....54
Figure 2-S3. Related to Figure 3: Loss of AGO4 disrupts localization of SB associated proteins in early pachytene. .....57
Figure 2-4. Loss of *Ago4* Results in Loss of miRNAs Originating from Chromosome X and Wide-Scale Alterations in the Expression of Most miRNA Families .....61
Figure 2-S4 Related to Figure 4: Alternative normalization of miRNA data, length distribution of pachytene small RNA populations and Fluorescence *in* situ hybridization for miRNA 206. .....63
Figure 2-S5. Figure S5 related to figure 4: miR/miR* ratios between *Ago4*$^{+/+}$ and *Ago4*$^{-/-}$ pachytene small RNA samples. .....66
Figure 2-5. RNAseq Profiling of Purified Spermatocytes from Different Stages of Prophase I and from Premeiotic Testes .....69
Figure 2-6. Loss of AGO4 Induces Early Entry into Meiosis in Postnatal Testes....74
Figure 2-7. Model for the Role of AGO4 in Meiotic Silencing .....79
Figure 3-1. Phenotypic Analysis of *Dicer* cKO males. .....97
Figure 3-2. Phenotypic Analysis of *Dgcr8* cKO males .....98
Figure 3-3. Quantification of TUNEL Staining from Dicer and Dgcr8 testes sections. .....100
Figure 3-4. Loss of DICER disrupts localization of SB associated Proteins, RNAP II and Chromosomal abnormalities at the Sex Chromosomes during Pachynema .....102

Figure 3-5. Loss of DGCR8 disrupts localization of SB associated Proteins, RNAP II and Chromosomal abnormalities at the Sex Chromosomes during Pachynema ..... 103
Figure 3-6. Losses of Dicer and Dgcr8 have unique frequencies of chromosomal abnormalities.. ..... 105
Figure 3-7. *Dicer* and *Dgcr8* cKO spermatocytes are able to progress beyond pachytene checkpoint ..... 109
Figure 3-8. Loss of DICER and DGCR8 disrupts localization of proteins associated with recognizing, spreading and placement of epigenetic marks in pachytene spermatocyte. ..... 112
Figure 4-1. Model for RITs-LIKE meiotic silencing by AGO4 and miRNAS at the X-Chromosome. ..... 123
Figure AI-1: Deletion of *Ago314* ..... 129
Figure AI-2: PCR confirmation fo Fermline transmission of *Ago314* construct .. 129
Figure AII-1. Localization of miR-24. ..... 137
Figure AII-2. Localization of miR-Let7d ..... 138
Figure AII-3. Localization of miR-743a ..... 139
Figure AII-4. Localization of miR-34c ..... 140
Figure AII-5. miRNA FISH Controls ..... 141
Figure AIII-1. Laser Capture Microdissection of Pachytene Stage Sex Bodies ..... 146
Figure AIV-1. Cytological analysis of Ts($17^{16}$)65Dn spermatocytes ..... 151
Figure AIV-2. Small RNA cloning analysis of Ts($17^{16}$)65Dn spermatocytes ..... 152

LIST OF TABLES

Table 1-1. Male Germline Specific RNAi knockout mouse models……..35

Table 1-2. Female Germline Specific RNAi knockout mouse models……..37

Table 2-S1. Table S1 Related to Figure 1: Summary of phenotypic data for *Ago4*$^{+/+}$ and *Ago4*$^{-/-}$ littermate males at day 70 pp……..49

Table 2-S2. Related to Figure 4: MicroRNA hairpins for all members of the 15 most highly expressed microRNA families in WT pachytene cells. .....67

Table 2-S3. Related to Figure 5: Summary of RNAseq data at Leptonema/Zygonema and at Pachynema .....71

Table AIII-1. Summary of Locked Nucleic Acid miRNA probes. .....136

## LIST OF ABBREVIATIONS

| | |
|---|---|
| AGO1 | Argonaute 1 |
| AGO2 | Argonaute 2 |
| AGO3 | Argonaute 3 |
| AGO4 | Argonaute 4 |
| ALG-1 | Argonaute Like Gene 1 |
| ALG-2 | Argonaute Like Gene 2 |
| ATM | Ataxia Telangiectasia Mutated |
| ATR | Ataxia Telangiectasia and Rad3 related |
| BRCA1 | Breast Cancer type 1 susceptibility protein |
| CDK2 | Cyclin Dependent Kinase 2 |
| CHK2 | Checkpoint protein homolog 2 |
| cKO | Conditional Knock Out |
| Day #pp | Day #post partum |
| DDX4 | Deadbox protein 4 |
| DGCR8 | DiGeorge Syndrome Critical Region 8 |
| DMC1 | Disrupted Meiotic cDNA 1 |
| DSB | Double Strand Break |
| dsRNA | Double Stranded RNA |
| DTC | Distal Tip Cells |
| e(#) | Embryonic Day # |
| Endo-siRNA | Endogenous Small Interfering RNA |
| ES Cell | Embryonic Stem Cell |
| FISH | Fluorescence *In Situ* Hybridization |
| GCNA-1 | Germ Cell Nuclear Antigen 1 |
| H1T | Histone 1 Testes specific |
| H2AX | Histone 2A Family member X |
| H3K9me3 | Histone 3 Lysine 9 tri-methylation |
| HEK | Human Embryonic Kidney |
| IACUC | Institutional Animal Care and Use Committee |
| KO | Knock Out |
| LCMD | Laser Capture Micro Dissection |
| LINC-RNA | Long Intergenic Non Coding RNA |
| LNA | Locked Nucleic Acid |
| LEPT | Leptonema/Leptotene |
| MI | Meiosis I |
| MII | Meiosis II |
| MDC1 | Mediator of DNA damage Checkpoint 1 |
| miR | miRNA |
| miRISC | miRNA RISC |
| miRLC | miRNA Loading Complex |
| miRNA | micro RNA |
| MLH1 | Mut-L Homolog 1 |

| | |
|---|---|
| MLH3 | Mut-L Homolog 3 |
| MMR | MisMatch Repair |
| mRNA | messenger RNA |
| MSCI | Meiotic Sex Chromosome Inactivation |
| MSH4 | Mut-S Homolog 4 |
| MSH5 | Mut-S Homolog 5 |
| MSUC | Meiotic Silencing of Unpaired Chromatin |
| MSUD | Meiotic Silencing of Unpaired DNA |
| PAR | PsuedoAutosomal Region |
| PCR | Polymerase Chain Reaction |
| PGC | Primordial Germ Cell |
| piRNA | PIWI Interacting RNA |
| PIWI | P-element Induced Wimpy Testes |
| pre-miRNA | Precursor miRNA |
| pri-miRNA | Primary miRNA |
| PTGS | Post Transcriptional Gene Silencing |
| qRT-PCR | Quantitative Reverse Transcription PCR |
| RA | Retinoic Acid |
| RAD51 | Radiation Senstivie 51 |
| RDRP | RNA dependent RNA polymerase |
| RISC | RNA Induced Silencing Complex |
| RITS | RNA Induced Transcriptional Silencing |
| RNF8 | Ring Finger Protein 8 |
| RNAi | RNA Interference |
| RNAPII | RNA Polymerase II |
| SB | Sex Body |
| SC | Synaptonemal Complex |
| SD | Sexual Dimorphism |
| siRISC | siRNA RISC |
| siRLC | siRNA Loading Complex |
| ssRNA | Single Stranded RNA |
| SUMO1 | Small Ubiquitin-like Modifier 1 |
| SYCE2 | Synaptonemal Complex Central Element Protein 2 |
| SYCP1 | Synaptonemal Complex Protein 1 |
| SYCP2 | Synaptonemal Complex Protein 2 |
| SYCP3 | Synaptonemal Complex Protein 3 |
| TGS | Transcriptional Gene Silencing |
| TRBP | Tar RNA Binding Protein |
| TOPBP1 | DNA Topoisomerase 2-binding protein 1 |
| TUNEL | Terminal Deoxynucleotidyl transferase dUTP NickEnd Label |
| ubiH2A | Ubiquitylated Histone 2A |
| WT | Wild Type |
| ZYG | Zygonema/Zygotene |

# PREFACE

The primary emphasis of this dissertation is the involvement of small RNAs and associated proteins in the development and regulation of mammalian spermatogenesis. This work is composed of four main chapters, each focusing on a different aspect of small RNA mediated regulation in maintaining male fertility. Chapter one reviews what is currently known about RNAi related components in both male and female meiosis and emphasizes that there is a significant degree of sexual dimorphism in the involvement of different small RNA species in each sex. Chapter two derives from the bulk of my PhD training and describes the phenotypical analysis of one of the effector of small RNA mediated regulation, Argonaute-4 (*Ago4*). Chapter three focuses on genetically dissecting the roles of two of the major small RNA populations present in spermatogenesis, miRNAs and endo-siRNAs by evaluating the conditional loss of *Dgcr8* and *Dicer*. Part four summarizes the connection of these findings, while exploring a few of the unanswered questions that remain.

Extended research in these areas, outside the focus of the main chapters, is examined to a lesser extent and discussed briefly within four appendices associated mostly with chapter two.

# CHAPTER 1

## Small RNA Sexual Dimorphism during Mouse Meiosis

This chapter was written by Modzelewski AJ as a literature review on RNAi and its link to regulation in the male germ line. The article will be revised and submitted for peer-review with Cohen PE.

### 1.1 Introduction

Mammalian meiosis is a tightly regulated process in which an organism passes on genetic information, preserving the species, and occasionally imparting some physiological advantage to its offspring. Germ cells undergo one round of DNA replication followed by two rounds of cellular division. In the case of females, the end product is a single oocyte, while in males four spermatozoa are generated, each providing one-half of the genetic material required for initiating new life. This cycle has occurred, unbroken, for over one billion years where an enormous level of regulation and coordination must be utilized to allow for the faithful inheritance of genetic information.

RNA interference (RNAi) exists in nearly all eukaryotes and predates the divergence of plants, animals and fungi. Believed to have originated over one billion years ago, RNAi coincides with the emergence of sexually reproducing organisms. Since the discovery of small RNA function in 1998 (Fire et al., 1998), it has been reported that every mammalian tissue and cell type exhibits regulation governed by at least one of the known small RNA pathways (Wu et al., 2012a). In mammals, three classes of small non-coding RNAs ranging from ~20-30nts have been a major focus of investigation. These classes are microRNAs (miRNAs, 21-22nt), endogenous small interfering RNAs (endo-siRNA, 21nt) and PIWI interacting RNAs (piRNAs, 23-30nts). Although most studies have been focused on soma and cell culture, only recently has it been shown through the conditional deletion of various RNAi related genes that endo-siRNAs and miRNAs play essential roles throughout male and female germlines. In females, small RNAs are

required for proper follicle recruitment regulated by granulosa cells (Lei et al., 2010), and chromosome segregation in oocytes (Murchison et al., 2007). In males, small RNAs are essential for sertoli cell function, tubule organization (Kim et al., 2010a) proliferation of spermatogonia and early development of spermatocytes (Hayashi et al., 2008) as well as chromatin condensation and spermatid elongation (Korhonen et al., 2011). No doubt additional functions are left to be discovered.

Although there are germline specific small RNAs in both male and females, only a few examples of specific small RNA functions have been reported in either sex, therefore it is likely that small RNAs will continue to emerge as key regulators of reproductive events. The overall contribution of small RNAs in reproduction has not been fully elucidated, however, recent reports suggest that small RNAs function in a sexually dimorphic nature in the mammalian germline, in that endo-siRNAs (but not miRNAs) are essential for proper oocyte development (Suh et al., 2010)(Garcia-Lopez and Del Mazo, 2012). In males, on the other hand, it seems that all small RNA species (miRNA, endo-siRNA and piRNA) are function during spermatogenesis (Wu et al., 2012b), (Yadav and Kotaja, 2013). Males and females appear to have evolved distinct small RNA regulatory processes to govern proper meiotic progression, however the underlying mechanisms and differences are only just beginning to be understood. Therefore, small RNA function cannot be generalized when considering male and female gametogenesis, in spite of the similarities in the molecular events of meiotic progression.

## 1.2 Overview of small RNA biogenesis pathways

Small RNA regulation has taken on various forms throughout different eukaryotic species. The presence of regulatory small RNAs ranges from an apparent absence in *S. cerevisea* (0 Dicer, 0 Argonautes: (Drinnenberg et al., 2009), *A. thaliana* (4 Dicers, 10 Argonautes: (Watanabe, 2011)), to the

overwhelming number of RNAi components in *C. elegans* (1 Dicer, 27 Argonautes: (Yigit et al., 2006). Mammals fall somewhere in the middle with 1 Dicer and 7 Argonaute proteins making up three distinct RNAi mechanisms (Meister, 2013). Both the miRNA and endo-siRNA pathways are involved in post-transcriptional gene silencing (PTGS) in the mammalian cytoplasm. The contribution of the remaining small RNA class (piRNAs) has been extensively studied and we would like to direct interested readers to excellent reviews on the subject (Ishizu et al., 2011; Malone et al., 2009).

miRNA typically originate as clusters found on all chromosomes except on the Y chromosome (Kozomara and Griffiths-Jones, 2011). RNA Polymerase II (RNAPII) then transcribes these regions into elaborate stem-loops structures called primary miRNAs (pri-miRNA), usually containing 1 to 6 miRNA precursors. These precursors are recognized in the nucleus by the initiating components of miRNA regulation: DGCR8 (DiGeorge Syndrome Critical Region 8) and DROSHA, collectively termed the microprocessor complex. DGCR8 is an RNA binding protein that is responsible for first recognizing the pri-miRNA (Faller et al., 2007) and binds to ssRNA-dsRNA junctions to direct DROSHA function. DROSHA is class 2 RNase III enzyme that interacts with the RNA bound DGCR8 and cleaves the pri-miRNA approximately 11bp away from the ssRNA-dsRNA junction. This action results in the characteristic stemloop structures of approximately 70 base pairs long made up of a double stranded stem region and a 33bp single stranded loop structure, now termed pre-cursor miRNAs or pre-miRNAs (Han et al., 2007). This cleavage event leaves a distinguishing 2nt 3' overhang, which is recognized by the nucleoplasmic shuttle protein, EXPORTIN-5, that exports the pre-miRNA to the cytoplasm in a Ran-GTP dependent manner (Murchison et al., 2005).

Once in the cytoplasm, the pre-miRNA comes into contact with DICER and TRBP (Tar RNA Binding Protein). DICER is a class III endoribonuclease that binds to the 3' end of the hairpin just before the loop structure and cleaves, leaving an imperfect miRNA duplex of approximately 22nt long with 2nt 3' overhangs (Lund and Dahlberg, 2006). Cleavage is enhanced by the stabilization of DICER-

substrate interactions by TRBP as well as the structural properties of the pre-miRNA substrate (Chakravarthy et al., 2010). This duplex, now double stranded mature miRNA, is bound by the miRNA Loading Complex (miRLC), which consists of DICER and TRBP (Maniataki and Mourelatos, 2005). The miRLC transfers the miRNA duplex to an Argonaute protein where the duplex miRNA is unwound as the miRLC dissociates and the strand with the less stable 5' end (guide strand) is loaded into the AGO protein while the passenger strand is presumably degraded (Schwarz et al., 2003). The AGO protein along with its miRNA cargo is now called the RNA Induced Silencing Complex (RISC) and is capable of carrying various cellular functions.

Endogenous siRNAs have been reported to exist in mammalian embryonic stem (ES) cells, oocytes and spermatocytes, even though mammals lack a discernable RNA dependent RNA polymerase (RDRP), which was thought to be essential for endo-siRNA production (Babiarz et al., 2008) (Watanabe et al., 2006) (Song et al., 2011). Endo-siRNAs originate from cis/trans derived loci and inverted repeats found throughout the genome (Kim et al., 2009). These molecules act as DICER substrates, thereby obviating the requirement of the microprocessor as seen in miRNA biogenesis. These small RNAs are then processed similarly to the miRNA pathway, however, RISC loading and subsequent silencing action is distinct from the miRNA pathway. Unlike miRNA loading and unwinding, siRNAs are reported to only be loaded into RISC with AGO2 as the core effector (Liu et al., 2004). During siRNA RISC (siRISC) loading, the perfectly matched duplex RNA is transferred from the siRNA RLC (siRLC) to AGO2 and the strand destined to become the passenger strand is cleaved through catalytic action of the AGO2 PIWI domain (Matranga et al., 2005). In a manner nearly identical to this initial cleaving event, the loaded guide strand is used to scan for perfectly matching target RNA, and once bound, this target is subsequently cleaved by AGO2, effectively reducing the pool of the particular mRNA as the major mode of silencing in this pathway. The remaining Argonautes, AGO1,3 and 4, are all able to associate with both miRNAs and siRNAs, however,

AGO3 and 4 appear to have lost the catalytic ability to cleave RNA targets. All four are believed to have largely redundant roles in non-cleavage miRNA based silencing while AGO2 (and to a unknown extent, AGO1) function in siRNA mediated cleavage silencing (Su et al., 2009). A more thorough understanding of the individual roles of each Argonaute protein is only currently being formulated and interesting roles for each are beginning to emerge (Van Stry et al., 2012), (Modzelewski et al., 2012).

## 1.3 Mammalian Gametogenesis and Sexual Dimorphism

In order for germ cells to participate in sexual reproduction, they must go through a meiotic cell cycle, a process in which a mitotically dividing stem cell first synthesizes a new copy of its genome, recombines genetic material and then divides twice. In males, this results in 4 haploid spermatozoa, and in females, a single oocyte. This is the principal example of sexual dimorphism (SD) (Liu et al.), a term that is usually used to describe the secondary sexual characteristic differences between males and females (McPherson and Chenoweth, 2012), however, it also relates to any biological, cellular or molecular process that varies between the sexes (Morelli and Cohen, 2005). SD is a theme that exists between males and females to a surprising degree throughout development and nowhere more so evident than in the germline.

The same basic molecular events must occur in both male and female meiosis, and to some extent, they do. The most obvious difference is the timing and eventual haploid end products. In mice, males and females both initiate the meiotic program at around e11 in response to the secretion of retinoic acid (RA) from neighboring Sertoli and other cells. This activates a cascade of molecular events in a *Stra8* dependent manner. This cascade is allowed to persist in females, so that the entirety of germ cells proceed through meiosis during embryonic development and arrest at the end of prophase I. However, in males at embryonic day 12 (e12), anti-meiotic factors are expressed that block the

cascade through oxidation of RA by CYP2B1, and other mechanisms (Hogarth and Griswold, 2010). It is not until day 5pp that RA is able to bind to the surface of type A spermatogonia and meiosis is initiated (Gely-Pernot et al., 2012). In contrast to females, where every germ cell enters and completes a semi-synchronous wave of meiotic events during embryonic development, male meiosis is entirely a postnatal event. The first wave of male meiosis is synchronous, while subsequent non-synchronous waves persist throughout the adult life of the animal (Handel and Eppig, 1998).

The major molecular events of both male and female meiosis occur during prophase I and are largely conserved, however mutations of key proteins lead to drastically different meiotic phenotypes between the sexes. Prophase I consists of five distinct stages where many key events have been shown to occur. The first stage, leptonema, is initiated by programmed double strand breaks (DSBs) catalyzed by the type II topoisomerase, SPO11. The breaks are then recognized by the single strand DNA (ssDNA) binding RecA homologs, DMC1 and RAD51, to mediate subsequent single strand invasion at recombination nodules. In males, mutations in *Dmc1* lead to arrest zygonema, while females arrest at a later stage (Yoshida et al., 1998), (Pittman et al., 1998). Also during this stage, as the chromosomes begin to condense, a meiosis specific proteinacious structure called the synaptonemal complex (SC) begins to form, which facilities DSB repair events and acts as a scaffold by physically tethering the homologous chromosomes together throughout prophase I. By zygonema, the chromosomes are further condensed and begin to pair with one another, facilitated by the accumulation of SC components in a zipper-like fashion between the homologous chromosomes, now termed bivalents. Interestingly, while mutations in the SC components lead to arrest of spermatocytes during zygonema, oocytes somehow progress through the whole of meiosis and produce offspring (Kolas and Cohen, 2004). Some of the RAD51 and DMC1 binding sites are selected for repair events leading to recombination, in which the mismatch repair (MMR) proteins MSH4 and MSH5 localize to these intermediates structures. Defects in either of these

genes prevent spermatocytes from entering the next stage, while oocytes are not depleted until day 6pp (Kneitz et al., 2000), (Edelmann et al., 1999). By pachynema, the bivalents are fully paired. In females, the SC core lengths are significantly longer than that of their male counterparts. The MMR proteins, MSH4 and MSH5, recruit MLH1 and MLH3 to a subset of recombination nodules and facilitate the exchange of genetic information by resolving these recombination intermediates into either crossover or non-crossover gene conversion events. Errors in these genes result in metaphase I arrest in males while oocytes are seen to arrest after fertilization at the two-cell stage (Morelli and Cohen, 2005). The next stage, diplonema, is characterized by the dissociation of the SC and separation of homologous chromosomes except at sites of recombination, which reveal structures called chiasmata. In females, all developing oocytes pause at this stage in a form of suspended animation called dictyate arrest. The final stage is called diakensis, where the chromosomes further repel from each other and chiasmata are more clearly visible.

One of the major differences between how male and female meiosis progress is the presence of the Y-chromosome in males. In females, the two X-chromosomes pair with each other and act essentially as autosome for the purpose of meiosis and recombination. In males, however, the X and Y share only a small portion of homology called the pseudo autosomal region (PAR) that pair and undergo recombination. For reasons that are not completely understood, spermatocytes undergo a unique process of heterochromatinization at the X and Y-chromosomes that repress the expression of all protein coding genes on these chromosomes (Song et al., 2009). Silencing during meiosis is mediated by two related processes, Meiotic Sex Chromosome Inactivation (MSCI; (Turner, 2007)) which monitors the X and Y chromosomes, into a subdomain called the sex body (SB; (Handel et al., 1994) and Meiotic Silencing of Unpaired Chromatin (MSUC; (Schimenti, 2005b)), which monitors the synaptic status of the autosomes. Interestingly, while MSCI is an absolute requirement of meiotic progression in spermatocytes, the activation of MSUC in either sex results in arrest, even though

the machinery between to two mechanisms are seemingly identical. The mechanism behind how this process is implemented is not well characterized, but it is believed that the formation of the SB allows for the unpaired chromatin of the XY bivalents to bypass the meiotic checkpoints present during prophase I (Baarends and Grootegoed, 2003b). Interestingly, it was found that although the protein coding transcripts from the SB are repressed, a large proportion of the miRNA clusters are actively expressed (Song et al., 2009), suggesting possible small RNA mediated functionality in initiating or maintaining the silenced status of the unpaired X and Y chromosomes.

## 1.4 Why are germ cells unique in terms of the Small RNA pathways?

Much of what is known about mammalian small RNA biology has been extrapolated from *in vitro* and cell culture studies, as well as by inference from other organisms. Although these are sufficient proxies for some mammalian tissue types, germ cells are notoriously difficult to culture and are therefore under represented in these types of analyses. Moreover, their unique cell cycle, transcriptional regulation, and genetics make germ cells fundamentally different from somatic cells in terms of their molecular regulation. Gene expression analysis of various RNAi component transcripts in different mouse tissues has shown that these transcripts display distinct expression patterns and are co-regulated in a tissue specific manner. Interestingly, it was found that in general, RNAi components are most highly expressed in brain and testis (Gonzalez-Gonzalez et al., 2008a). More specifically, of the four mammalian Argonaute genes, *Ago4* (and to a lesser extent *Ago3*) display their highest level of expression in the testis. Closer examination of these expression levels during spermatogenesis showed that *Ago4* is most highly expressed in the pachytene stage of meiosis, and this high level of expression persists until the elongated spermatid stage.

Based on *ex vivo* studies, it is not expected that each Argonaute would have distinct functions in regards to miRNA-guided regulation. The Tuschl lab investigated the small RNA:AGO binding partners with tagged AGO proteins. The tagged proteins were expressed in HeLa S3 and HEK 293 cells and small RNAs were collected from purified immunoprecipitation experiments (Meister et al., 2004a). These libraries were essentially identical, suggesting that in these cell types, all four AGO proteins bind to small RNA in a sequence independent manner. In an inducible ES cell line deficient in AGO1-4, the Wang lab determined that the loss of all four AGO proteins resulted in disrupted miRNA silencing and de-repression of the pro-apoptotic protein, Bim. The re-introduction of any one member of the *Ago* clade rescued the cells from this effect, implying that the four AGOs are equivalent in miRNA silencing in ES cells (Su et al., 2009).

The male and female germlines have the unique characteristic of harboring distinct classes of small RNAs, not found elsewhere in the adult animal. During two prominent phases of mammalian spermatogenesis, piRNAs are expressed and utilized by the PIWI subfamily of Argonaute proteins to enact essential germ cell development and retrotransposon repressive functions ((Kuramochi-Miyagawa et al., 2010), (Aravin et al., 2006), (Girard et al., 2006), (Grivna et al., 2006a), (Watanabe et al., 2006)). In the oocyte, endo-siRNAs have also been implicated in restricting the functions of retrotransposons in female meiosis ((Watanabe et al., 2007), (Tan et al., 2009)). Since a portion of the cycle of retrotransposition occurs within the nucleus, it is tempting to speculate that piRNAs and endo-siRNAs function there as well, as they have been shown to do in other organisms ((Fagegaltier et al., 2009), (Burkhart et al., 2011)). Endo-siRNAs have also been recovered in embryonic stem cells and isolated mouse spermatocytes and are predicted to target hundreds of RNA targets and thousands of DNA targets, however, more in vivo studies are needed determine what their roles may be (Babiarz et al., 2008) (Song et al., 2010).

In mammals, RNAi had thus far been implied to be a solely cytoplasmic phenomenon. Using fluorescence correlation and cross-correlation spectroscopy

it was shown in er293 cells that two distinct RISCs exist, one in the cytoplasm that is 20 fold larger than a nuclear complex (Ohrt et al., 2008). Recent findings from the Suzuki lab visually demonstrated nuclear distribution of Ago-associated siRNA, where they determined that during retroviral infection in human cell culture, *Ago1* and *Ago2* are able to induce transcriptional gene silencing (TGS) in a RNA Induced Transcriptional Silencing (RITS) like mechanism (Ahlenstiel 2012). These studies are in line with the previous demonstration of miRNA localization within the nuclei of mouse spermatocytes by the Moens lab. Using miRNA fluorescence in-situ hybridization (miR FISH), it was demonstrated that miRNAs display distinct localization patterns, particularly at the transcriptionally silenced X and Y-chromosomes (sex body), a DNA poor region termed the dense body and in some instances, the autosome cores (Marcon et al., 2008b). These finding strongly imply that not only are these RNAi components found within the nucleus, but they are capable of inducing TGS regulation under certain conditions. The precedence for TGS occurring in a meiotic setting has already been shown in the bread mold, *Nuerospora crassa*. In this organism, meiotic progression and RNAi are inseparable. The disruption of the organism's sole *Ago* gene, siRNAs or RNA Dependent RNA Polymerase (RDRP) results in sterility ((Shiu et al., 2001), (Raju et al., 2007). These finding lend credence to possible meiosis specific roles for small RNAs and RNA binding proteins in the nuclei of metazoan and other higher order eukaryotes.

## 1.5 Small RNA pathways in male germ cells

The investigation of RNAi machinery in meiotic cells has been hindered by the fact that homozygous mutations in genes encoding many of the core components of RNAi are embryonically lethal. Thus, our current knowledge stems from the generation of various conditional knockout (cKO) animals at distinct developmental time points using a vast repertoire of temporally inducible *Cre* recombinases. This approach has been applied to various tissues

and time points in both male and female germlines. These analyses provide a framework to begin unraveling the complex relationship between small RNAs and mammalian reproduction.

DROSHA is essential for the initial processing of pri-miRNA in the mammalian nuclei. Thus far, DROSHA has only been shown to be involved in the biogenesis of miRNAs via the generation of the characteristic ~70nt hairpin structure known as pre-miRNAs. For this reason, disrupted DROSHA function is expected to only alter canonical miRNA biogenesis, leaving the remaining small RNA populations unaffected. The loss of *Drosha* during spermatogenesis has so far only been investigated at day 3pp, a time point prior to the onset of meiosis in the male mouse. It was found that these mice are infertile and display severe spermatogenic cell depletion in adult cKO seminiferous tubules. mRNA expression levels are altered in both pachytene spermatocytes and round spermatids, including genes normally suppressed during meiotic progression (Wu et al., 2012b). Although only a single developmental time point, these finding reflect an essential role for *Drosha* and miRNAs in male spermatogenesis.

DICER has been investigated throughout various timepoints and tissues during male meiosis in the mouse. Since DICER is involved in processing various forms of double stranded RNA, it is therefore is involved in the canonical biogenesis of both miRNA and endo-siRNA, and its loss would results in massive depletions of both species. The removal of *Dicer* at e10 resulted in proliferation defects in both primordial germ cells (PGCs) and spermatogonia. Spermatogenesis was seen to show signs of arrest in the *Dicer* deleted testes of four-week-old males with the vast majority of tubules showing no signs of germ cells. Although *Dicer* cKO males reaching 8 months of age were infertile, younger males of 8-16 weeks were able to produce offspring, presumably due to the efficiency of the inducible *Cre* system selected (Hayashi et al., 2008). When *Dicer* is removed from sertoli cells at e14, developmentally relevant genes are down regulated a day 0. At day 3pp, large numbers of sertoli cells are seen undergoing apoptosis and the subsequent loss of germ cells was observed so that by day 6pp,

the remaining tubules are highly disorganized and leads to the total loss of spermatogenesis (Kim et al., 2010a). Later, when *Dicer* is deleted at e18 in germ cells, testis size is drastically reduced and the males were rendered infertile, although these animals did produce few spermatozoa. These findings link small RNAs in the regulation of spermatogenesis and sperm productions (Romero et al., 2011). The loss of *Dicer* starting at day 3pp from type A spermatogonia resulted in disrupted meiotic silencing, arrest during pachyenema and abnormal sperm formation (Wu et al., 2012b) (Greenlee et al., 2012). At the slightly later time point of day 5pp, epididymal spermatozoa displaying prominent morphological abnormalities followed the loss of *Dicer* in type A spermatogonia. The cause of infertility was recognized to be due to improper chromatin organization in the haploid elongating spermatid (Korhonen et al., 2011). Together, these finding strongly suggest the involvement of small RNAs in virtually all aspects of spermatogenesis. The distinct phenotypes and causes for infertility by removing *Dicer* at slightly different time points highlights the extensive degree of temporal regulation imparted by small RNA mediated mechanisms.

Of the four Argonaute proteins, only AGO2 has been shown to function in both the miRNA and endo-siRNA pathways, while the remaining three non-slicing Argonautes (AGO1, 3 and 4) are involved in only the miRNA pathway. Therefore, the loss of AGO2 limits the functions of both endo-siRNAs and miRNAs, while the loss of the non-slicing AGOs perturbs only miRNA function. Although *Ago1* and *Ago3* deletions have not been assessed in a meiotic setting, both *Ago2* and *Ago4* have. The loss of *Ago2* has been characterized in e10 germ cells and was not associated with an overt meiotic defect in the embryo or adult animal (Hayashi et al., 2008). Since AGO2 functions with siRNAs, this result suggests that the role of these particular small RNAs is not essential in spermatogenesis. Given the high degree of conservation between AGOs, and their shared role in the miRNA pathway (Su et al., 2009), the lack of a fertility defect is most likely due to compensation in the miRNA pathway by the remaining Argonaute proteins. Existing as a double knockout in all tissues, the *Ago1-3* deficient mouse was

generated but the analysis was not aimed at studying the germ line. However, it was reported that no discernable decrease in litter size, male to female ratio or Mendelian inheritance was observed when characterizing the mutant mice (Van Stry et al., 2012).

Although both miRNA and endo-siRNAs are present in spermatocytes, whether or not both small RNA types are required for mouse spermatogenesis is not clear. The lack of an *Ago2* associated defect would imply that endo-siRNAs are dispensable. However, the non-overlapping phenotypes associated with *Drosha* (miRNA) and *Dicer (miRNA and endo-siRNA)* would argue otherwise. Additional meiotic phenotypic analyses will be required to elucidate the overall function of small RNA populations in male gametogenesis.

| Gene | Cre - Expression | Tissue | Phenotype | Reference |
|---|---|---|---|---|
| *Drosha* | *Stra8* Day 3pp | Spermatogonia | Disrupted spermatocyte and spermatid development. Altered mRNA expression levels and comparatively more severe than the *Stra8-Cre Dicer cKO.* | Wu 2012 |
| *Dicer* | *Tnap* e10 | Primordial Germ Cells | PGC proliferation defects. | Hayashi 2008 |
| *Dicer* | *Amh* e14 | Sertoli Cell | Loss of sertoli cell function and disorganized tubule formation. | Kim 2010 |
| *Dicer* | *Ddx4* e18 | Prospermatogonia | Defects in haploid cell development, sperm head abnormalities. | Romero 2011 |
| *Dicer* | *Stra8* Day 3pp | Spermatogonia | Altered MSCI, spermatogenic failure. | Wu 2012, Greenlee 2012 |
| *Dicer* | *Ngn3* Day 5pp | Spermatogonia | Defective chromatin organization, elongated spermatid abnormalities. | Korhonen 2011 |
| *Ago2* | *Tnap* e10 | Primordial Germ Cells | None detected. | Hayashi 2008 |
| *Ago4* | *ActinB* ubiquitous | Global | Premature entry into meiosis, defects in MSCI. | Modzelewski 2012 |

**Table1: Male Germline Specific RNAi knockout mouse models**. Table describing the various testes conditional knockout of RNAi components. Column 1 lists the targeted gene. Column 2 described the Cre-promotor and timing of excision. Column 3 tells the target tissue. Column 4 describes meiotic phenotypes. Column 5 lists references.

## 1.6 Small RNA pathways in female germ cell

Less is known about the particulars of small RNA function in female meiosis, however recent experiments describe essential roles for various RNAi components both temporally and in different female mouse tissues.

To assess the overall contributions of both miRNAs and siRNAs in mouse ovaries, specifically in granulosa cells and the affect this has on oocytes, *Dicer* was deleted at e11.5. Comparison between mutant and wild type (WT) littermates at various developmentally relevant time points determined that the cKO mice had a larger primordial follicle pool in the neonatal ovary, and by later stages, many more degenerate follicles were observed. Gene regulation was altered in a temporal and gene specific manner, suggesting that small RNAs are important throughout multiple stages of granulosa cell function (Lei et al., 2010).

When oocytes are specifically depleted of *Dicer* transcripts at around day 10-12pp, their growth and development are normal however spindles are highly disorganized at meiosis I (MI) and meiosis II (MII) due to kinetochore attachment failure and improper chromosome congression. Additionally, misregulation of maternal transcripts in oocytes matured *in vitro* for 16hrs was reported as well as the upregulation of distinct transposable element classes was reported, possibly implicating a role for endo-siRNAs and miRNAs in guarding the female genome in a piRNA fashion during this vulnerable stage (Murchison et al., 2007).

DGCR8 is the binding partner of DROSHA and forms the microprocessor complex for initial miRNA processing. For this reason, DGCR8 is involved in only miRNA biogenesis, while siRNAs are theoretically intact. Therefore, the deletion of *Dgcr8* generates an animal or tissue void of canonical miRNAs. To dissect the roles of miRNAs and endo-siRNAs in the oocyte, a *Dgcr8* cKO mouse was generated by deletion at day 10pp. Surprisingly, the loss of *Dgcr8* in oocytes resulted in no discernable abnormalities in terms of oocyte development, maturation and fertilization. Implantation was unaffected and phenotypically normal offspring were produced when fertilized with WT sperm. Although

miRNAs are present, and in some cases highly abundant, these results hint at miRNA function being suppressed in the oocyte and essentially dispensable for proper oocyte maturation and preimplantation, however it is required for proper embryonic development beyond the formation of the epiblast and trophectoderm lineages (Suh et al., 2010).

The loss of *Ago2* at day 10pp in the oocyte displayed very similar phenotypical defects associated with the *Dicer* cKO at the same time point. These oocytes are able to mature, but displayed severe spindle formation defects and chromosomal arrangement. Interestingly, the loss of *Ago2* also resulted in the loss of nearly all miRNAs normally present in the oocyte, suggesting that AGO2 is somehow involved in the biogenesis or stability of miRNAs here. The *Dicer* and *Ago2* cKO defects diverge when comparing the downstream affects of their loss on the transcript level. Only a small proportion of altered genes overlapped between the two mutants, while the majority of differentially expressed genes are seemingly unrelated to the observed phenotype (Kaneda et al., 2009).

| Gene | Cre-Expression | Tissue | Phenotype | Reference |
|---|---|---|---|---|
| *Dicer* | *Amhr2* e11.5 | Follicular Granulosa Cells | Larger primordial follicle pool and increased number of degenerate follicles. | Lei 2011 |
| *Dgcr8* | *Zp3* Day 10pp | Oocyte | None detected in oogenesis. | Suh 2010 |
| *Dicer* | *Zp3* Day 10pp | Oocyte | Severe chromosome congression defects. | Murchison 2007 |
| *Ago2* | *Zp3* Day 10pp | Oocyte | Defective spindle formation and chromosomal arrangement. | Kaneda 2009 |

**Table1: Female Germline Specific RNAi knockout mouse models**. Table describing the various testes conditional knockout of RNAi components. Column 1 lists the targeted gene. Column 2 described the Cre-promotor and timing of excision. Column 3 tells the target tissue. Column 4 describes meiotic phenotypes. Column 5 lists references.

Taking the male and female reports together, it is clear that the requirement of different small RNA populations adds to the list of sexually dimorphic processes that exist in the mammalian germ lines. In males, the miRNA and piRNA pathways are indispensible for maintaining fertility and perpetuating the species. The loss of both *Dicer* and *Drosha* results in infertile male mice but

with non-overlapping phenotypes, while *Ago2* is lost without consequence, leading to some confusion as to whether endo-siRNAs are needed. In females, miRNAs are seemingly dispensable in the developing oocyte, while endo-siRNA function is essential. Although piRNAs haven't been recovered in oocyte small RNA sequencing experiments, one hypothesis is that oocyte specific endo-siRNAs have adopted the role of genome guardian to protect the genetic material from transposable element insertions (Murchison et al., 2007). The purpose of this proposed division of labor is not clear and many more mouse models, compound knockout and genetic manipulation is necessary to further appreciate the inherit differences between RNAi regulated male and female meiosis.

## 1.7 Perspectives and looking to the future

RNAi components are expressed and translated in all tissues and at every developmental stage (Gonzalez-Gonzalez et al., 2008a). Much of what is known and extrapolated about these mechanisms stems from the manipulation of cells in culture, but the temporal and tissue specific nuances of these regulatory elements are just now being investigated.

Since the original discovery twenty years ago (Lee et al., 1993) and subsequent functional characterization (Fire et al., 1998), small RNA mediated regulatory events are appearing under every biological rock. Our view of how these mechanisms work in mammals relies heavily on work done in model organisms that are separated by millions of years of evolution. As ancient mechanisms, the core process appears to be the same; small RNAs are made, processed and loaded into an Argonaute and together enact some regulatory function. The particulars of how, when and why these processes occur are necessary for our understanding of every biological system and developmental time point. Importantly, miRNAs have immense therapeutic potential and are already being actively pursued in this regard due to the observations that even individual molecules have the ability regulate entire cellular processes (Wu et al.,

2013). These effects are difficult to ascertain in *ex vivo* studies, where cell signaling, hormonal effects and overall biological relevance are largely unrepresented. As the list of small RNA classes grows every year, and their individual functions are being better annotated, it is not surprising that evidence for unique mammalian RNAi mechanisms are being uncovered (Ahlenstiel et al., 2012) (Sampey et al., 2012), and it is feasible to predict that given the high degree of specialization observed in different tissues, unique small RNA mediated mechanisms will be discovered that are distinct to their tissue of origin, as seen in spermatogenesis (Modzelewski et al., 2012).

The germ line provides a challenging but important model to study the immense catalogue of mammalian small RNAs. Spermatogenesis is unique in that it harbors all three known cytoplasmic RNAi mechanisms: miRNA, siRNA and piRNA pathways. Initial characterization of the various knockout models during male meiosis suggests that endo-siRNAs are dispensable for normal meiotic progression, while both miRNAs and piRNAs are critical, although there is some source of doubt in this assessment. Conversely, oogenesis contains two species, with miRNAs being functionally suppressed, and endo-siRNAs having taken on a novel genome guardian role similar to the piRNA pathway. Even though both meiotic systems work towards the eventual goal of generating haploid gametes, the processes involved are largely distinct, both in terms of molecular and regulatory events. Using *in vivo* strategies such as the ones described here provides the unique opportunity to study how the same basic machinery can work in nearly unrecognizable ways. Although cell culture studies have deciphered much of what we know about small RNA regulation, it will perpetually lack the biological relevance of a living tissue. Studying the role of small RNAs in intact, *in vivo*, biological contexts, such as the highly specialized and quickly evolving mammalian germline, will provide the necessary insight to better understand potential RNAi mechanisms that exist throughout all mammalian systems.

To this end, a thorough and systematic analysis of the core components of RNAi in both male and female germlines will be necessary to elucidate the sex specific roles of small RNA regulation during gametogenesis. This approach is being undertaken by the Cohen lab to fully characterize the role of miRNAs and endo-siRNAs in prophase I of meiosis. Parallel analysis of small RNA biogenesis components, *Dgcr8* and *Dicer*, reveal the overall roles of miRNAs and endo-siRNAs, respectively, in the regulatory processes during meiotic progression. Loss of *Ago4*, which is most highly expressed in pachytene cells, uncovered a role for small RNAs in meiotic silencing. The cumulative loss of the three non-slicing AGOs, *Ago3-1-4*$^{-/-}$ will further dissect the roles of small RNAs and loss of all four *Agos*, will show what the presence of small RNAs has when their potential functions have been removed.

# CHAPTER 2

## AGO4 REGULATES ENTRY INTO MEIOSIS AND INFLUENCES SILENCING OF SEX CHROMOSOMES IN THE MALE MOUSE GERMLINE.

This work was submitted March 2012 and first published on August 2, 2012, doi:10.1016/j.devcel.2012.07.003. The manuscript was published as Andrew J. Modzelewski, Rebecca J. Holmes, Stephanie Hilz, Andrew Grimson and Paula E. Cohen. **AGO4 Regulates Entry into Meiosis and Influences Silencing of Sec Chromosomes in the Male Mouse Germline.** Developmental Cell; Volume 23, Issue 2, 14 August 2012, 251-264. Minor modifications have been made for reprint here.

### 2.1 Abstract

The four mammalian Argonaute family members are thought to share redundant functions in the microRNA pathway, yet only AGO2 possesses the catalytic "slicer" function required for RNA interference. Whether AGO1, AGO3, or AGO4 possess specialized functions remains unclear. Here we show that AGO4 localizes to spermatocyte nuclei during meiotic prophase I, specifically at sites of asynapsis and the transcriptionally silenced XY sub-domain, the sex body. We generated *Ago4* knockout mice and show that *Ago4*$^{-/-}$ spermatogonia initiate meiosis early, resulting from premature induction of retinoic acid-response genes. During prophase I, the sex body assembles incorrectly in *Ago4*$^{-/-}$ mice, leading to disrupted meiotic sex chromosome inactivation (MSCI). This is associated with a dramatic loss of microRNAs, >20% of which arise from the X chromosome. Thus, AGO4 regulates meiotic entry and MSCI in mammalian germ cells, implicating small RNA pathways in these processes.

## 2.2 Introduction

Argonaute proteins form two clades within a larger super-family, based on their sequence homology (Cenik and Zamore, 2011; Czech and Hannon, 2011). The PIWI clade includes *Mili, Miwi1*, and *Miwi2* in mice, which are required for retrotransposon silencing in the germ line and normal progression through prophase I in male meiosis (Aravin et al., 2006; Girard et al., 2006; Grivna et al., 2006b), in conjunction with the PIWI-interacting RNAs (piRNAs). The second clade are the AGO proteins, of which there are four in mammals (AGO1-4(Steiner and Plasterk, 2006). However, only AGO2 is capable of mediating small RNA-directed endonucleolytic cleavage of mRNA targets, the hallmark of RNA interference (RNAi; (Liu et al., 2004; Meister et al., 2004b; Song et al., 2003). No individual functions have yet been ascribed to the other mammalian AGOs, but they can all associate with several distinct classes of small RNAs, including microRNAs (miRNAs) and small interfering RNAs (siRNAs).

Endogenous siRNAs and miRNAs are found in the male germ line (Song et al., 2011; Watanabe et al., 2006) and, while some associate with AGO proteins (Kim et al., 2006), their precise roles are unknown. Small RNAs may function in the process of meiotic silencing of unpaired chromosomes, a common feature of prophase I in a number of organisms (Maine, 2010). During meiosis in *Neurospora crassa*, for example, the presence of unsynapsed DNA triggers the post-transcriptional silencing of any homologous sequences. This process, called

Meiotic Silencing of Unpaired DNA (MSUD), requires Ago-protein function and small RNA involvement (Raju et al., 2007; Shiu et al., 2001).

The high expression of mouse *Ago4* (and *Ago3)* in the male mouse germ line (Gonzalez-Gonzalez et al., 2008b) indicates that similar meiotic functions for AGO proteins may also exist in mammals. Two distinct levels of meiotic silencing in the male germ line have been described: Meiotic Silencing of Unsynapsed Chromatin (MSUC; (Schimenti, 2005a) and Meiotic Sex Chromosome Inactivation (MSCI; (Fernandez-Capetillo et al., 2003). MSUC monitors complete pairing before permitting progression through prophase I, and protects genome from transposon mobilization by silencing regions that fail to pair because of hemizygous transposon insertions (Turner et al., 2005). MSCI, on the other hand, is unique to the sex chromosomes and results in their heterochromatinization and compartmentalization into a specialized nuclear sub-domain known as the Sex Body (SB; (Handel, 2004). This enables the unpaired sex chromatin to bypass meiotic synapsis check points and is essential for meiotic progression in males (Baarends and Grootegoed, 2003a). Although neither the mechanism is fully understood, it is notable that the miRNA genes located on the X-chromosome evade MSCI, perhaps indicating a role for small RNAs in silencing (Song et al., 2009).

To examine the role of AGO4 in mammals, we generated an *Ago4* null mouse line. *Ago4*$^{-/-}$ mice are viable, but males have fertility defects including reduced testis size and lower sperm counts. AGO4 localizes to the SB during pachynema of prophase I, and loss of *Ago4* perturbs SB morphology leading to an

influx of RNA Polymerase II, and an associated failure to silence many sex-linked transcripts, resulting in apoptosis. Interestingly, our analysis also reveals an unexpected role for AGO4 in the onset of meiosis, in that spermatogonia from *Ago4*$^{-/-}$ males enter prophase I prematurely. These findings reveal a role for non-slicing Argonautes in mammalian germ cell development.

## 2.3 Results and Discussion

*AGO4 localizes to the sex body during prophase I of meiosis*

In adult mouse testis, *Ago4* mRNA expression is highest at prophase I during pachynema (Gonzalez-Gonzalez et al., 2008b), the stage at which homologous autosomes are completely synapsed (paired) and the SB is formed. AGO4 protein localization was assessed on chromosome-spread preparations from prophase I spermatocytes of WT adult male testes (day 70 pp), together with staining of the synaptonemal complex (SC) using antibodies against the lateral element protein, SYCP3 (Figure 1A). AGO4 staining was evident in the nucleus, with the most intense staining at the SB (Figure 1Aii), where it co-localizes with γH2AX (Figure 1Aiii). The AGO4 SB staining pattern was lost when the antibody was pre-incubated with the immunizing peptide, indicating specificity of the signal for AGO4 (Figure S1A) and no AGO4 staining was observed from *Ago4*-deficient males (Figure S1B,C). Only faint punctate staining was observed in oocytes (Figure 1B), which do not possess an SB.

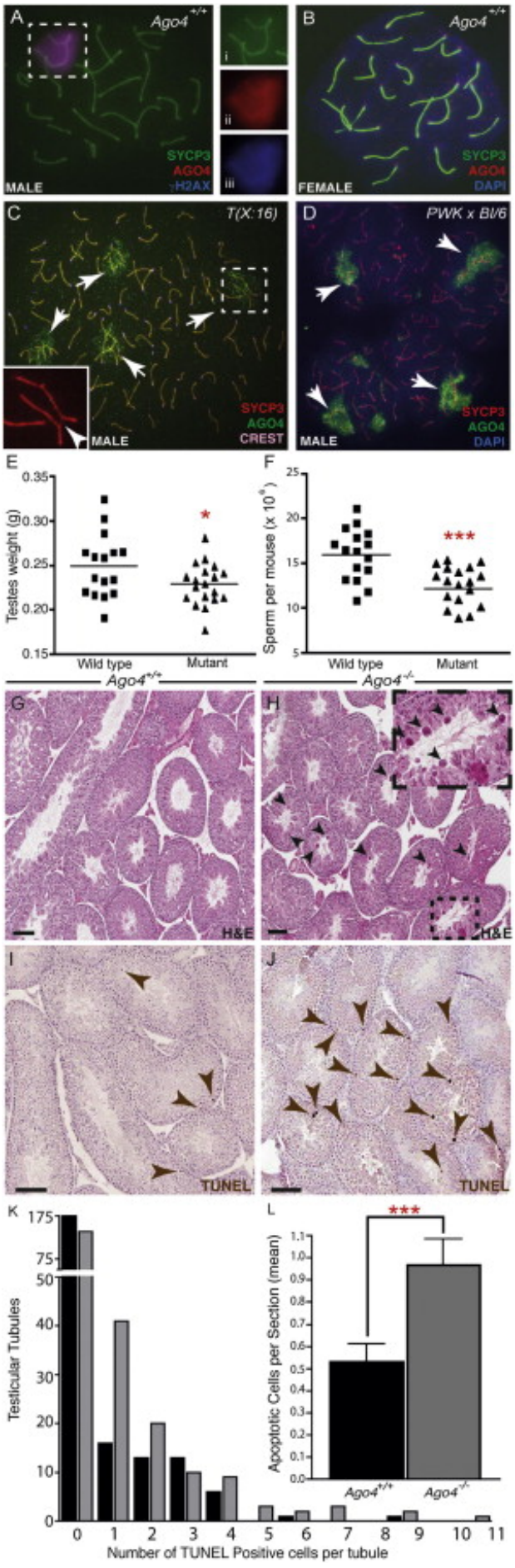


**Figure 1. AGO4 Localization and Phenotypic Analysis of *Ago4*$^{-/-}$ Males(A–D) AGO4 localization on chromosome spreads from wild-type (Nicolosi et al.) and induced asynaptic mouse models.** (A) Spermatocyte from a WT mouse stained with anti-SYCP3 (i, green), anti-AGO4 (ii, red), and anti-γH2AX (iii, blue). (B) Pachytene stage oocyte from WT mouse stained with anti-SYCP3 (green) and anti-AGO4 (red) antibodies and DAPI to highlight DNA (blue). (C and D) Pachytene stage spermatocytes from a T(X:16) male translocation mouse (C) and a PWK × C57BL/6J hybrid mouse (D) that both exhibit significant levels of asynapsis (arrows), stained with anti-SYCP3 (red), CREST autoimmune serum (pink localization on centromeres in C only), and anti-AGO4 (green) antibodies. Asynapsis induced by chromosome 16 to X translocation in (C) is marked by white arrowhead (inset). Dashed-line boxes in (A) and (C) identify the region that is further magnified in the corresponding inset panels.(E) Testes from *Ago4*$^{-/-}$ mice (n = 19) are significantly reduced in size compared to WT (n = 16; $^{*}p < 0.05$, t test).(F) Caudal epididymal sperm counts shown in millions. Sperm counts from *Ago4*$^{-/-}$ mice (▲ n = 19) are reduced when compared to WT (▪ n = 16; $^{***}p < 0.0005$, t test).(G and H) Testis sections from (G) *Ago4+/+* and (H) *Ago4*$^{-/-}$ mice with H&E. Scale bars, 100 μm. Large multinucleated cells are apparent in *Ago4*$^{-/-}$ mice (arrowheads and inset).(I and J) TUNEL staining and quantitation of testis sections from (I) *Ago4+/+* and (J) *Ago4*$^{-/-}$ mice.(K and L) *Ago4+/+* (black bars) and *Ago4*$^{-/-}$ mice (gray bars) expressed per tubule (K) or per section (L) showing significant increase in *Ago4*$^{-/-}$ mice (n = 230, 45.2% increase; $^{***}p < 0.0005$, t

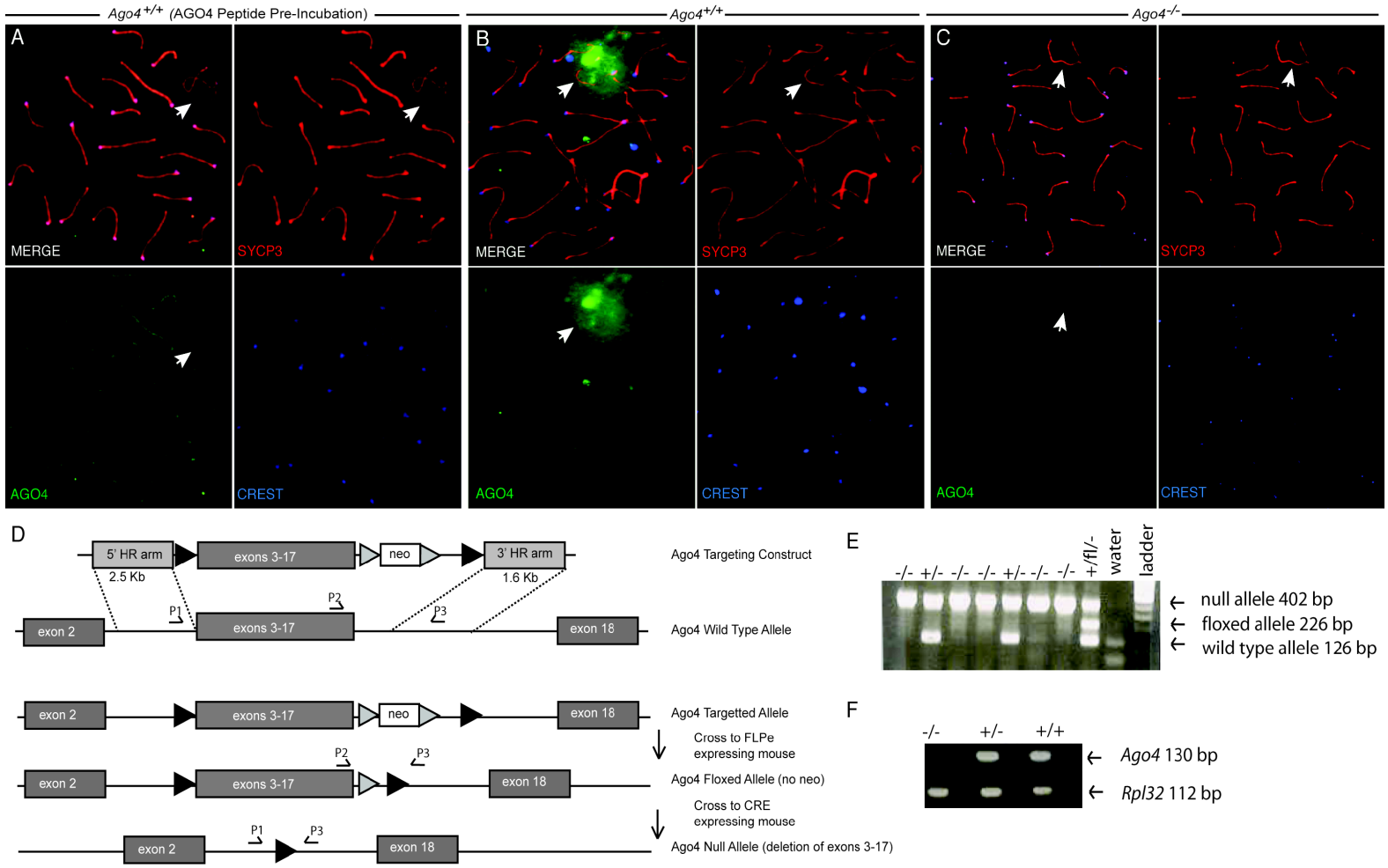
Ago4 +/+ (AGO4 Peptide Pre-Incubation)
Ago4+/+
Ago4-/-
A
B
C
MERGE
SYCP3
AGO4
CREST
D
5' HR arm
2.5 Kb
exons 3-17
neo
3' HR arm
1.6 Kb
exon 2
exon 18
P1
P2
P3
Ago4 Targeting Construct
Ago4 Wild Type Allele
Ago4 Targetted Allele
Cross to FLPe expressing mouse
Ago4 Floxed Allele (no neo)
Cross to CRE expressing mouse
Ago4 Null Allele (deletion of exons 3-17)
E
-/- +/- -/- -/- +/- -/- -/- +/fl/- water ladder
null allele 402 bp
floxed allele 226 bp
wild type allele 126 bp
F
-/- +/- +/+
Ago4 130 bp
Rpl32 112 bp

**Figure S1 Related to Figure 1: Pre-Incubation of AGO4 antibody with immunizing peptide abolishes AGO4 localization. An additional AGO4 antibody shows an identical pattern to the original antibody used, and is absent in *Ago4*$^{-/-}$ spermatocytes. Generation of *Ago4*$^{-/-}$ mouse via targeted deletion of *Ago4* exons 3-17.** Pachytene stage spermatocytes with SB (white arrows) from (A,B) *Ago4*$^{+/+}$ mice and (C) *Ago4*$^{-/-}$ mice stained with anti-AGO4 (green), anti-SYCP3 (red) and anti-CREST (blue). Chromosome spreads in which the AGO4 antibody was first incubated with the immunizing peptide (A) shows no apparent AGO4 signal. SYCP3 only image shows normal localization of synaptonemal complex (SC), typical of a pachytene stage spermatocyte. AGO4 only image displays SC-like staining pattern with a lack of sex-body localization, as previously seen with this antibody. Persistence of SC core staining and absence of SB staining suggests that the SB localization is the actual target of this antibody, while the SC staining is an artifact or a nonspecific localization pattern. CREST only image confirms that stained cells are pachytene, because only a single focus is detectable per chromosome core indicating complete synapsis of all chromosomes. An additional commercially available antibody (abcam ab52724) was used to demonstrate the localization pattern of AGO4 on (B) *Ago4*$^{+/+}$ chromosome spreads. As in Figure 1A, AGO4 localizes to the SB. This localization pattern is not observed in (C) *Ago4*$^{-/-}$chromosome spread preparations. (D) *Ago4* targeting construct, *Ago4* wild type (Nicolosi et al.) allele, *Ago4* floxed allele (no neo), and *Ago4* null allele (deletion of exons 3-17). The targeting construct was engineered using BAC recombination with BAC# RP23-260E11 as the backbone. The targeting construct was electroporated into ES cells (strain 129P2). Correctly targeted ES cells were injected into blastocysts and transferred to pseudo pregnant females. Chimeric mice were bred and germ line transmission obtained. Removing the neo cassette flanked by FRT sites (grey triangles) in *FLPe* transgenic mice produced the floxed allele (no neo) with LoxP sites (black triangles) flanking *Ago4* exons 3-17. Removing exons 3-17 in *Cre* transgenic mice produced the *Ago4* null allele. (E) PCR analysis of DNA from progeny of a *Cre* transgenic and an *Ago4* floxed allele cross used primers in (D) to detect the WT (P2-P3), floxed allele (P2-P3) and the recombined *Ago4* null allele (P1-P3). The 402 bp amplicon can only be amplified from the fully recombined allele as the positions of the primers spans over 25kb in WT mice. The floxed allele and WT allele amplicons are generated by primers P2 and P3 resulting in a 100 bp increase in amplicon in the floxed allele due to the presence of the LoxP site and a small amount of polylinker sequence. The +/fl/- genotype is generated from mice that have not undergone 100% recombination of the *Ago4* allele and were not used in further studies. (F) RT-PCR analysis of WT, heterozygous and *Ago4* null mice. The expected, 130 bp, *Ago4* amplicon is absent in *Ago4*$^{-/-}$ (Pittman et al.) mice and present in heterozygous and WT animals. Amplification of *Rpl32* served as a control for cDNA quality.

To explore whether the meiotic localization of AGO4 to the X and Y chromosomes is a consequence of their lack of pairing, we examined the localization of AGO4 in two mouse models displaying varying degrees of induced autosomal asynapsis in spermatocytes: mice carrying a TX(16:X)16H translocation (Figure 1C), or hybrid offspring of two divergent strains (PWKxB6, Figure 1D). In both cases, significant degrees of autosomal asynapsis were evident by the staining pattern for SYCP3 (Figure 1C Arrowhead), and AGO4 co-localized to all these sites (Figure 1C, D arrows). Given that these asynapsed regions of chromatin, are silenced during prophase I (Handel, 2004), these observations suggest a role for AGO4 in meiotic silencing.

*Loss of Ago4 results in reduced testis size and epididymal spermatozoa together with increased apoptosis of spermatogenic cells*

We generated a floxed *Ago4*$^{-/-}$ mouse line which, following Cre-driven excision of a *LoxP*-flanked region, lacks exons 3-17 of the gene (Figure S1D and Supplemental Experimental Procedures). The recombinant allele was backcrossed for six generations from the mixed 129/C57 background onto a pure C57Bl/6J background. Backcrossed homozygous *Ago4*$^{-/-}$ male and female mice were healthy and viable, and male and female offspring were observed at the expected frequencies (Male: 54%, Female: 46%, n=121). Furthermore, *Ago4*$^{-/-}$ males exhibit normal mating behavior with no decrease in litter sizes from *Ago4*$^{+/+}$ males (Supplemental Table 1). However, testis weights in *Ago4*$^{-/-}$ adult

mice were reduced by 13% compared to *Ago4*$^{+/+}$ mice (Figure 1E, Supplementary Table 1). Similarly, epididymal spermatozoa counts were also abnormal in *Ago4*$^{-/-}$ mice, reduced by 22% compared to WT littermates (Figure 1F, Supplemental Table 1).

| Observation and Metric | Mean | SEM | N | Significant | p Value (unpaired T Test) |
|---|---|---|---|---|---|
| ♂ *Ago4*$^{+/+}$ x 2 ♀ *Ago4*$^{-/-}$ Plug Date (days) | 1.7 | 0.3226 | 10 | no | 0.2051 |
| ♂ *Ago4*$^{-/-}$ x 2 ♀ *Ago4*$^{+/+}$ Plug Date (days) | 2.4 | 0.2631 | 7 | | |
| ♂ *Ago4*$^{+/+}$ x 2 ♀ *Ago4*$^{-/-}$ Litter Size (pups) | 8 | 0.7454 | 10 | no | 0.33 |
| ♂ *Ago4*$^{-/-}$ x 2 ♀ *Ago4*$^{+/+}$Litter Size (pups) | 6.9 | 0.8289 | 7 | | |
| *Ago4*$^{+/+}$ Body Weight (g) | 26.22 | 0.5077 | 16 | no | 0.1416 |
| *Ago4*$^{-/-}$ Body Weight (g) | 27.78 | 0.8514 | 19 | | |
| *Ago4*$^{+/+}$ Testes Weight (g) | 0.249 | 0.008872 | 16 | yes* | 0.0262 |
| *Ago4*$^{-/-}$ Testes Weight (g) | 0.2284 | 0.005407 | 19 | | |
| *Ago4*$^{+/+}$ Testes Weight (% of Animal Weight) | 0.9511 | 0.03271 | 16 | yes** | 0.0013 |
| *Ago4*$^{-/-}$ Testes Weight (% of Animal Weight) | 0.8298 | 0.02031 | 19 | | |
| *Ago4*$^{+/+}$ Sperm Count (x$10^6$) | 15.91 | 0.7172 | 16 | yes*** | 0.0004 |
| *Ago4*$^{-/-}$ Sperm Count (x$10^6$) | 12.11 | 0.6319 | 19 | | |
| *Ago4*$^{+/+}$ TUNEL count (cells per tubule) | 0.5313 | 0.08174 | 230 | yes*** | 0.0007 |
| *Ago4*$^{-/-}$ TUNEL count (cells per tubule) | 0.9696 | 0.1163 | 230 | | |

**Table S1 Related to Figure 1: Summary of phenotypic data for *Ago4*$^{+/+}$ and *Ago4*$^{-/-}$ littermate males at day 70 pp.**

*Testes from Ago4*$^{-/-}$ *males undergo increased apoptosis*

Histological analysis with H&E staining revealed similar cellular composition of the seminiferous epithelium in *Ago4*$^{+/+}$ and *Ago4*$^{-/-}$ males (Figure 1G-H). In the latter, however, we observed abnormally large, densely staining cells within the seminiferous tubular lumen (Figure 1H). TUNEL staining of testis

sections (Figure 1I-J) revealed a significant increase in apoptotic cells within the prophase I layers of the seminiferous epithelium of *Ago4*$^{-/-}$ mice compared to WT (Figure 1I,J, arrows; Figure 1K,L). These results demonstrate that *Ago4*$^{-/-}$ mice exhibit an increase in testicular apoptosis, reduced testes weight, and lowered sperm counts, phenotypes previously observed in MSCI-compromised animals (Turner et al., 2004).

*Loss of AGO4 results in increased AGO3 protein*

Given the high degree of sequence similarity (Cenik and Zamore, 2011), together with the high expression of *Ago3* in testis, we reasoned that overlapping functions might exist between mammalian Argonaute genes. Therefore, we used quantitative reverse transcription PCR (qRT-PCR) to measure the expression of all four AGO family members in testes of *Ago4*$^{+/+}$ and *Ago4*$^{-/-}$ mice. As expected, both *Ago3* and *Ago4* mRNA are highly expressed in adult testes, and at higher levels than in all other tissues examined (Figure 2A,B). *Ago1* was expressed at lower and more uniform levels throughout all of the tissues and *Ago2* expression was higher in non-meiotic tissues (Figure S2). Loss of *Ago4* resulted in a significant increase in *Ago3* expression specifically in testis (Figure 2B, $p<0.05$, t-test), while *Ago1* and *Ago2* transcripts were not affected by the loss of AGO4 (Figure S2). Together, these data suggest that *Ago3* and *Ago4* may function redundantly in the male germline, such that loss of *Ago4* results in a compensatory elevation in *Ago3* mRNA.

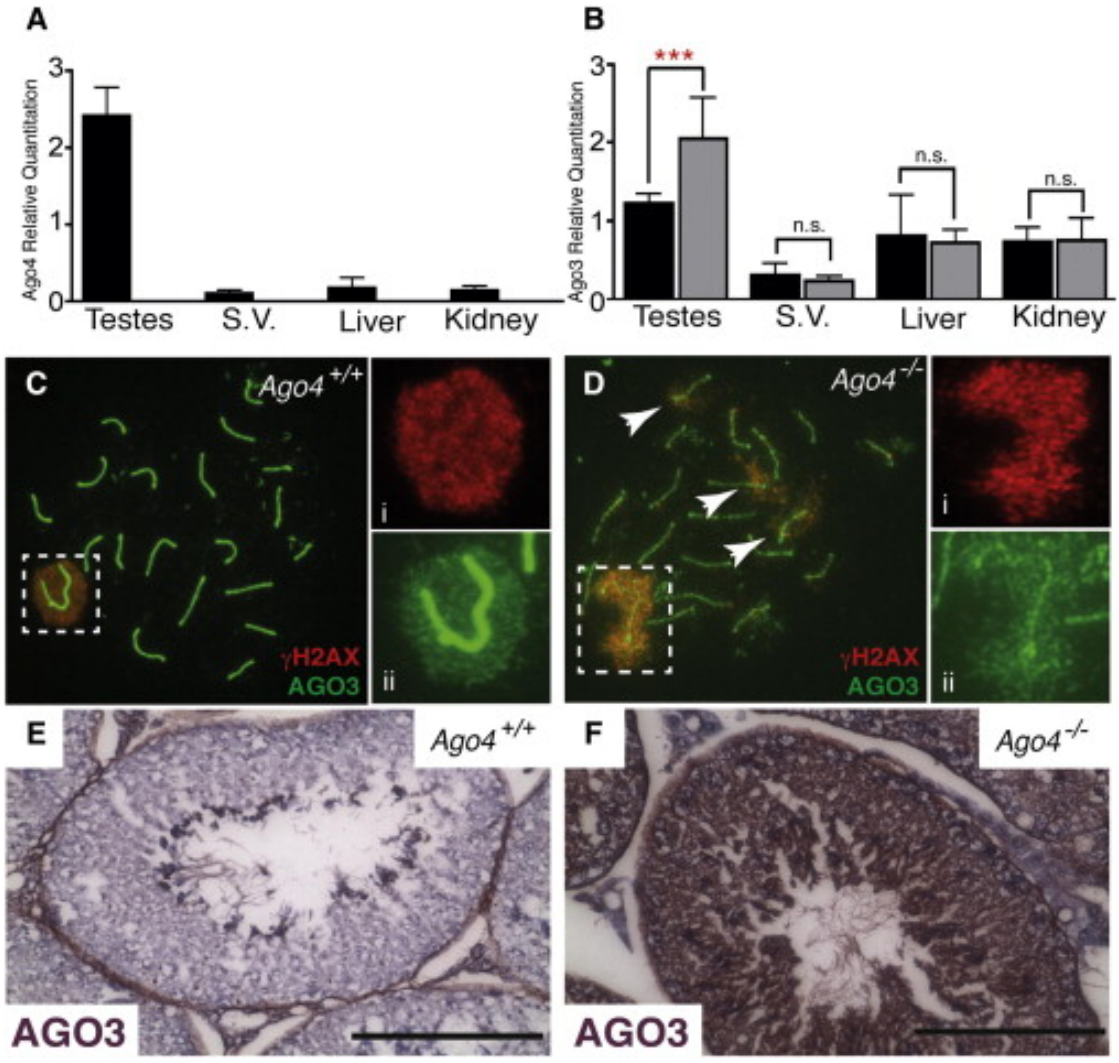


**Figure 2. Upregulation of *Ago3* mRNA and Protein in the Testis of *Ago4*$^{-}$/$^{-}$ Males.** (A and B) Quantitative RT-PCR analysis of *Ago4* (A) and *Ago3* (B) expression in total RNA from whole testes, seminal vesicle (S.V.), liver, and kidney isolated from *Ago4+/+* (n = 5, black bars) and *Ago4*$^{-}$/$^{-}$ (n = 5, gray bars) adult littermates (***p < 0.001, t test). Error bars, SEM. n.s., not significant.(C and D) Spermatocyte spreads from *Ago4+/+* (C) and *Ago4*$^{-}$/$^{-}$ (D) males stained with anti-γH2AX (red, Ci and Di) and anti-AGO3 (green, Cii and Dii) antibodies and DAPI (blue). "Pseudosex body" regions in (D) denoted by arrows. Dashed-line boxes identify the region that is further magnified in the corresponding inset panels. In both cases these boxes define the SB.(E and F) Testis sections from *Ago4+/+* (E) and *Ago4*$^{-}$/$^{-}$ (F) stained with anti-AGO3 antibody to demonstrate increased AGO3 signal within germ cells of *Ago4*$^{-}$/$^{-}$ males.See also Figure S2.

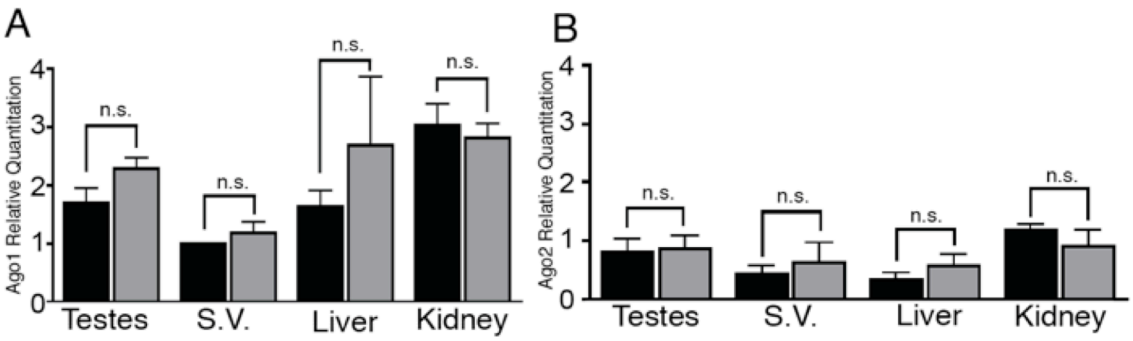


**Figure S2 related to Figure 2: *Ago1* and *Ago2* are not up-regulated in *Ago4* null testes.** Gene expression analysis of (A) *Ago1*, (B) *Ago2* from whole testes, seminal vesicle, liver and kidney total mRNA isolated from *Ago4*$^{+/+}$ (n=5, black bars) and *Ago4*$^{-/-}$ null (n=5, grey bars) littermates. Analysis indicates that no significant differential gene expression was found (student's unpaired t-test).

We next investigated whether AGO3 protein shows similar localization to AGO4 on male prophase I chromosome spreads. Like AGO4, AGO3 localized preferentially to the SB at pachynema in WT spreads (Figure 2Ci). When examining the AGO3 staining pattern on *Ago4*$^{-/-}$ spreads, however, we found that the chromatin domain occupied by AGO3 signal was dramatically expanded (Figure 2D). Indeed, both AGO3 and γH2AX extended beyond the SB into areas of chromatin associated with the autosomes (Figure 2D, arrows). In mouse mutants that exhibit similar disruption of the SB appearance, these extended γH2AX domains have been termed "pseudo-sex bodies" (Barchi et al., 2005; Bellani et al., 2005; Daniel et al., 2011).

AGO3 localization was also assessed by immunohistochemistry of whole testis sections from *Ago4*$^{+/+}$ and *Ago4*$^{-/-}$ adult males. In WT testis, AGO3 localized to meiotic cells and was absent in the non-meiotic spermatogonial cells (Figure 2E). In *Ago4*$^{-/-}$ testis, AGO3 signal was increased (Figure 2F), as expected, but still

restricted to spermatogenic cells. Thus, the loss of *Ago4* results in increased expression of *Ago3* in the testis. We conclude that some functions of AGO4 in the male germline may be redundant with AGO3 and, if so, this would imply that the testis weight and sperm count phenotypes observed in *Ago4*$^{-/-}$ mice result from only a partial defect in these shared functions.

*Loss of AGO4 disrupts sex body formation and alters the localization of key sex body components*

To examine more closely the SB morphology of *Ago4*$^{-/-}$ males, we investigated the localization of the SC central element protein, SYCP1, together with SYCP3 during prophase I (Figure 3A). In *Ago4*$^{-/-}$ spreads, SYCP1 localized to unsynapsed regions of the X and Y (Figure 3B) approximately 4-fold more frequently than in the WT (Figure 3C, *Ago4*$^{+/+}$ 6.3%. *Ago4*$^{-/-}$ 22.8% of 300 pachytene spermatocytes, $p<0.0005$, $\chi^2$-test), indicating that loss of AGO4 perturbs SC formation and/or integrity. Importantly, initial events of prophase I progression, including the processing of double strand breaks for recombination, and crossover formation, appeared normal in *Ago4*$^{-/-}$ males (data not shown). The mislocalization of SC components in the *Ago4*$^{-/-}$ SB, together with the importance of SB integrity for meiotic sex chromosome inactivation (MSCI), led us to hypothesize that AGO4 may play a role in transcriptional silencing of the X

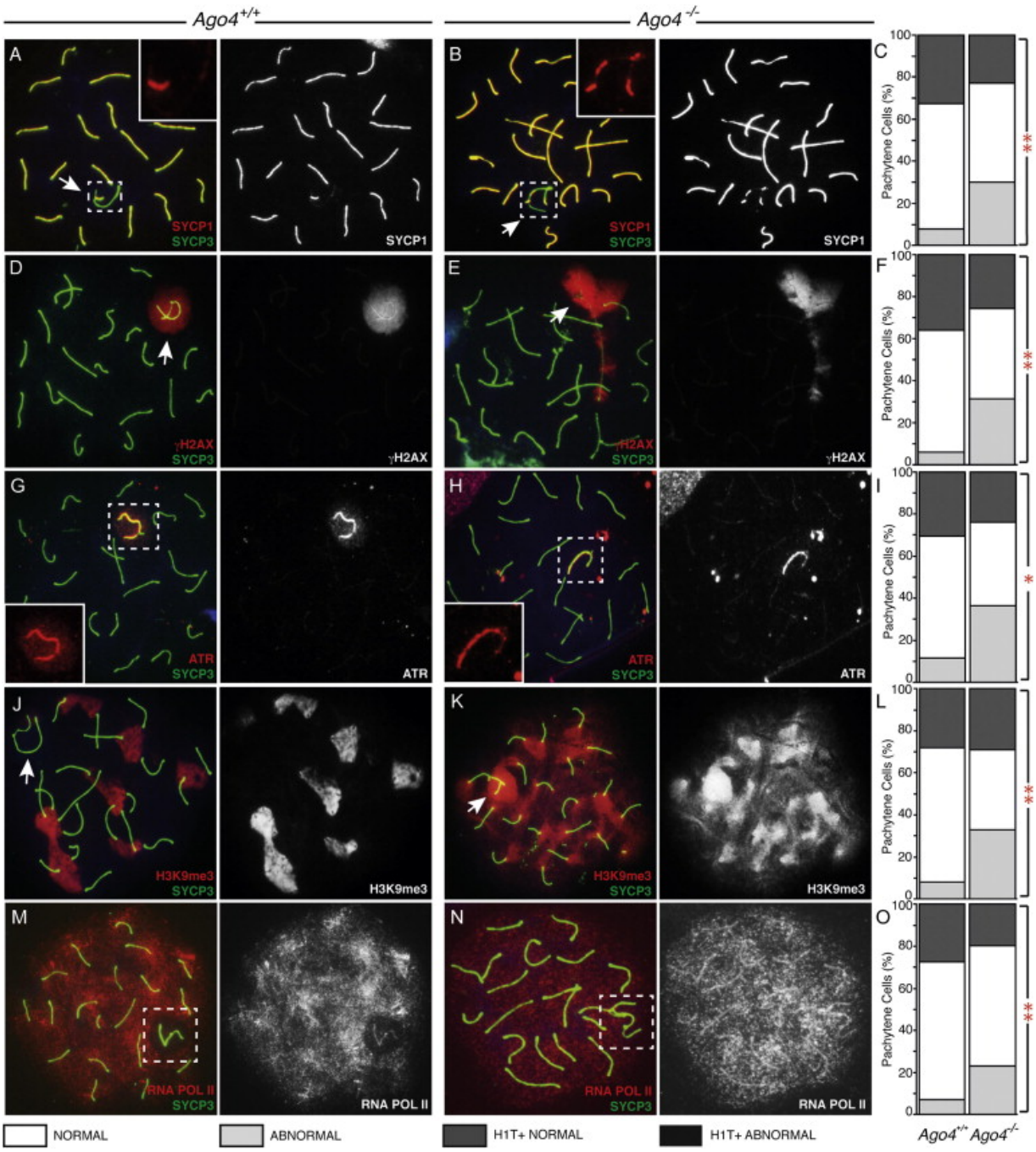


**Figure 3. Loss of AGO4 Disrupts Localization of SB-Associated Proteins and RNAP II during Pachynema** Pachytene stage spermatocytes with SB (white arrows) from *Ago4+/+* (A, D, G, J, and M) and *Ago4*$^{-}$*/*$^{-}$ (B, E, H, K, and N) mice, stained with anti-SYCP3 (green). For all quantitation graphs (C, F, I, L, and O), WT (left bar) and *Ago4*$^{-}$*/*$^{-}$ (right bar).(A–C) SYCP1 in red. Insets show magnification of SYCP1 in SB (n = 300 per genotype; $^{**}p < 0.005$, $\chi^2$ test).(D–F) γH2AX in red (n = 300; $^{**}p < 0.005$, $\chi^2$ test).(G–I) ATR in red (n = 200; $^{*}p < 0.05$, $\chi^2$ test).(J–L) H3K9Me3 in red (n = 300; $^{**}p < 0.005$, $\chi^2$ test).(M–O) RNAP II staining in red (n = 200; $^{**}p < 0.01$, $\chi^2$ test).See also Figure S3.

and Y chromosomes. To test this, we utilized a repertoire of antibodies (γH2AX, TOPBP1, ATR, pCHK2, SUMO1, UbiH2A) against SB components to assess the integrity and functionality of this structure. The histone variant H2AX (Histone 2A family member X) is phosphorylated during prophase I by the ATM and ATR kinases to become γH2AX (Turner et al., 2004). SB-associated H2AX phosphorylation is mediated by ATR during pachynema, a stage at which γH2AX is found almost exclusively in the SB and at any remaining asynapsed regions on autosomes (Figure 3D). However, a large proportion of *Ago4*$^{-/-}$ pachytene cells (Figure 3E,F, 31% versus 5.5% in WT; n=300, $p<0.0005$, $\chi^2$-test), exhibit expanded γH2AX staining beyond the SB, often associating with synapsed autosomes, or pseudo-sex-bodies. The localization of γH2AX during diplonema is unaffected by loss of AGO4 (data not shown), and in fact, such defects appear to be restricted to early pachytene spermatocytes. To illustrate this, we used an antibody against the testis specific histone variant H1T, which localizes to chromatin from late pachynema (Lin et al., 2000). We found no instances in which the altered pseudo-SB staining of γH2AX, or other SB markers, coincided with the appearance of H1T in late pachytene or diplotene cell populations (*Ago4*$^{+/+}$ n=289, *Ago4*$^{-/-}$ n=241 Figure S3K,L,M). Together, these results suggest that the SB morphology defects occur in early pachynema in *Ago4*$^{-/-}$ mice. Defective *Ago4*$^{-/-}$ spermatocytes are likely to be eliminated by the pachytene checkpoint, as evidenced by the increased TUNEL staining.

One explanation for aberrant γH2AX localization in *Ago4*$^{-/-}$ mice is failure to recruit ATR, which we investigated by staining for both ATR and TopBP1, a regulator of ATR (Kumagai et al., 2006). In WT mice, ATR staining is pronounced on the X and Y chromosome cores and through the SB starting from pachynema (Figure 3G). In *Ago4*$^{-/-}$ pachytene cells, however, ATR is frequently mislocalized (Figure 3H,I, n=200 cells, $p<0.0005$, $\chi^2$-test). A range of aberrant staining patterns were observed, including a complete loss of signal at the SB, reduced X chromosome core localization, and almost complete loss of Y chromosome core localization. TopBP1 localization is similarly altered by the loss of *Ago4* (Figure S3A,B). The loss of ATR at the SB coincides with increased signal on autosome cores, potentially utilizing the limited store of ATR that would normally be required to induce MSCI.

We corroborated ATR mislocalization in *Ago4*$^{-/-}$ mice using an antibody against the phospho-(Ser/Thr)ATM/ATR substrate motif (Figure S3C) and an antibody specific to phosphorylated CHK2 (Weiss et al., 2002), a substrate of ATM/ATR (Figure S3E). In both cases, ATM/ATR substrate and pCHK2 were absent in pachytene spermatocyte spreads from *Ago4*$^{-/-}$ mice (Figure S3D and S3F).

SUMO1 and ubiH2A are proteins implicated in meiotic silencing (Brown et al., 2008; Vigodner, 2009). SUMO1 first appears in zygonema localizing to the X and Y cores (not shown) and persists into pachynema (Figure S3G). During pachynema, the ubiH2A histone mark emerges and localizes

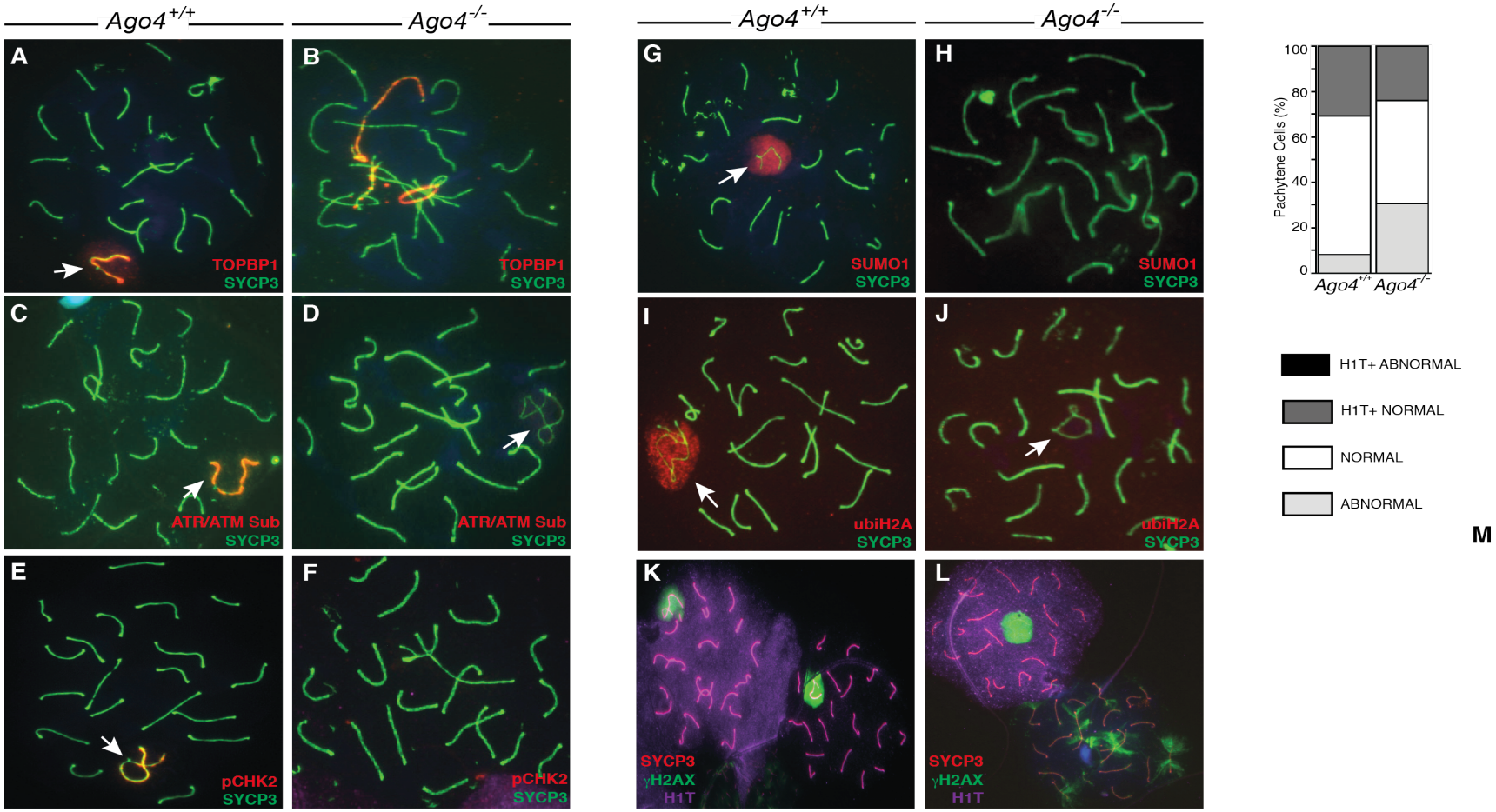
Ago4+/+
Ago4-/-
A
TOPBP1
SYCP3
B
TOPBP1
SYCP3
C
ATR/ATM Sub
SYCP3
D
ATR/ATM Sub
SYCP3
E
pCHK2
SYCP3
F
pCHK2
SYCP3
Ago4+/+
Ago4-/-
G
SUMO1
SYCP3
H
SUMO1
SYCP3
I
ubiH2A
SYCP3
J
ubiH2A
SYCP3
K
SYCP3
γH2AX
H1T
L
SYCP3
γH2AX
H1T
100
80
60
40
20
0
Pachytene Cells (%)
Ago4+/+
Ago4-/-
H1T+ ABNORMAL
H1T+ NORMAL
NORMAL
ABNORMAL
M

**Figure S3 related to Figure 3: Loss of AGO4 disrupts localization of SB associated proteins in early pachytene.** Pachytene stage spermatocytes with SB (white arrows) from *Ago4*$^{+/+}$ (A, C, E, G, I) and *Ago4*$^{-/-}$ (B, D, F, H, J) mice stained with anti-SYCP3 (green). TOPBP1 (red) localizes to the X and Y cores during pachynema (A). In the *Ago4*$^{-/-}$ spermatocytes (B), this pattern is largely maintained however there are additional TOPBP1 positive cores. Much like ATR, the anti-ATM/ATR substrate staining (red) localizes to the XY cores during pachynema (C). In the *Ago4*$^{-/-}$ spermatocytes (D), however, the localization pattern is absent. A specific target of ATR/ATM, pCHK2 (red), localizes to the XY cores during pachynema (E). In the *Ago4*$^{-/-}$spermatocytes (F), however, this localization is also absent. SUMO1 (red) localizes to the SB during pachynema (G), in a pattern similar to γH2AX. In the *Ago4*$^{-/-}$ spermatocytes (H), the localization pattern is absent. While concentrated to the X and Y cores in WT (I), the ubiH2A (red) pattern is absent in *Ago4*$^{-/-}$ spermatocytes (J). Pachytene stage spermatocytes from *Ago4*$^{+/+}$ (K) and *Ago4*$^{-/-}$ (L) mice stained with anti-SYCP3 (red), anti-γH2AX (green) and anti-H1T (purple): H1T localizes specifically to chromosomes found in mid-late pachynema, diplonema and persists until the elongated spermatid stage. (K) Both early (lower cell) and late (higher cell) pachytene cells are shown. Only the late, (higher) cell is positive for H1T. In the *Ago4*$^{-/-}$ pachytene spermatocytes (L), H1T localizes specifically to the late (higher) cell while absent from the early (lower) cell, which displays a substantial level of γH2AX mislocalization. The co-localization of H1T and altered (pseudo) sex bodies was never observed in H1T positive pachytene cells. (M) *Ago4*$^{+/+}$: n=289, *Ago4*$^{-/-}$: n=241.

to the SB (Figure S3I; (Baarends et al., 2005). SUMO1 and ubiH2A localization is abolished in a subset of *Ago4*$^{-/-}$ cells (Figures 3H,J). Together, these studies reveal that a subset of spermatocytes in *Ago4*$^{-/-}$ males fail to assemble a normal SB structure, leading to the appearance of pseudo-sex bodies and mislocalization of key SB markers.

*Ago4*$^{-/-}$ *mice fail to correctly silence the X and Y chromosomes during meiosis.*

The defects we observed in SB components prompted us to determine whether silencing of the sex chromosomes during meiosis was normal in the absence of AGO4. The tri-methylation modification of H3K9 is associated with repressed heterochromatinized DNA. During prophase I in WT male mice, H3K9me3 is primarily restricted to autosomal centromeres and the majority of the SB (Kim et al., 2007; Tachibana et al., 2007); Figure 3J). In early pachynema, loss of *Ago4* results in diffuse H3K9me3 localization in a significant portion of cells (Figure 3K,L; n=300. $P<0.0005$, $\chi^2$-test). These results suggest that AGO4 contributes to the establishment of chromatin marks associated with silencing, but as meiosis progresses aberrant cells are either eliminated or overcome the defect.

To further assess transcriptional activity of the sex chromosomes, we compared the localization of RNA Polymerase II (RNAP II) in WT and *Ago4*$^{-/-}$ pachytene spermatocytes. As expected, in *Ago4*$^{+/+}$ cells, RNAP II is absent from sites of silencing and heterochromatin (Figure 3M) and is excluded from the SB

through pachynema. This exclusion is no longer maintained in a significant fraction of pachytene spermatoctyes from *Ago4*$^{-/-}$ males (Figure 3N,O, *Ago4*$^{+/+}$*:* 7%, *Ago4*$^{-/-}$*:* 25.5% n=200. $p<0.0005$, $\chi^2$-test), matching the frequency of mislocalization we observed for SB components and further indicating a silencing defect in *Ago4*$^{-/-}$ spermatocytes.

*Loss of Ago4 leads to down-regulation of specific microRNA families.*

Since Argonaute proteins function with small RNAs, we hypothesized that the phenotypes in *Ago4*$^{-/-}$ animals reflect alterations in the small RNAs. We therefore cloned and sequenced small RNAs (18-30 nts) from purified pachytene cells isolated from *Ago4*$^{+/+}$ and *Ago4*$^{-/-}$ littermates. We obtained 21.2 and 14.7 million genome-matching reads from the *Ago4*$^{+/+}$ and *Ago4*$^{-/-}$ samples, respectively, a sequencing depth sufficient to robustly profile the small RNAs of pachytene cells.

piRNAs are the most abundant small RNAs in pachytene cells (Pillai and Chuma, 2012; Siomi et al., 2011), and loss of *Ago4* only minimally perturbed these piRNA populations (Figure S4F,G), as expected. By contrast, loss of *Ago4* had a substantial effect on the miRNAs present in pachytene cells. Overall, we observed an approximately 2.3-fold reduction (Figure 4 and S4) in reads matching miRNA hairpins in *Ago4*$^{-/-}$ pachytene cells (Fig 4A and 4A; 6% *Ago4*$^{+/+}$, 2.6%*Ago4*$^{-/-}$). However, this reduction was not consistent among different miRNA families, indicating some degree of miRNA specificity for AGO4 (Fig 4C-D,S4C-D,

S5). Approximately 20% of the global miRNA down-regulation came from miRNAs expressed from the X chromosome, and interestingly, all miRNAs

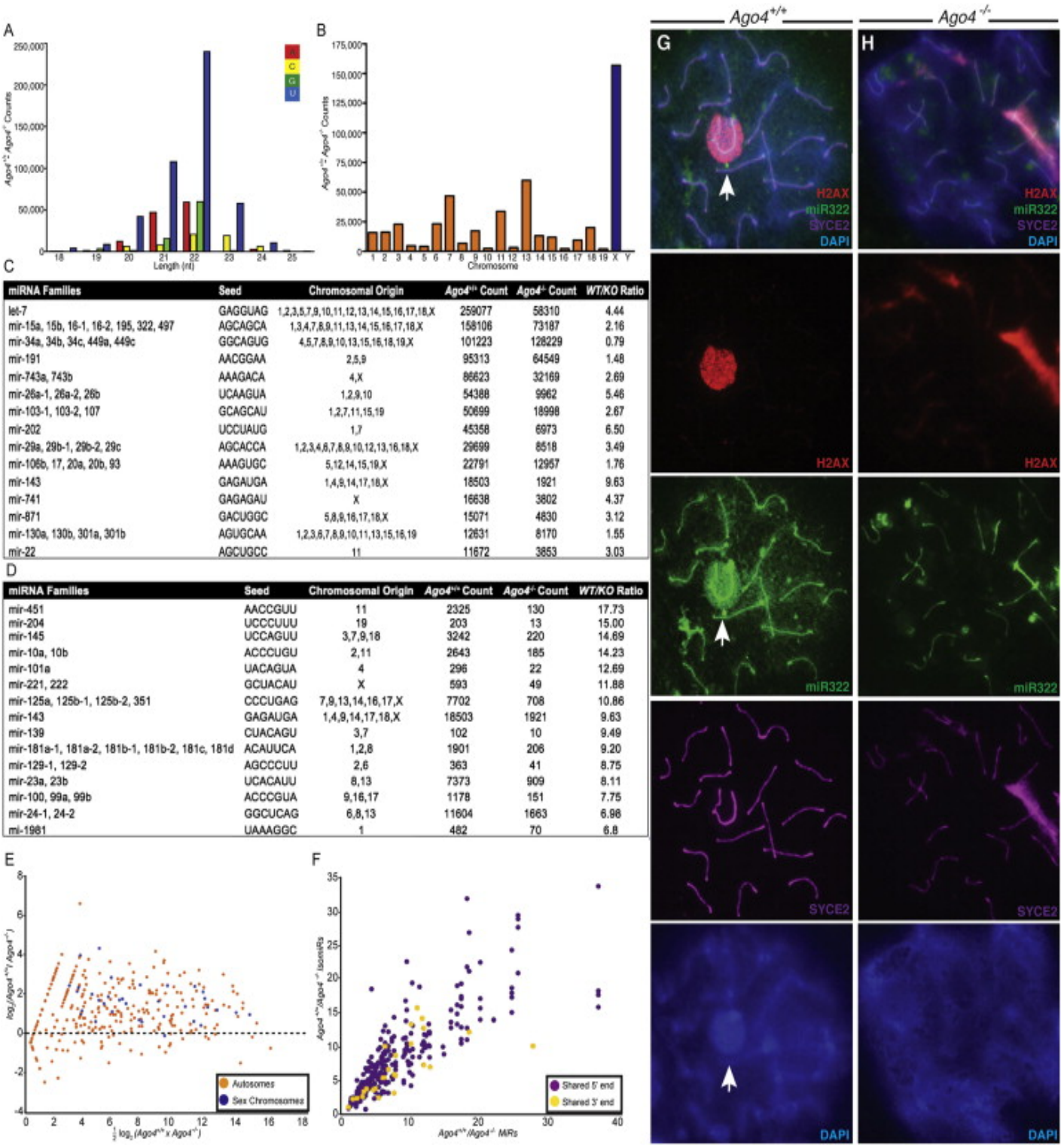


| miRNA Families | Seed | Chromosomal Origin | Ago4+/+ Count | Ago4-/- Count | WT/KO Ratio |
|---|---|---|---|---|---|
| let-7 | GAGGUAG | 1,2,3,5,7,9,10,11,12,13,14,15,16,17,18,X | 259077 | 58310 | 4.44 |
| mir-15a, 15b, 16-1, 16-2, 195, 322, 497 | AGCAGCA | 1,3,4,7,8,9,11,13,14,15,16,17,18,X | 158106 | 73187 | 2.16 |
| mir-34a, 34b, 34c, 449a, 449c | GGCAGUG | 4,5,7,8,9,10,13,15,16,18,19,X | 101223 | 128229 | 0.79 |
| mir-191 | AACGGAA | 2,5,9 | 95313 | 64549 | 1.48 |
| mir-743a, 743b | AAAGACA | 4,X | 86623 | 32169 | 2.69 |
| mir-26a-1, 26a-2, 26b | UCAAGUA | 1,2,9,10 | 54388 | 9962 | 5.46 |
| mir-103-1, 103-2, 107 | GCAGCAU | 1,2,7,11,15,19 | 50699 | 18998 | 2.67 |
| mir-202 | UCCUAUG | 1,7 | 45358 | 6973 | 6.50 |
| mir-29a, 29b-1, 29b-2, 29c | AGCACCA | 1,2,3,4,6,7,8,9,10,12,13,16,18,X | 29699 | 8518 | 3.49 |
| mir-106b, 17, 20a, 20b, 93 | AAAGUGC | 5,12,14,15,19,X | 22791 | 12957 | 1.76 |
| mir-143 | GAGAUGA | 1,4,9,14,17,18,X | 18503 | 1921 | 9.63 |
| mir-741 | GAGAGAU | X | 16638 | 3802 | 4.37 |
| mir-871 | GACUGGC | 5,8,9,16,17,18,X | 15071 | 4830 | 3.12 |
| mir-130a, 130b, 301a, 301b | AGUGCAA | 1,2,3,6,7,8,9,10,11,13,15,16,19 | 12631 | 8170 | 1.55 |
| mir-22 | AGCUGCC | 11 | 11672 | 3853 | 3.03 |

| miRNA Families | Seed | Chromosomal Origin | Ago4+/+ Count | Ago4-/- Count | WT/KO Ratio |
|---|---|---|---|---|---|
| mir-451 | AACCGUU | 11 | 2325 | 130 | 17.73 |
| mir-204 | UCCCUUU | 19 | 203 | 13 | 15.00 |
| mir-145 | UCCAGUU | 3,7,9,18 | 3242 | 220 | 14.69 |
| mir-10a, 10b | ACCCUGU | 2,11 | 2643 | 185 | 14.23 |
| mir-101a | UACAGUA | 4 | 296 | 22 | 12.69 |
| mir-221, 222 | GCUACAU | X | 593 | 49 | 11.88 |
| mir-125a, 125b-1, 125b-2, 351 | CCCUGAG | 7,9,13,14,16,17,X | 7702 | 708 | 10.86 |
| mir-143 | GAGAUGA | 1,4,9,14,17,18,X | 18503 | 1921 | 9.63 |
| mir-139 | CUACAGU | 3,7 | 102 | 10 | 9.49 |
| mir-181a-1, 181a-2, 181b-1, 181b-2, 181c, 181d | ACAUUCA | 1,2,8 | 1901 | 206 | 9.20 |
| mir-129-1, 129-2 | AGCCCUU | 2,6 | 363 | 41 | 8.75 |
| mir-23a, 23b | UCACAUU | 8,13 | 7373 | 909 | 8.11 |
| mir-100, 99a, 99b | ACCCGUA | 9,16,17 | 1178 | 151 | 7.75 |
| mir-24-1, 24-2 | GGCUCAG | 6,8,13 | 11604 | 1663 | 6.98 |
| mi-1981 | UAAAGGC | 1 | 482 | 70 | 6.8 |

**Figure 4. Loss of *Ago4* Results in Loss of miRNAs Originating from Chromosome X and Wide-Scale Alterations in the Expression of Most miRNA Families** (A) The difference between miRNAs cloned from pachytene cells of WT and*Ago4*$^{-}$/$^{-}$ males, distributed by miRNA length and base identity of the most 5′ nucleotide.(B) For miRNAs with a single chromosomal origin, the difference between WT and mutant counts of these miRNAs is shown by chromosome (autosomes in orange; X chromosome in blue).(C and D) miRNA families, grouped by common "seed" (nucleotides 2–7), with the highest expression in WT pachytene cells (C) and those showing the largest decrease in expression in the*Ago4*$^{-}$/$^{-}$ (D).(E) MA plot showing the intensity of expression (x axis) versus change in expression (y axis) for WT and mutant miRNAs reveals a preferential decrease in miRNA levels in the mutant for miRNAs originating from the sex chromosomes.(F) Comparison of the ratio of WT to mutant miRNA counts between each miRNA and other variant species derived from the same hairpin.(G and H) miRNA fluorescence in situ hybridization for miR-322 using pachytene stage spermatocytes from *Ago4+/+* (G) and *Ago4*$^{-}$/$^{-}$ (H) mice stained with anti-γH2AX (red), anti-SYCE2 (purple), and DAPI (blue).See also Figures S4 and S5 and Table S2.

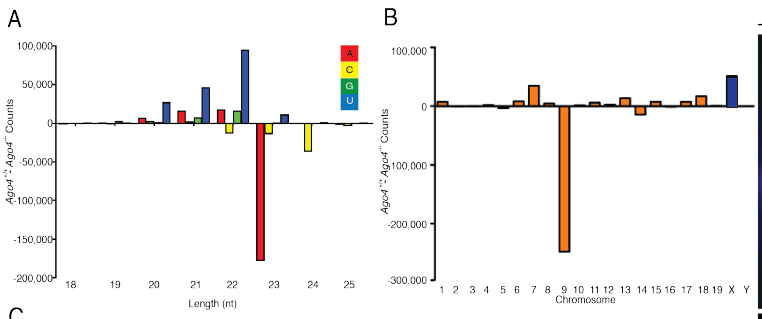


C

| miRNA Families | Seed | Chromosomal Origin | *Ago4*$^{+/+}$ Count | *Ago4*$^{-/-}$ Count | *WT/KO* Ratio |
|---|---|---|---|---|---|
| let-7 | GAGGUAG | 1,2,3,5,7,9,10,11,12,13,14,15,16,17,18,X | 259077 | 139111 | 1.86 |
| mir-15a, 15b, 16-1, 16-2, 195, 322, 497 | AGCAGCA | 1,3,4,7,8,9,11,13,14,15,16,17,18,X | 158106 | 174604 | 0.91 |
| mir-34a, 34b, 34c, 449a, 449c | GGCAGUG | 4,5,7,8,9,10,13,15,16,18,19,X | 101223 | 305917 | 0.33 |
| mir-191 | AACGGAA | 2,5,9 | 95313 | 153995 | 0.62 |
| mir-743a, 743b | AAAGACA | 4,X | 86623 | 76747 | 1.13 |
| mir-26a-1, 26a-2, 26b | UCAAGUA | 1,2,9,10 | 54388 | 23767 | 2.29 |
| mir-103-1, 103-2, 107 | GCAGCAU | 1,2,7,11,15,19 | 50699 | 45324 | 1.13 |
| mir-202 | UCCUAUG | 1,7 | 45358 | 16637 | 2.73 |
| mir-29a, 29b-1, 29b-2, 29c | AGCACCA | 1,2,3,4,6,7,8,9,10,12,13,16,18,X | 29699 | 20321 | 1.46 |
| mir-106b, 17, 20a, 20b, 93 | AAAGUGC | 5,12,14,15,19,X | 22791 | 30912 | 0.74 |
| mir-143 | GAGAUGA | 1,4,9,14,17,18,X | 18503 | 4584 | 4.04 |
| mir-741 | GAGAGAU | X | 16638 | 9071 | 1.83 |
| mir-871 | GACUGGC | 5,8,9,16,17,18,X | 15071 | 11524 | 1.31 |
| mir-130a, 130b, 301a, 301b | AGUGCAA | 1,2,3,6,7,8,9,10,11,13,15,16,19 | 12631 | 19491 | 0.65 |
| mir-22 | AGCUGCC | 11 | 11672 | 9192 | 1.27 |

D

| miRNA Families | Seed | Chromosomal Origin | *Ago4*$^{+/+}$ Count | *Ago4*$^{-/-}$ Count | *WT/KO* Ratio |
|---|---|---|---|---|---|
| mir-451 | AACCGUU | 11 | 2325 | 311 | 7.46 |
| mir-204 | UCCCUUU | 19 | 203 | 30 | 6.57 |
| mir-145 | UCCAGUU | 3,7,9,18 | 3242 | 524 | 6.17 |
| mir-10a, 10b | ACCCUGU | 2,11 | 2643 | 441 | 5.98 |
| mir-101a | UACAGUA | 4 | 296 | 53 | 5.46 |
| mir-221, 222 | GCUACAU | X | 593 | 117 | 5.04 |
| mir-125a, 125b-1, 125b-2, 351 | CCCUGAG | 7,9,13,14,16,17,X | 7702 | 1690 | 4.55 |
| mir-143 | GAGAUGA | 1,4,9,14,17,18,X | 18503 | 4584 | 4.04 |
| mir-139 | CUACAGU | 3,7 | 102 | 23 | 4.20 |
| mir-181a-1, 181a-2, 181b-1, 181b-2, 181c, 181d | ACAUUCA | 1,2,8 | 1901 | 491 | 3.87 |
| mir-129-1, 129-2 | AGCCCUU | 2,6 | 363 | 97 | 3.72 |
| mir-23a, 23b | UCACAUU | 8,13 | 7373 | 2168 | 3.40 |
| mir-100, 99a, 99b | ACCCGUA | 9,16,17 | 1178 | 361 | 3.26 |
| mir-574 | ACGCUCA | 5 | 34 | 10 | 3.18 |
| mir-409 | GGUUACC | 12 | 53 | 17 | 3.05 |

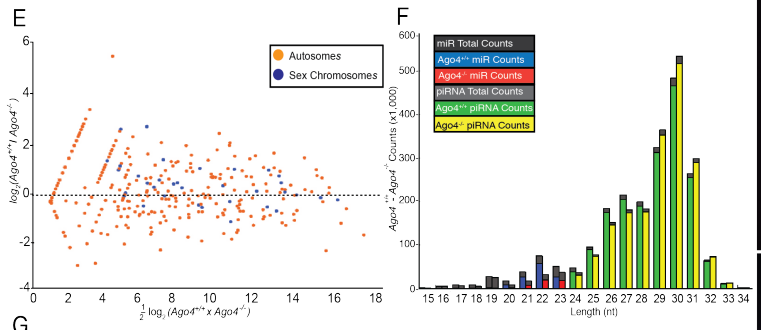


G

| | *Ago4*$^{+/+}$ Counts | % Total or Genome Derived | *Ago4*$^{-/-}$ Counts | % Total or Genome Derived |
|---|---|---|---|---|
| Quality Reads Sequenced | 28929223 | | 20182569 | |
| Genome Derived Reads | 21194467 | 73.3 | 14656855 | 72.6 |
| miRNAs | 1275849 | 6.0 | 381771 | 2.6 |
| piRNAs | 15994110 | 75.5 | 11788558 | 80.4 |
| rRNAs | 75439 | 0.4 | 10271 | 0.1 |

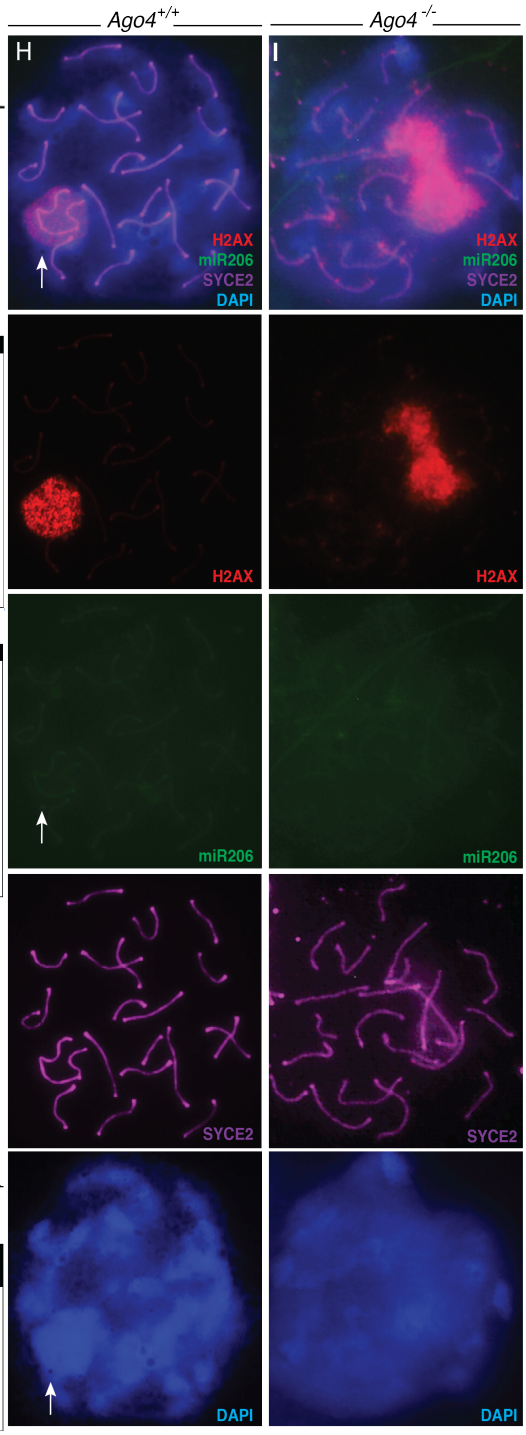

**Figure S4 related to Figure 4: Alternative normalization of miRNA data, length distribution of pachytene small RNA populations and Fluorescence *in* situ hybridization for miRNA 206.** Normalization of sequenced libraries allows for comparisons of small RNA populations between samples, and numerous methods of normalization for small RNA sequencing libraries exist. For all data presented in the text, we chose to normalize the mutant read counts to the total genome-matching WT counts, a method which assumes proportionality between the two libraries and allows for the relative small RNA species compositions of the two samples, WT and knock-out, to be compared. Here, we present a re-analysis of the data in Figure 4A-E. In Figure 4, mutant miRNAs and all other read counts are normalized to total genome-matching WT counts, whereas in this supplemental figure all counts for sequenced mutant miRNAs are normalized to the counts for WT miRNAs (the WT miRNA count was 3.34 times that of the knock-out). This internal normalization within the sequenced miRNAs better highlights the redistribution of the miRNA population in the knock-out as compared to the WT. (A) The difference between microRNAs in the WT and *Ago4*$^{-/-}$, shown by subtracting the mutant counts from the WT and distributed by microRNA length and base identity of the most 5′ nucleotide, shows populations of microRNAs lost or gained in the mutant relative to WT. (B) For microRNAs with a single chromosomal origin, the difference between WT and mutant counts of these microRNAs is shown by chromosome. (C) and (D) microRNA families, grouped by common 'seed' (nucleotides 2-7), with the highest expression in WT pachytene cells (C) and those showing the largest decrease in expression in the *Ago4*$^{-/-}$ (D) are shown with their family seed sequence, the total WT and *Ago4*$^{-/-}$ counts, and the ratio of WT to mutant counts. An MA plot (E) showing the intensity of expression (x-axis) versus change in expression (y-axis) for WT and mutant. Another method for normalization, based on the assumption that AGO4, as an Argonaute protein, would interact with miRNAs and siRNAs but not piRNAs, would be to normalize to the total number of piRNA counts in each sample; because the percent of piRNAs in both populations is roughly equal, normalization by this method is virtually identical to normalization by total genome-matching reads (seen in Figure 4).

All genome matching small RNAs isolated and sequenced from WT and *Ago4*$^{-/-}$ pachytene spermatocytes are shown here distributed by length (F). Reads identified computationally as miRNAs (WT: blue, knock-out: red) make up approximately 6% and 2.6% of the total WT and knock-out small RNA population, and piRNAs (WT: green, knock-out: yellow) constitute 75% and 80%, respectively, of the total population. A small number of reads also matched ribosomal RNA: 0.4% and 0.1% from the WT and *Ago4*$^{-/-}$ samples, respectively.

encoded on the X are significantly less abundant ($p<0.01$; Wilcoxon-rank sum test) in *Ago4*$^{-/-}$ cells whereas not all autosomal miRNAs are decreased (Fig 4B-E, S4B-E).

We considered two explanations for the alterations in the miRNA profile of *Ago4*$^{-/-}$ cells. First, AGO proteins might associate with miRNAs at different efficacies, thus, in the absence of AGO4, the sequenced miRNAs would represent the propensities of AGO1, AGO2 and AGO3 to form complexes with specific miRNAs. Second, the altered profile might be a downstream consequence of altered transcriptional regulation of miRNA genes. To distinguish between these possibilities, we compared the change in abundance for each mature miRNA sequence to each variant miRNA sequence originating from the same precursor. The normal processing of miRNA precursors (Ruby et al., 2006; Ruby et al., 2007) results in the production of a mature miRNA species together with rarer shorter or longer variant miRNAs. Such variations can alter propensities for association with AGO proteins (Okamura et al., 2009; Wang et al., 2011) while alterations in the transcription of miRNA genes would be reflected equally by all variant products (isomiRs) of a particular miRNA. We found that changes in the abundance of pairs of miRNAs and variant miRNA species were significantly correlated (Fig 4F; $R=0.68$; $P\leq10^{-45}$; Figure S5, Supplemental Table 2), a result most consistent with transcriptional differences for miRNA genes in *Ago4*$^{-/-}$ cells. Interestingly, when comparing miRs and isomiRs with shared 5′ ends and shared 3′ ends, those with shared 5′ ends were somewhat ($P=0.09$)

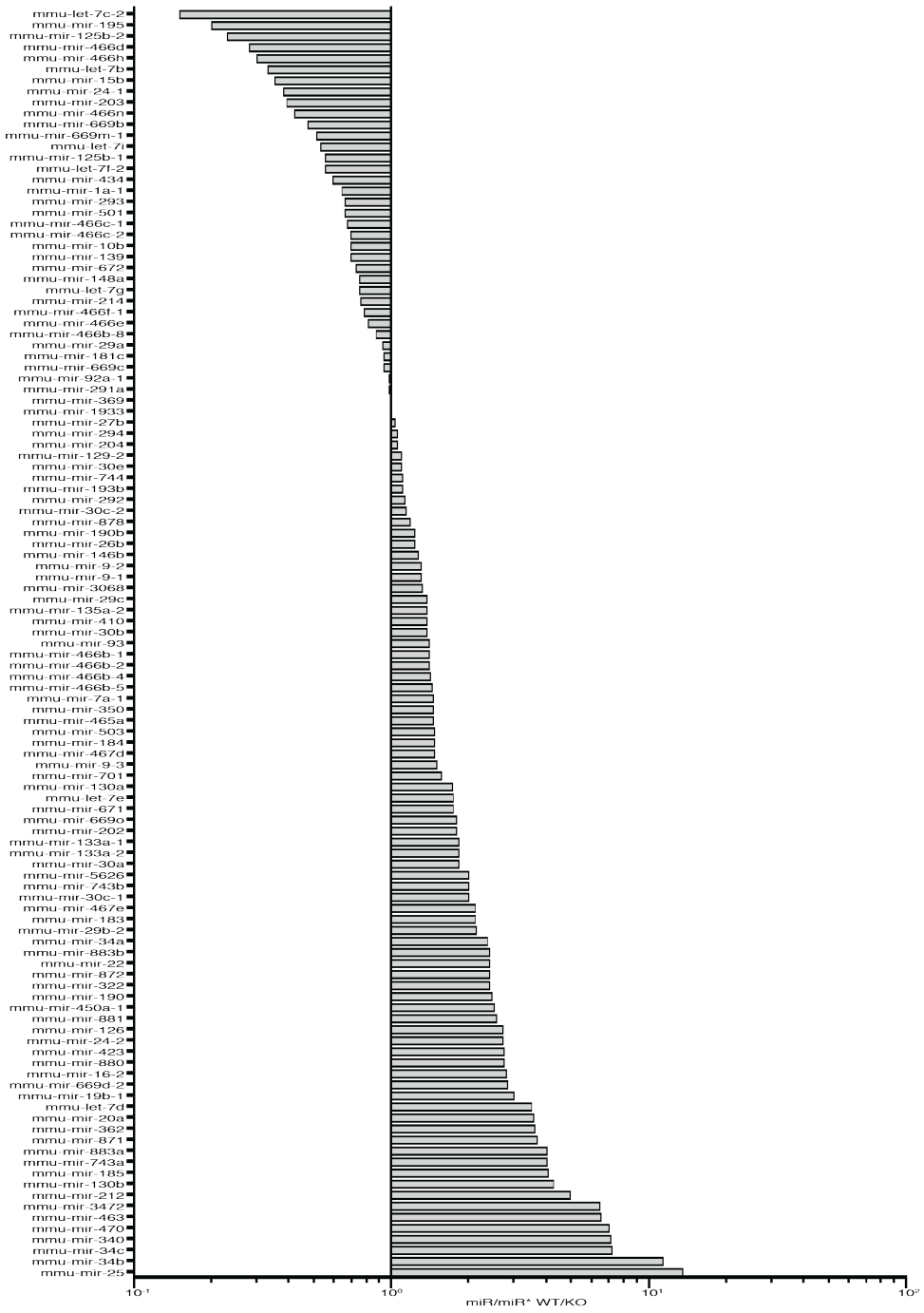


**Figure S5 related to figure 4: miR/miR* ratios between *Ago4*$^{+/+}$ and *Ago4*$^{-/-}$ pachytene small RNA samples.** For each miRNA hairpin, the most abundant transcript (Chu et al.) and the miR* (the transcript produced from the opposite side of the hairpin as a result of Dicer/Drosha processing of the miR) were identified, and counts in both *Ago4*$^{+/+}$ and *Ago4*$^{-/-}$ were determined for each. The miR/miR* ratio was then calculated for each hairpin for both *Ago4*$^{+/+}$ and *Ago4*$^{-/-}$ samples. They are shown here ranked in order of the *Ago4*$^{+/+}$ to *Ago4*$^{-/-}$ ratio.

**Table S2 related to Figure 4: MicroRNA hairpins for all members of the 15 most highly expressed microRNA families in WT pachytene cells.** Small RNA sequences isolated from WT and *Ago4*$^{-/-}$ mice were aligned to known mouse microRNA hairpins. For each microRNA hairpin, the name of the hairpin is given. Beneath is the full-length sequence for the hairpin, followed by the secondary structure predicted for the hairpin using RNA fold. A dot denotes a non-pairing base, while a bracket denotes a base participating in pairing. Below each structure, all sequences that aligned to the hairpin are shown. The sequence with the highest count in the WT animal is colored red. For each sequence, the number of times it was sequenced in *Ago4*$^{+/+}$ and *Ago4*$^{-/-}$ animals is given to the right, together with a total for all sequences in the hairpin (Total Counts, at the bottom of each column). The ratio of sequencing reads between *Ago4*$^{+/+}$ and *Ago4*$^{-/-}$ was calculated (*Ago4*$^{+/+}$/*Ago4*$^{-/-}$). The number of genome matches for each sequence (Lin et al.) and the chromosomal origins (CO) are also given. A '>3' in the chromosomal origin column denotes sequences matching the genome more than three times, for which possible chromosomal origins are not listed. *(see accompanying Excel spreadsheet)*

more correlated (Figure 4F; R values of 0.70, red) than those with shared 3′ ends (R=0.41, blue). These results are consistent with loss of *Ago4* resulting in both changes in miRNA transcription, together with different propensities for certain miRNA species to form complexes with different AGO proteins. Importantly, loss of AGO4 results in a significant reduction in specific microRNAs, and despite increased RNAP II in the SB, a significant fraction of these arise from the X chromosome.

To correlate changes in small RNA species identified by small RNA cloning with changes in their localization, we examined the localization of microRNAs originating from the X chromosome. For example, miR-322 is known to escape MSCI (Song et al., 2009), and was shown in our small RNA cloning to be dramatically down-regulated in the absence of AGO4. We find miR-322 localizes to the SB in WT spermatocytes (Figure 4G), while its localization is decreased in

those *Ago4*$^{-/-}$ pachytene spermatocytes that display aberrant SB morphology (Figure 4H). Furthermore, we confirm the SB localization of miR-24 as demonstrated previously (Marcon et al., 2008a), and observed no signal from miR-206, consistent with the small RNA cloning data (Figure S4H,I). Together, these studies demonstrate that certain miRNAs are dependent on AGO4 and suggest an accumulation of some miRNA species in the SB during pachynema.

*Expression profiling of pachytene spermatocytes reveals loss of silencing of sex-linked genes*

To better understand alterations in gene expression that result from loss of *Ago4*, we used RNAseq to profile the transcriptome of *Ago4*$^{-/-}$ and WT cell populations. Our profiling was performed on whole testis extracts at day 3-4 and day 8-9 pp, both comprised solely of somatic cells and spermatogonia, together with isolated meiotic cell fractions from adult testis at leptonema/zygonema and at pachynema. RNA from adult kidney and seminal vesicles served as controls for each genotype. Contrary to our expectation, we found no evidence for a global failure in sex chromosome silencing in *Ago4*$^{-/-}$ pachytene cells (Figure 5A). However, numerous Y-linked transcripts did show upregulated expression in the absence of *Ago4*, including *Zfy2* and *Ube1y1* (Figure 5B,C). *Zfy2* is one of the "suicide" genes (along with *Zfy1*) whose expression in the absence of MSCI results in apoptosis (Royo et al., 2010). *Zfy2* expression was elevated approximately 2-fold in pachytenes from *Ago4*$^{-/-}$ males ($p<0.03$).

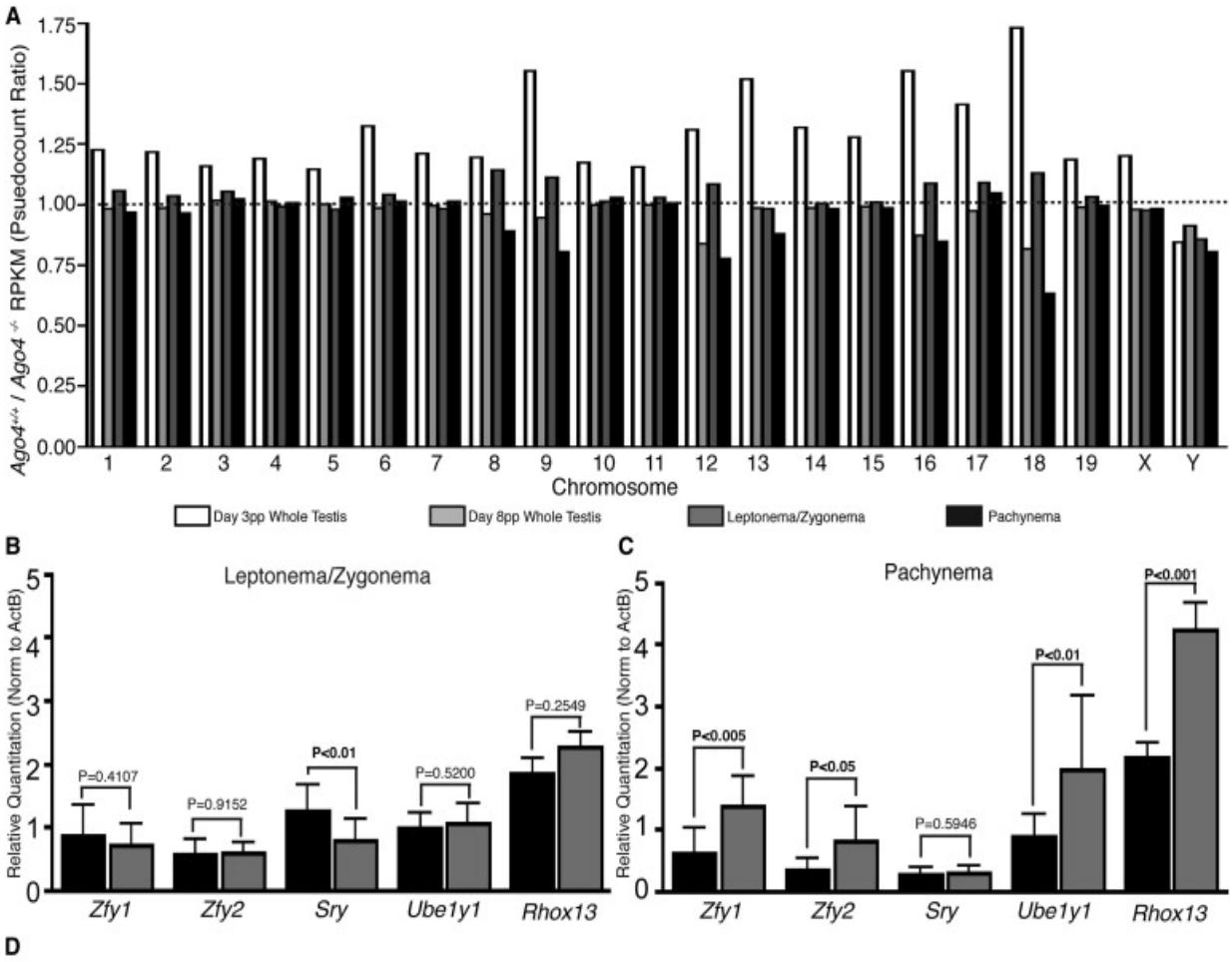


D

| PreMeiotic Day 3 pp | p Value | PreMeiotic Day 8 pp | p Value | Leptonema/Zygonema | p Value | Pachynema | p Value |
|---|---|---|---|---|---|---|---|
| Gland morphogenesis | $4.95 \times 10^{-4}$ | M phase of meiotic cell cycle | $1.35 \times 10^{-5}$ | Cell motility | 0.004583 | Cell motion | $7.53 \times 10^{-4}$ |
| Amebodial cell migration | $1.38 \times 10^{-5}$ | Meiosis | $1.35 \times 10^{-5}$ | Localization of cell | 0.004583 | Heart development | 0.012200 |
| Positive regulation of gene expression | $1.80 \times 10^{-5}$ | Meiotic cell cycle | $1.64 \times 10^{-5}$ | Cell motion | 0.012358 | Cell motility | 0.002326 |
| Tube development | $1.84 \times 10^{-5}$ | Meiosis I | $2.20 \times 10^{-5}$ | Lymphocyte mediated immunity | 0.014733 | Localization of cell | 0.002326 |
| Epithelial tube morphogenesis | $1.94 \times 10^{-5}$ | Chromosome organization involved in meiosis | $1.72 \times 10^{-4}$ | Leukocyte adhesion | 0.015524 | Muscle organ development | 0.005639 |
| Epithelium development | $1.99 \times 10^{-5}$ | Synapsis | $1.72 \times 10^{-4}$ | Gene silencing | 0.019912 | Reproductive developmental process | 0.006017 |
| Morphogenesis of an epithelium | $2.67 \times 10^{-5}$ | Male meiosis | $2.73 \times 10^{-4}$ | Leukocyte mediated immunity | 0.019912 | Reproductive process in a multicellular organism | 0.006049 |
| Tube morphogenesis | $3.57 \times 10^{-5}$ | Synaptonemal complex assembly | $3.96 \times 10^{-4}$ | Adaptive immune response* | 0.021371 | Multicellular organism reproduction | 0.006049 |
| Positive regulation of macromolecule metabolic process | $4.13 \times 10^{-5}$ | Sister chromatid cohesion | $3.96 \times 10^{-4}$ | Adaptive immune response | 0.021371 | Sperm motility | 0.008891 |
| Positive regulation of RNA metabolic process | $6.25 \times 10^{-5}$ | Synaptonemal complex organization | $5.58 \times 10^{-4}$ | Regulation of cell motion | 0.023741 | Blood vessel morphogenesis | 0.009230 |

**Figure 5. RNAseq Profiling of Purified Spermatocytes from Different Stages of Prophase I and from Premeiotic Testes** (A) Differential expression between WT and *Ago4*$^{-/-}$ transcript levels was determined by RNAseq and depicted by ratios of WT to *Ago4*$^{-/-}$ mRNA levels by chromosome.(B and C) Quantitative RT-PCR analysis of XY-linked gene expression in total RNA from isolated (B) leptotene/zygotene and (C) pachytene spermatocytes from *Ago4+/+* (n = 3, black bars) and *Ago4*$^{-/-}$ (n = 3, gray bars) adult littermates (significant values in bold). Error bars, SEM.(D) GO analysis of transcripts showing significant differential expression ($q < 0.05$) in mRNA levels; the most significant groups of transcripts differentially expressed are shown for each cell type.See also Table S3.

Importantly, the increased transcription seen for certain sex-linked genes in the absence of AGO4 is likely contributed only by those pachytene cells showing SB aberrations, such that the overall extent of the loss of silencing is likely lost in the heterogeneous population of aberrant and normal pachytene cells obtained for RNAseq analysis, suggesting that the effect of AGO4 loss on MSCI is under-estimated by our RNAseq analysis.

Many aspects MSCI initiation and maintenance remain elusive. Establishment of MSCI requires H2AX phosphorylation by ATR in the SB. Thus, during meiotic prophase I, ATR and γH2AX accumulate on sex chromatin in spermatocytes (Fernandez-Capetillo et al., 2003; Turner et al., 2004; Turner et al., 2005). The prevailing model proposes that to maintain MSCI, the limited pool of ATR functions to prevent expression of toxic Y-linked genes (Royo et al., 2010). Thus, ATR must be recruited to the SB by first being depleted from the autosomes following synapsis. In various SC or recombination repair mouse mutants, therefore, ATR persists on the autosomes due to the more generalized MSUC mechanism, resulting in up-regulation of gene expression from the sex chromosomes including *Zfy1/Zfy2*. It is the expression of these genes that results in meiotic arrest, rather than any effects of recombination failure *per se* (Royo et al., 2010). Importantly, RNAseq analysis of RNA from the leptotene/zygotene and pachytene stages did not show any differences in expression of *Atr* or *Brca1* between WT and mutant (Supplemental Table 3). These genes are essential for

phosphorylation of H2AX during MSCI (Turner et al., 2004), suggesting that the derepression of XY-linked genes is not due to failure to phosphorylate H2AX.

| Gene | Leptotene/Zygotene | | | | | | |
|---|---|---|---|---|---|---|---|
| | KO | WT | log2(fold_change) | test_stat | p_value | q_value | significant |
| *Brca1* | 6.80993 | 4.60323 | -0.564992 | 1.81888 | 0.0689291 | 0.496595 | no |
| *Atr* | 42.6561 | 36.5765 | -0.221835 | 1.42425 | 0.154375 | 0.613546 | no |
| *Hormad1* | 14.2659 | 11.0588 | -0.367383 | 1.56684 | 0.117151 | 0.588194 | no |
| *Hormad2* | 7.07559 | 7.29965 | 0.0449771 | -0.085119 | 0.932166 | 0.988489 | no |

| Gene | Pachytene | | | | | | |
|---|---|---|---|---|---|---|---|
| | KO | WT | log2(fold_change) | test_stat | p_value | q_value | significant |
| *Brca1* | 3.98426 | 2.08843 | -0.931894 | 2.5842 | 0.00976047 | 0.203812 | no |
| *Atr* | 118.828 | 107.637 | -0.142702 | 0.773398 | 0.439287 | 0.852473 | no |
| *Hormad1* | 18.216 | 17.3525 | -0.0700685 | 0.22987 | 0.818193 | 0.969458 | no |
| *Hormad2* | 44.4241 | 47.3571 | 0.0922376 | -0.616576 | 0.537514 | 0.899902 | no |

**Table S3 related to Figure 5:** Summary of RNAseq data at Leptonema/Zygonema and at Pachynema for genes involved directly in MSCI to demonstrate that there were no appreciable changes detected in the overall mechanism of meiotic silencing, and that the action of *Ago4* must function together with these proteins rather than regulating their expression. For example, loss of MSCI is not simply due to failure to express *Atr* and *Brca1,* two mediators of H2AX phosphorylation.

The derepression of certain XY-linked transcripts was examined further by performing qRT-PCR on RNA from isolated leptotene/zygotene and pachytene spermatocytes (Figure 5B,C, respectively). Three out of four Y-linked genes examined (*Zfy1, Zfy2, Ube1y1*) and one X-linked gene (Rhox13) showed significant increases in expression in *Ago4*$^{-/-}$ spermatocytes compared to WT specifically at pachynema (Figure 5C), indicating that many XY-linked genes escape MSCI in the absence of AGO4.

Given our model for AGO4 involvement in MSCI, it was somewhat surprising to see only a modest loss of silencing in the SB, associated with modest

persistence of ATR on the X, but not the Y, chromosome, and only a slight increase in ATR localization on the autosomes. This could reflect partial redundancy with AGO3, which is up-regulated in *Ago4*$^{-/-}$ spermatocytes. Alternatively, this partial loss of MSCI could reflect the fact that only ~30% of cells observed in early pachynema have abnormal SB morphologies, which are likely eradicated by apoptosis, thus those that survive are functionally intact with respect to MSCI processes. This possibility is supported by the finding that all abnormal SBs are observed in cells that are H1T-negative, indicative of early pachynema, while only normal SB morphologies are observed in cells that are H1T-positive, indicative of late pachynema.

*Loss of Ago4 drives premature entry into meiosis*

While comparing gene expression profiles between *Ago4*$^{-/-}$ and WT littermate males, gene ontology (GO) analysis of RNAseq data revealed a dramatic up-regulation of transcripts encoding proteins involved in spermatogonial proliferation in *Ago4*$^{-/-}$ testes on day 3-4 pp relative to WT, together with a distinct induction of genes regulating meiotic entry within day 8-9 pp *Ago4*$^{-/-}$ testes (Figure 5D). This suggests that loss of AGO4 facilitates spermatogonial differentiation and proliferation leading to premature meiotic initiation. In WT mice, meiotic initiation is brought about by the production of Retinoic acid (RA) via the action of the RALDH2 enzyme (the product of the *Aldh1a2* gene) in Sertoli (and other) cells of the postnatal testis. The oxidation of RA by the P450 enzyme, CYP26B1, prevents RA-induced meiotic entry in fetal testes at a time when fetal

oocytes initiate meiosis because they lack this enzyme (Hogarth and Griswold, 2010). In postnatal males, at around day 5-6 pp, RA binds to the retinoic acid receptor G (RARG) on the surface of Type A spermatogonia (Gely-Pernot et al., 2012) and induces a cascade of genes, including *Stra8, Esco2*, and *Uba6* (Hogarth et al., 2011), while negative regulators of meiotic onset act to repress *Stra8* function and promote spermatogonial maintenance. These negative regulators of meiotic induction include *Nanos2* and *Fgf9* (Suzuki and Saga, 2008).

Genes involved in spermatogonial stem cell maintenance and proliferation were up-regulated in RNA samples from day 3-4 pp *Ago4*$^{-/-}$ testes (Figure 6A). These included *Sox2* (Figure 6A) and *Sox9* (not shown), members of the Sox family of transcription factors that are involved in the reactivation of stem cell pluripotency (Yabuta et al., 2006). Similarly, the RNA binding protein, *Lin28b*, was up-regulated along with its downstream target, *Prdm1*, while *let7* was down-regulated, in *Ago4*$^{-/-}$ testes. Under the influence of RA, LIN28b is required to repress the somatic mesodermal program by sequestering the let-7 miRNA family, which in turn allows PRDM1 to act as an inducer of germ cell lineages (Bowles and Koopman, 2010). Thus, the day 3-4 pp GO analysis of RNA from whole *Ago4*$^{-/-}$ testes revealed a switch from spermatogonial stem cell maintenance to one of spermatogonial proliferation and/or differentiation.

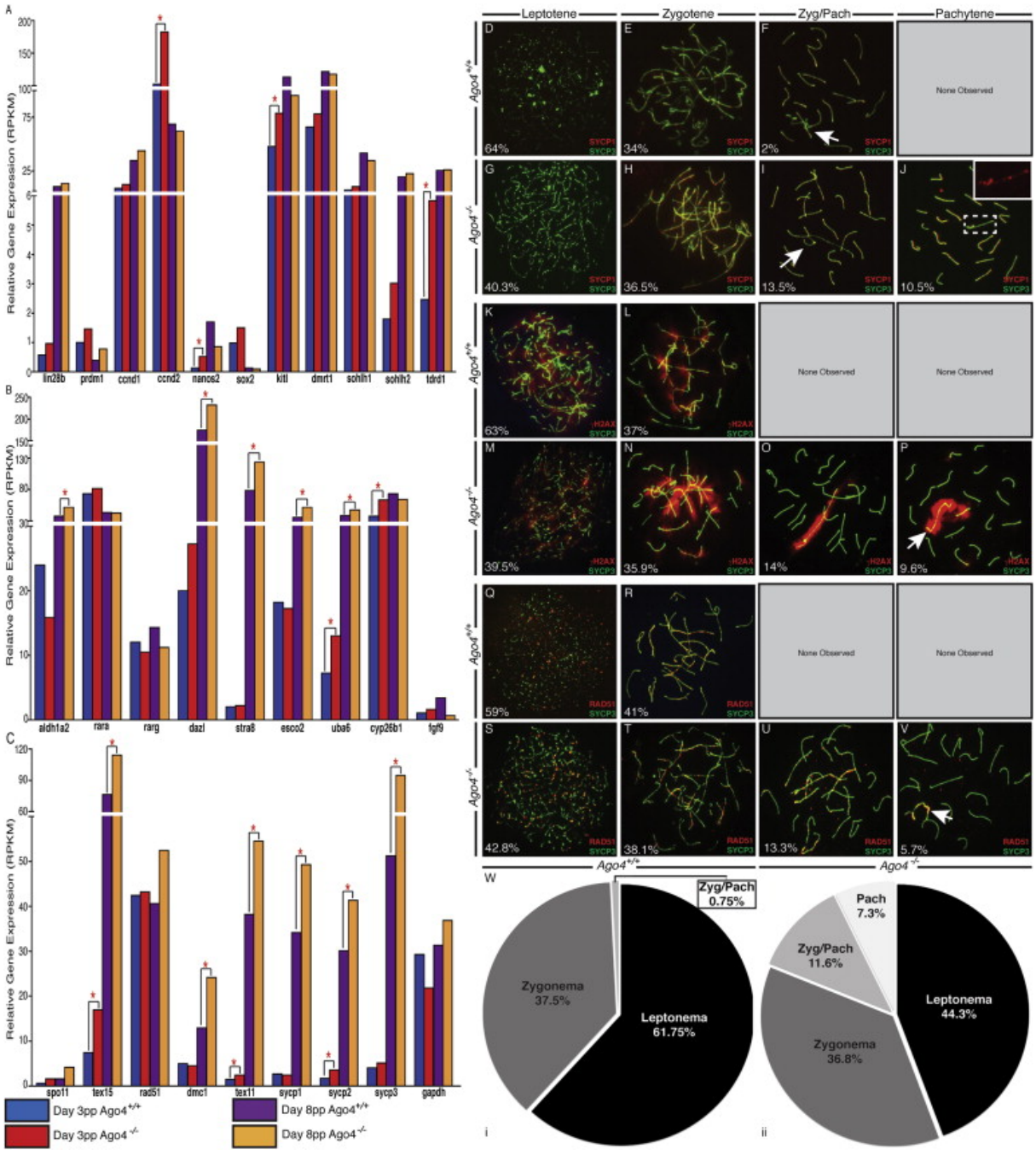
A
Relative Gene Expression (RPKM)
lin28b
prdm1
ccnd1
ccnd2
nanos2
sox2
kitl
dmrt1
schlh1
schlh2
tdrd1
B
Relative Gene Expression (RPKM)
aldh1a2
rara
rarg
dazl
stra8
esco2
uba6
cyp26b1
fgf9
C
Relative Gene Expression (RPKM)
spo11
tex15
rad51
dmc1
tex11
sycp1
sycp2
sycp3
gapdh
Day 3pp Ago4+/+
Day 3pp Ago4-/-
Day 8pp Ago4+/+
Day 8pp Ago4-/-
Leptotene
Zygotene
Zyg/Pach
Pachytene
Ago4+/+
Ago4-/-
None Observed
SYCP1
SYCP3
γH2AX
RAD51
W
Zyg/Pach 0.75%
Zygonema 37.5%
Leptonema 61.75%
Pach 7.3%
Zyg/Pach 11.6%
Leptonema 44.3%
Zygonema 36.8%
i
ii

**Figure 6. Loss of AGO4 Induces Early Entry into Meiosis in Postnatal Testes** (A–C) Quantification of transcripts from RNAseq performed on premeiotic testis from *Ago4+/+* and *Ago4*$^{-}$*/*$^{-}$ males at day 3–4 pp (blue [*Ago4+/+*] and red [*Ago4*$^{-}$*/*$^{-}$] bars) and day 8–9 pp (purple [*Ago4+/+*] and orange [*Ago4*$^{-}$*/*$^{-}$] bars). GAPDH is shown as a control. Genes with a significant degree of differential expression between *Ago4+/+* and *Ago4*$^{-}$*/*$^{-}$ males ($q < 0.05$) are indicated with an asterisk (*). Genes in (A) are associated with spermatogonial proliferation and/or differentiation. Genes in (B) are involved in the initiation of meiosis, via RA. Genes involved in early prophase I progression are in (C).(D–V) Chromosome immunofluorescence from day 8–9 pp testes from *Ago4*$^{+/+}$ (D–F, K, L, Q, R, and Wi) and *Ago4*$^{-}$*/*$^{-}$ (G–J, M–P, S–V, and Wii) littermates stained with anti-SYCP3 (green), together with anti-SYCP1 (D–J), anti-γH2AX (K–P), or anti-RAD51 (Q–V), all in red. Progression through prophase I is depicted by horizontal panels from left to right. If no image is given for a particular stage of prophase I, then that stage was not observed in the staining for this genotype. Percent (%) cells found at each stage is shown.(Wi and Wii) Quantification of prophase I stages for *Ago4+/+* and *Ago4*$^{-}$*/*$^{-}$, respectively ($n = 400$). $\chi^2$ analysis revealed significant differences between the two populations (***$p < 0.0001$).

At day 8-9 pp in *Ago4*$^{-/-}$ testes, *Cyp26b1, Nanos2* and *Fgf9* levels are all reduced while *Aldh1a2, Rarg* and *Stra8* levels are greatly enhanced compared to *Ago4*$^{+/+}$ males. Similarly, *Esco2* and *Uba6* show premature increases in expression at day 8-9 pp in the *Ago4*$^{-/-}$ testes (Figure 6B). These alterations in the induction of RA pathway suggest that the absence of AGO4 results in premature induction of meiotic genes approximately 5 days earlier than in the WT.

Early meiotic initiation in young *Ago4*$^{-/-}$ male pups was supported by the onset of expression of genes known to be essential and specific to meiotic prophase I, which usually occurs around day 9 pp in the male mouse (Goetz et al., 1984). These include the genes encoding SPO11, the topoisomerase that generates double strand breaks (DSB) that initiate meiotic recombination; the RecA homologs, DMC1 and RAD51, which process DSBs to facilitate homology searching and recombination (reviewed by (Handel and Schimenti, 2010); TEX15, which facilitates loading of the RecA homologs (Yang et al., 2008); and the synaptonemal complex components, SYCP1 and SYCP3 (Figure 6C).

To confirm the early onset of prophase I at the cytological level, chromosome preps were examined from pups at day 5-6 pp and day 8-9 pp. At day 5-6 pp, no cells were found to be in prophase I in *Ago4*$^{+/+}$ males, whereas a large number of cells from *Ago4*$^{-/-}$ males were found to be in pre-leptonema (not shown). This difference was even more dramatic by day 8-9 pp, when large numbers of spermatocytes from *Ago4*$^{-/-}$ males were found to have entered, and progressed through, the early stages of prophase I. Progression through prophase I was demonstrated by staining with antibodies against SYCP3,

together with SYCP1 (Figure 6D-J), or with γH2AX (Figure 6K-P), and with RAD51 (Figure 6Q-V). In all cases, the major alteration to the spermatocyte pool in *Ago4*$^{-/-}$ males appeared to be a decrease in total leptotene cells (collective counts shown in figure 6W, n=400, $p<0.005$ t-test), and a concomitant increase in zygonema/pachynema intermediate cells ("Zyg/Pach" Figure 6W, n=400, $p<0.005$ t-test). The emergence of pachytene cells in *Ago4*$^{-/-}$ males was approximately 5-6 days earlier than in WT males. Interestingly, all spermatocytes observed to reach the pachytene stage in the young mutant pups (Figure 6J,P) displayed defects identical to the altered staining patterns described earlier for spermatocytes from adult males. This observation suggests that meiotic progression in the adult can be partially rescued, perhaps by AGO3, while the initial waves of meiotic prophase I in early postnatal life are more wholly dependent on AGO4.

Together, our observations demonstrate early entry into meiosis in *Ago4*$^{-/-}$ males caused by premature induction of RA response genes that trigger meiotic initiation. These studies are in line with a recent report which demonstrates that the *C. elegans* Argonautes ALG-1 and ALG-2 are required for germ cell proliferation and entry into meiosis (Bukhari et al., 2012). In the worm, ALG-1 and ALG-2 localize to distal tip cells (DTC), specialized somatic cells in the gonad that regulate the switch from mitosis to meiosis (Kimble and Crittenden, 2007) suggesting a cell non-autonomous miRNA mechanism for regulating meiotic entry.

## 2.4 Conclusion

The studies described herein demonstrate a role for AGO4 in the nucleus of male germ cells. Our data support a model whereby AGO4-associated small RNAs directly participate in MSCI (Figure 7). Consistent with the discovery of nuclear RNAi components in human cells (Ahlenstiel et al., 2011; Robb et al., 2005), our study reveals distinct localization patterns for both AGO3 and AGO4 within the nuclei of mouse spermatogenic cells, along with certain miRNAs. These observations support the idea that AGO4 may recruit small RNAs to the SB, or *vice versa*. Importantly, we show that in the absence of AGO4, disproportionate numbers of down-regulated miRNAs originate from the X chromosome, and that miRNA localization in the SB is markedly reduced. This loss of miRNAs specifically from X and Y is contrary to expectation given the increased localization of RNAP II in the SB, but is in line with the fact that X-linked miRNAs have been found to escape repression during MSCI of prophase I (Song et al., 2009).

Given the localization of AGO4 to asynapsed regions and the SB in pachynema, together with its co-localization with mediators of MSCI (ATR and γH2AX), and the dependence of these mediators on AGO4, the results presented herein indicate a role for AGO4 in the initiation and/or maintenance of transcriptional silencing during prophase I. We hypothesize that this transcriptional regulation is regulated by AGO4 in a manner reminiscent of the RITS complex seen in *S. pombe* and *C. elegans* (van Wolfswinkel and Ketting,

2010). While small RNAs have been postulated to be involved in MSCI (Burgoyne et al., 2009), our data provide direct evidence for AGO4 in these events (Figure 7).

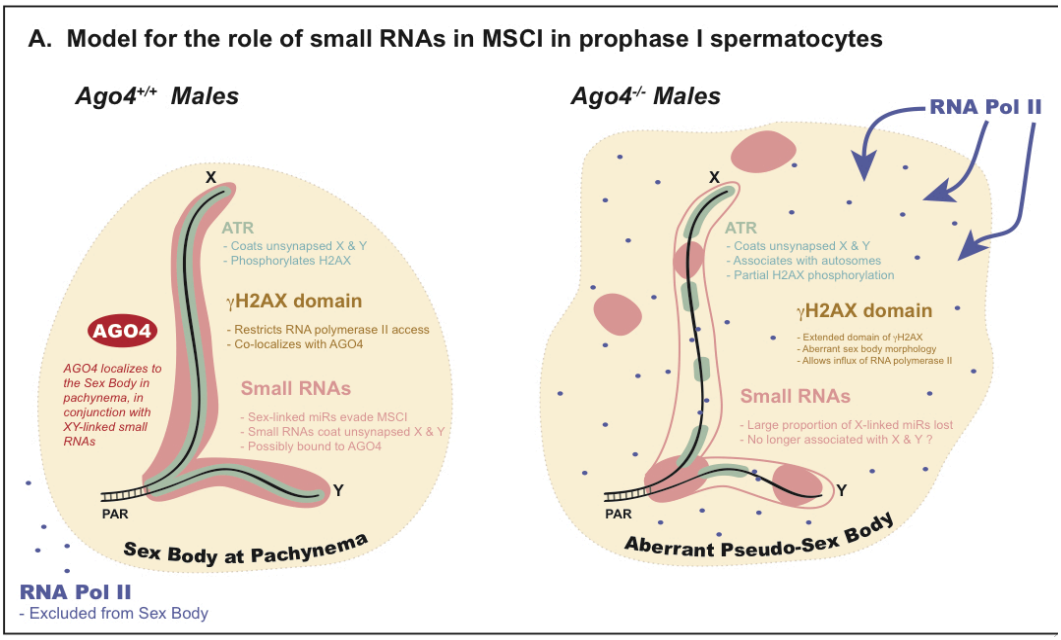


**Figure 7. Model for the Role of AGO4 in Meiotic Silencing** In WT males at pachynema (left side), the SB domain is defined by localization of γH2AX (yellow background), whose phosphorylation is mediated by the ATR kinase, which coats the unsynapsed lengths of the X and Y chromosomes (green). Sex chromosomes are also coated with small RNAs (pink) at this time. We propose that the presence of these RNA species may depend on AGO4, and the sum effect is the exclusion of RNAP II from the SB and silencing of the sex chromosomes by MSCI. In the absence of AGO4 (right side), ATR localization is drastically reduced along abnormal SB morphology. Sex-linked small RNAs are drastically reduced and no longer reside in the SB, leading to RNAP II infiltration and failed silencing. These effects are distinct from those involving RA signaling and meiotic initiation described in Figure 6.

The role of AGO4 in meiotic initiation appears to originate in at least two cell types: the RA producing Sertoli cells and the spermatogonia. However, AGO4 expression appears to be confined to the germ lineages, leading us to postulate an indirect effect on RA production by the somatic cells of the testis. In this scenario, loss of AGO4 results in loss of a signal from the germ cells to the Sertoli cells that would usually repress RA production. The action of AGO4 in the germ cells themselves may be directed towards RA signal transduction and/or towards

downstream mediators. Indeed, treatment of fetal testes with trichostatin A, an inhibitor of class I/II histone deacetylases, promotes premature activation of *Stra8* expression and early meiotic entry (Wang and Tilly, 2010), suggesting epigenetic regulation of these events. Moreover, there is evidence supporting the role of RNA binding proteins and small RNAs in self-renewal of spermatogonial stem cells (Niu et al., 2011), as well as in the response of spermatogonia to RA signaling (Griswold et al., 2012; Ro et al., 2007). For example, DAZL, an RNA-binding protein expressed in germ cells, which is up-regulated on day 8-9 pp in the absence of AGO4, facilitates germ cell responses to RA to promote meiotic initiation (Gill et al., 2011; Lin et al., 2008; Lin and Page, 2005). In contrast, two miRNA clusters have been implicated during spermatogonial differentiation in mice, *miR-17-92* and *miR-106b-25* (Tong et al., 2011), and both are down-regulated in *Ago4*$^{-/-}$ testes.

Taken together, our studies demonstrate important roles for AGO4 in meiotic induction and progression in male mice. Of particular note is the observation that AGO4 is found in the nucleus of prophase I cells, suggesting the existence of a RITS-like complex at the level of heterochromatin in meiotic cells. Finally, it is important to note that the two roles for AGO4 in mammalian germ cells that we describe appear to be distinct, since treatment of vitamin A deficient mice with RA does not lead to MSCI defects or meiotic disruption (van Pelt and de Rooij, 1990). Indeed, it is plausible that the early meiotic entry and the MSCI events require different roles for AGO4 in the context of their nuclear and

cytoplasmic activities. Continued studies are aimed at elucidating the mechanisms of AGO4 involvement in these mammalian germ cell events.

## 2.5 Materials & Methods

*Generation of Ago4 mutant mice.*

An *Ago4* targeting construct, containing a 2.5-kbp 5′ arm from intron 2 of *Ago4*, a LoxP site, 25.4 kb of *Ago4* from exons 3-17, an *Frt*-flanked *Pgk-neo* cassette, a second LoxP site and a 1.6-kbp 3′ arm within intron 17 of Ago4 (Figure S1D-F), was used to generate chimeric mice using standard mouse mutagenesis techniques. Following FlpE and CRE-mediated excision of the *Frt*-flanked and *LoxP*-flanked cassettes, respectively, the resulting $Ago4^{-/-}$ allele (lacking exons 3-17) was bred to homozygosity onto a C57BL/6 background.

*Testes weights, Sperm counts and Histology*

Whole testes were removed from $Ago4^{+/+}$ and $Ago4^{-/-}$ littermates and weighed, and epididymal sperm counts assessed (Edelmann et al., 1996). For histological analysis, testes were fixed in Bouins (for H&E staining) or in 10% formalin (for all other staining and for TUNEL) overnight at 4°C. Paraffin embedded tissues were sectioned at 5 μm before dewaxing and histological staining.

*Chromosome spreading and immunofluorescent staining*

Prophase I chromosome spreads and antibody staining were prepared as previously described, (Holloway et al., 2008; Holloway et al., 2011 ; Kolas et al.,

2005; Lipkin et al., 2002) using antibodies from various sources (see supplemental Experimental Procedures).

*RT-PCR and Q-PCR*

Total RNA was extracted from whole tissue or isolated spermatocytes using TRIZOL reagent (Invitrogen). Reverse transcription was performed using Superscript III (Invitrogen). For real-time PCR analysis, TaqMan probes (Applied Biosystems, Carlsbad CA, USA) were used on the 7500 Real Time PCR System (Applied Biosystems). Raw data was analyzed using the 7500 System Sequence Detection Software (Applied Biosystems). Probesets are provided in supplemental Experimental Procedures.

*Isolation of mouse spermatogenic cells*

Testes from adult *Ago4*$^{+/+}$ and *Ago4*$^{-/-}$ adult mice (day 70-80 pp) were removed, weighed and decapsulated prior to enrichment of specific spermatogenic cells types using the STA-PUT method based on separation by cell diameter/density at unit gravity (Bellve, 1993). Purity of resulting fractions was determined by microscopy based on cell diameter and morphology. Pachytene cells were at approximately 95% purification with potential contamination from spermatocytes of slightly earlier or later developmental timing.

*mRNA transcript sequencing and analysis*

mRNA transcripts were isolated and prepared for sequencing using Illumina's TRUseq kit. The completed library was sequenced on an Illumina HiSeq 2000 and aligned to the genome using TopHat and Cuffdiff programs (Trapnell et al., 2009) to determine differential expression between WT and mutant samples. A q-value, which represents a false discovery rate-corrected p-value (Klipper-Aurbach et al., 1995), <.05 was chosen as the cutoff for determining whether differential gene expression was significant. For ontology analysis, genes with significant differential expression were analyzed using DAVID (Huang da et al., 2009a, b).

*Small RNA sequencing and Analysis*

Small RNA sequencing was performed as described previously (Grimson et al., 2008). Sequences were filtered to remove reads containing undefined bases ('N') and reads under 14 nt in length. Sequences were aligned to the genome using Bowtie (version 0.12.07, (Langmead et al., 2009)). MicroRNAs were determined by alignment of sequences to mouse miRNA hairpins (miRBase Release 18, (Griffiths-Jones, 2004; Griffiths-Jones et al., 2006; Griffiths-Jones et al., 2008)).

*miRNA Fluorescent In Situ Hybridization and Immunofluorescence.*

Slides were prepared and stained as described above with modifications to retain RNA (see supplemental Experimental Procedures). Following immunofluorescence with primary antibodies as described previously (Holloway

et al., 2010; Kolas et al., 2005), and using an anti-SYCE2 antibody (from Howard Cooke, Edinburgh, Scotland), Fluorescein conjugated Locked Nucleic Acid (LNA) probes (Exiqon, Denmark) were used to probe for mature miRNA localization. Probes were first denatured by incubation at 90°C for 4 minutes and hybridizations were carried out at the appropriate incubation temperature overnight. Slides were then washed, mounted with antifade (Prolong Gold, Molecular Probes) and visualized.

**Supplemental Experimental Procedures**

*Generation of Ago4 mutant mice.*

All mouse studies were conducted with the prior approval of the Cornell Institutional Animal Care and Use Committee (IACUC). The *Ago4*$^{pRH7.9}$ targeting vector was constructed by bacterial recombination using BAC RP23-260E11 as the genomic backbone. The final construct included a 2.5-kbp 5′ arm from intron 2 of *Ago4*, a LoxP site, 25.4 kb of *Ago4* from exons 3-17, an *Frt*-flanked *Pgk-neo* cassette, a second LoxP site and a 1.6-kbp 3′ arm within intron 17 of Ago4 (Figure S1D). The linearized construct was electroporated into ES cells and homologous recombination was verified at the 5′ end using a 2.6kb PCR product amplified only by the recombined allele. At the 3′ end, homologous recombination was verified by a 1.6kb PCR product that could only be amplified by the recombined allele. We prepared *Ago4*$^{pRH7.9}$ mice using standard embryonic stem cell culture and blastocyst injection methods and excised the *Frt*-flanked *neo* marker by crossing them with *FLPe* transgenic mice to produce the *Ago4*$^{noneo}$ allele (Figure S2). *Ago4*$^{noneo}$ mice were crossed with *ActB*-Cre mice (from Jackson Laboratories, Bar Harbor, ME) to produce the *Ago4*$^{-/-}$ fully targeted mutation mice lacking exons 3-17 of *Ago4*. Mice were backcrossed onto a C57BL/6 background.

*Testes weights and Sperm counts*

Whole testes were removed from *Ago4*$^{+/+}$ and *Ago4*$^{-/-}$ littermates and weighed. Mature spermatozoa were quantified by extracting the caudal epididymides, puncturing and incubating in media containing 4% BSA for 20 minutes to allow the sperm to swim out. 20 μl of this media was added to 480 μl of 10% formalin to fix the sperm and then the cells were counted using a hemocytometer.

*Histology and TUNEL staining*

Testes were removed from *Ago4*$^{+/+}$ and *Ago4*$^{-/-}$ littermate adult (70-80 dpp) mice, fixed overnight in 10% formalin at 4°C and then washed in 3 changes of 70% ethanol over a period of 48 hours. Fixed tissues were cut into 5 μm sections and processed for Hematoxylin and Eosin staining or immunohistochemical analyses using standard methods. TUNEL staining was performed using the Apoptag TUNEL staining kit (Chemicon, Temecula CA, USA). GCNA staining was performed to identify germ cells, as per standard methods.

*Chromosome spreading and immunofluorescent staining*

Tubules were minced in sucrose solution and fixed onto slides in 1% paraformaldehyde overnight, in a humidified chamber. Slides were washed in Photoflo (KODAK, Geneva NY) diluted in PBS (800 μL in 200 mL PBS), Triton X-100 diluted in PBS (1 mL and 199 mL PBS) and blocked in antibody dilution buffer (ADB) diluted in PBS (20 mL and 180 mL), before being stained with various primary antibodies (anti-AGO4 ab3600 Abcam, anti-AGO4 ab52724 Abcam, Cambridge MA USA, Anti-AGO3 for sections Abcam ab3593. Anti-AGO3 for spreads H00192669-A01 Novus Biologicals, Littleton CO, USA). Several Alexafluor™ secondary antibodies were used (Molecular Probes Eugene OR, USA) for immunofluorescent staining at 37°C for one hour. Slides were washed and mounted with Prolong Gold antifade (Molecular Probes). Primary antibodies and conditions used herein have been described previously (Holloway et al., 2008;

Holloway et al., 2011 ; Kolas et al., 2005; Lipkin et al., 2002), except for TOPBP1 (from Raimundo Freire, Tenerife, Spain), ATR (GeneTex GTX70133), ATR/ATM substrate (Cell Signaling #5851), pCHK2 (Cell Signaling #2661), SUMO1 (Cell Signaling #4931), ubiH2A (Millipore 05-678), H3K9me3 (Millipore 07-442), RNA polymerase II (Millipore 05-623, Covance MMS-129R), H1T (from Mary Ann Handel, Jackson Laboratories, Bar Harbor, ME).

*Image acquisition*

All slides were visualized using a Zeiss Imager Z1 microscope under 20X, 40X or 63X magnifying objectives, at room temperature. Fluorochromes used were Alexafluors (Molecular Probes) labeled with Cy3, Cy5 or FITC. Images were processed using AxioVision (version 4.7, Zeiss).

*RT-PCR and Q-PCR*

Probes used for the analysis are as follows: *Eif2c1 (Ago1)*: Mm00462977_m1 lot-568774, *Eif2c2 (Ago2)*: Mm03053414_g1 Lot-611742, *Eif2c3 (Ago3)*: Mm01188534_m1 Lot 714363, *Eif2c4 (Ago4)*: Mm00462665_g1 Lot-P100203. *Zfy1*: Mm00494343_g1 Lot-1061650, *Zfy2*: Mm00494350_m1 Lot-965381, *Sry:* Mm00441712_s1 Lot-1055318, *Ube1y1* Mm00495883_g1 Lot-949693, *Rhox13*: Mm01314699_m1 Lot-1095550.

*Statistical Analysis*

Statistical analyses were performed using GraphPad Prism version 4.00 for Macintosh (GraphPad Software, San Diego California USA, www.graphpad.com).

*Analysis of mRNA sequencing data*

Sequences were filtered to remove reads flagged as low quality by the Illumina pre-processing software. The first two 5′ nucleotides and the 3′ ends of reads with low sequencing quality scores were clipped from all reads. Resulting reads over 21 nucleotides were aligned to the transcriptome using the transcript

alignment program TopHat (version 1.3.0(Trapnell et al., 2009)) and an existing annotated genome file (Mus_musculus.NCBIM37.63.gff3). Cuffdiff (version 1.1.0(Roberts et al., 2011; Trapnell et al., 2010)), a tool for determining differential expression in sequencing data, was used to quantify the changes occurring in mRNA expression levels between WT and mutant samples. A q-value, which represents a false discovery rate-corrected p-value (Klipper-Aurbach et al., 1995), of $q<.05$ was chosen as the cutoff for determining whether differential gene expression was significant.

For ontology analysis, genes with significant differential expression were analyzed using the DAVID (version 6.7(Huang da et al., 2009a, b)) Functional Annotation tool. To determine which functional groups our genes fell under, we used the GO Fat Molecular Functions sub-category.

*Small RNA sequencing*

Technique as described previously (Grimson et al., 2008). Briefly, isolated pachytene spermatocytes from *Ago4*$^{+/+}$ and *Ago4*$^{-/-}$ littermate adult (70-80 dpp) mice were placed in TRIZOL (Invitrogen) and total RNA was extracted according to manufacturer's directions. The library was constructed as described(Grimson et al., 2008) and sequenced on the Illumina platform (Illumina, San Diego CA, USA).

*Small RNA Sequencing Analysis*

Sequences were filtered to remove reads containing undefined bases ('N') and reads under 14 nt in length. Sequences were aligned to the genome using Bowtie (version 0.12.07, (Langmead et al., 2009)). MicroRNAs were determined by alignment of sequences to mouse miRNA hairpins (miRBase Release 18, (Griffiths-Jones, 2004; Griffiths-Jones et al., 2006; Griffiths-Jones et al., 2008)).

*miRNA Fluorescent In Situ Hybridization and Immunofluorescence.*

Slides were prepared and stained as described above. The following modifications to the previous protocol were implemented to prevent RNA degradation throughout the chromosome spread preparation and immunofluorescence procedures: DEPC (Sigma Aldrich) treated water was used to create each buffer, Hypotonic extraction buffer (HEB) contained 2 mM Ribonucleoside Vanadyl complex (NEB S1402), EDTA was replaced with 125 mM EGTA so as to not dissociate the complex. Primary antibodies and conditions used herein have been described previously (Holloway et al., 2011 ; Holloway et al., 2010; Kolas et al., 2005), except for anti-SYCE2 (from Howard Cooke, Edinburgh, Scotland), which was used at 1:500.

Fluorescein conjugated Locked Nucleic Acid (LNA) probes (Exiqon, Denmark) used to probe for mature miRNA localization are as follows:

miR-322* Exiqon 21397-04 Batch number 214963

/56-FAM/TGTTGCAGCGCTTCATGTTT.

miR-206 Exiqon 18100-04 Batch number 214965

/56-FAM/CCACACACTTCCTTACATTCCA.

Briefly, after secondary antibody incubation, slides were washed in PBS three times and 40 nM of each probe in hybridization buffer (2x Buffer: 4X SSC, 50% Dextran Sulfate, 2 mg/mL BSA, 2 mM Ribonucleoside Vanadyl complex) were applied to each slide and incubated overnight at the appropriate temperature (Probe RNA Tm – 30$^{o}$C). Probes were first denatured by incubation at 90$^{o}$C for 4 minutes prior to addition to 2X hybridization buffer. Probe and buffer were then pre-incubated at the appropriate incubation temperature for 30 minutes prior to slide application followed by overnight hybridization. Slide were then washed under three stringency conditions:

A: 42$^{o}$C, 50% Deionized formamide, 1X SSC, pH 7.2-7.4, 3 Washes

B: 42°C, 2X SSC, pH 7.2-7.4, 3 Washes

C: RT, 4X SSC, 4 mg/mL BSA, 0.1% Tween 20, pH 7.3, 1 Wash

Slides were washed and mounted with Prolong Gold antifade (Molecular Probes).

## 2.6 Acknowledgements

This work was supported by the Vertebrate Genomics Center at Cornell University (VERGE postdoctoral award to R.J.H. and predoctoral award to S.H.) and by funding from the NIH to P.E.C. (HD041012). A.M. was supported by NIH training grants in Genetics and Development (T32GM00761), and in Reproductive Genomics (T32HD052471); S.H. was supported by an NIH training grant in Biochemistry, Molecular and Cellular Biology. The authors acknowledge with gratitude the generosity of Dr. Mary Ann Handel (The Jackson Laboratory) for providing the anti-H1T antibody, Dr. Raimundo Freire (Tenerife, Spain) for providing the anti-TOPBP1 antibody, Drs. Ian Adams and Howard Cooke (University of Edinburgh, Scotland) for providing the anti-SYCE2 antibody, and Dr. George Enders (University of Kansas Medical Center) for providing the GCNA1 hybridoma supernatant. We are grateful to Ian Welsh for technical advice, and to Ewelina Bolcun-Filas, Jen Grenier, Kim Holloway, and Mark Roberson for reading this manuscript and for helpful suggestions. We also thank Kim Holloway for extensive guidance in preparing figures and editorial assistance. We thank Peter L. Borst for assistance in mouse care.

# CHAPTER 3

## Prophase I-specific Deletion of *Dgcr8* and *Dicer* result in altered Meiotic Sex Chromosome Inactivation, XY chromatin compaction and integrity.

This chapter describes work that is currently being undertaken in the Cohen lab by A.J. Modzelewski, and is a direct continuation of the published work presented in Chapter 2. All the work described herein was performed by A.J. Modzelewski, and will be continued after the defense of this thesis, partly in collaboration with Stephanie Hilz and Andrew Grimson. The work described in this chapter, therefore, will make up the larger part of a new manuscript, to be submitted in 2013"]

## 3.1 Abstract

RNAi is an essential mode of transcriptional regulation in every mammalian tissue type studied. The role of small RNAs have been found to essential for the transmission of genetic material during mouse spermatogenesis. However, the relative roles of two small RNA populations, micro (miRNA) and endogenous small interfering RNAs (endo-siRNA) in regulation of transcriptional activity in mammalian germ cells remain unclear, despite considerable interest over recent years. Previously, we uncovered novel roles for the small RNA binding protein, Argonaute 4 in mammalian meiosis, in which AGO4 is essential for the normal timing of meiotic initiation in males, and also for the essential process of meiotic sex chromosome inactivation (MSCI) during prophase I in mouse spermatocytes. Excitingly, the role of AGO4 in MSCI occurs in the nucleus (specifically the XY domain known as the Sex Body or SB), rather than in the cytoplasm where canonical Argonaute activities reside. To examine which small RNA species may participate in these novel nuclear functions of AGO4, we analyzed meiotic progression in mice harboring germ cell specific conditional deletions of *Dgcr8* and *Dicer* using a *Ddx4-Cre* promotor driven strategy, in which

both small RNA populations are lost, and just miRNAs are lost, respectively, in prospermatogonia at embryonic day 18 (e18). Testes homozygous mutant conditional mice for each of these genes are infertile, with the *Dicer* deficient animal displaying a slightly more severe meiotic phenotype at both the gross and histological levels. Cytological analyses of pachytene spermatocytes from both animals reveal errors in XY chromatin compaction and centromere/telomere integrity, with autosomes frequently fusing with the sex chromosomes and a tendency for the X and Y to circularize. Given the subtle differences between these mutants, with the *Dicer* cKO showing more severe aberrations during prophase I in males, our results indicate that endo-siRNAs play a less essential role in spermatogenesis than miRNAs.

## 3.2 Introduction

Small RNA mediated gene regulation has emerged as a principal mechanism of gene regulation in practically all species studied with evidence for the presence of regulatory components in the cytoplasm, nuclei, mammalian bloodstream, and in some organisms, through ingestion and even transgenerationally ((Gagnon and Corey, 2012), (Mitchell et al., 2008), (Timmons and Fire, 1998), (Vaucheret and Chupeau, 2012), (Montgomery et al., 1998)). Fundamental to continuation of life, a sexually reproducing species must be able to maintain the unbroken chain of propagation afforded to it by reproduction and meiosis.

Since the discovery of miRNAs and endo-siRNAs, only a handful of publications have touched on the subject of these small RNA species in relationship to reproduction in either male or female gametogenesis. In most

cases, the loss of even one of these RNAi related regulatory elements is not compatible with life, therefore analysis relies on the use of temporal and tissue specific *Cre*-mediated conditional mutations.

By analyzing conditional alleles of various RNAi components during different stages of gametogenesis, it was discovered that male and female meiosis require different populations of small RNAs to progress. Reports on the conditional deletion of proteins involved in small RNA biogenesis in oocytes reveal miRNAs are dispensable for oocyte development (Suh et al., 2010). In males, the requirements are unclear given the variability of meiotic phenotypes observed and conflicting results from these conditional deletion studies. These studies mainly concentrated on meiotic progression in general without focusing heavily on the specific stages, such as prophase I, where a large proportion of genetic defects result in meiotic arrest due to the activation of one of the various checkpoints present. Therefore, molecular explanations for the reported phenotypes have yet to be thoroughly analyzed throughout the different stages of meiosis.

Previous work from the Cohen lab reported on the loss of one of the effectors of RNAi, *Ago4*. These mice are subfertile, with reduced sperm numbers and incorrect sex body assembly leading to the disruption of meiotic sex chromosome inactivation (MSCI). During this analysis, evidence emerged for a non-canonical role for small RNAs in transcriptional gene silencing (TGS) within the nucleus: we demonstrated that AGO4 and associated small RNAs are required for proper meiotic silencing of the normally transcriptionally repressed X and Y chromosomes (Modzelewski et al., 2012). Given the normally cytoplasmic role for Argonaute proteins, abundance of endo-siRNAs and the high level of *Ago4* expression in pachytene spermatocytes, it is feasible that AGO4 may interact with

small RNA species that it has not previously been reported to associate with in this unusual context, such as endo-siRNAs. Therefore, the meiotic defects reported in *Ago4* deleted spermatocytes cannot be directly attributed to a single class of small RNAs without further investigation.

To help determine the overall roles of miRNAs and endo-siRNAs in mouse spermatogenesis, and to uncover more of the mechanism behind AGO4 mediated meiotic silencing, we report the first conditional deletion of *Dgcr8* in the mouse testis using the *Ddx4*-Cre deletor system. In parallel, we have also analyzed the loss of *Dicer* using the same *Cre*-lox system in order to genetically separate the contribution of miRNAs and endo-siRNAs in spermatogenesis. Our prediction was that the loss of miRNAs in the *Dgcr8* cKO would results in lack of fertility, in line with previous research. If endo-siRNAs are lost in addition to miRNAs, as is the case with *Dicer* cKO deletion, and these small RNAs do not participate in meiotic processes, as the literature suggests, then the *Dicer* cKO and *Dgcr8* cKO phenotypes should be identical. As expected, both animals are infertile, however the conditional deletion of *Dicer* results in a more severe meiotic phenotype when compared to the *Dgcr8* conditional deletion line, suggesting that endo-siRNAs are functional during spermatogenesis. In both cases, homozygous mutant cKO males have reduced testis size but while the *Dgcr8* cKO mouse retains about 15% the normal sperm number, the *Dicer* cKO deletion was devoid of mature epididymal spermatozoa. Chromosome spread analysis of spermatocytes showed similar silencing protein mislocalization and depletion. Importantly, the frequency at which the sex body displayed abnormalies in chromosomal structure and integrity was distinct between the *Dicer* and *Dgcr8* cKOs. Taken together, these data show that loss of *Dicer* or *Dgcr8* result in massive alterations in meiotic silencing, as seen in the *Ago4*$^{-/-}$ mutant mouse, as

well as chromosomal structure abnormalities during prophase I. The loss of both miRNAs and endo-siRNAs in the *Dicer* cKO is responsible for the more severe phenotype, strongly implying that both populations are required for normal progression through spermatogenesis however, miRNAs play a larger role based on the high degree of similarities in the observed defects.

## 3.3 Materials & Methods

*Mouse Breeding Strategies*— Female mice carrying homozygous floxed alleles for either *Dicer*$^{Fl/Fl}$ (B6;129S7-Dicer1$^{tm1Smr}$/J, Jax Stock: 012284), or *Dgcr8*$^{Fl/Fl}$ (Dr. Rui Yi, Univeristy of Colorado, Boulder) were first crossed to male mice carrying the *Ddx4*-cre transgene (FVB-Tg(Ddx4-cre)1Dcas/J, Jax Stock: 006954) to generate the desired *Dicer*$^{Fl/+}$ cre+ and *Dgcr8*$^{Fl/+}$*cre+* breeder males and crossed to *Dicer*$^{Fl/+}$ cre- and *Dgcr8*$^{Fl/+}$*cre-* breeder females, respectively. These crosses generated the experimental cohorts in which male mice displaying the *Dicer*$^{Fl/\Delta}$ cre+ and *Dgcr8*$^{Fl/\Delta}$ *cre-* genotypes were regarded as being conditional knockouts (cKO: *Dicer*$^{\Delta/\Delta}$ cre+ and *Dgcr8*$^{\Delta/\Delta}$ *cre+)* in the targeted cell types and used for subsequent analysis along with wildtype *(WT: +/+, cre+ or cre-)* and heterozygous (Δ/+, cre+or cre-) littermates.

*Testes weights, Sperm counts, Histology and TUNEL staining*

Whole testes were removed from *WT, heterozygous and cKO* littermates and weighed, and epididymal sperm counts assessed (Edelmann et al., 1996). For histological analysis, testes were fixed in Bouins (for H&E staining) or in 10% formalin (for all other staining and for TUNEL) overnight at 4°C. Paraffin embedded tissues were sectioned at 5 μm and processed for Hematoxylin and Eosin staining or immunohistochemical analyses using standard methods. TUNEL

staining was performed using the Apoptag TUNEL staining kit (Chemicon, Temecula CA, USA).

*Chromosome spreading and immunofluorescent staining*

Prophase I chromosome spreads and antibody staining were prepared as previously described, (Holloway et al., 2008; Holloway et al., 2011 ; Kolas et al., 2005; Lipkin et al., 2002) using antibodies from various sources. Primary antibodies and conditions used herein have been described previously (Holloway et al., 2008; Holloway et al., 2011 ; Kolas et al., 2005; Lipkin et al., 2002), except for ATR (GeneTex GTX70133), ATR/ATM substrate (Cell Signaling #5851), RAD51 (CalBiochem PC130), RNA polymerase II (Millipore 05-623, Covance MMS-129R), MDC1 and RNF8 (from Raimundo Freire, Tenerife, Spain), CDK1 (Abcam ab7954) and H3K9me3 (Millipore 07-442). Several Alexafluor™ secondary antibodies were used (Molecular Probes Eugene OR, USA) for immunofluorescent staining at 37°C for one hour. Slides were washed and mounted with Prolong Gold antifade (Molecular Probes).

*Image acquisition*

All slides were visualized using a Zeiss Imager Z1 microscope under 20X, 40X or 63X magnifying objectives, at room temperature. Fluorochromes used were Alexafluors (Molecular Probes) labeled with Cy3, Cy5 or FITC. Images were processed using AxioVision (version 4.7, Zeiss).

## 3.4 Results

*Dicer and Dgcr8 conditional knockouts are infertile and have reduced testes size and epididymal sperm number.*

To investigate the roles of miRNA and endo-siRNA populations in mouse spermatogenesis, we conditionally deleted either *Dicer* or *Dgcr8* in the germline of male mice by combining floxed alleles of these genes with the *Ddx4* promoter

driven *Cre* transgene, shown to effectively express the recombinase beginning at (e18) in mouse spermatogonia, a timepoint prior to the initiation of meiosis at around day 8pp but after the embryonic block of meiotic entry at around e12 (Gallardo et al., 2007). The benefit of this timepoint over other available *Cre* deletors is that the pre-meiotic development of the germ cells and the somatic compartments of the testis are left unaltered while ensuring all subsequent spermatocytes will have deletions prior to meiotic resumption. By crossing *Dicer*$^{Fl/+}$ cre+ and *Dgcr8*$^{Fl/+}$*cre+* males to *Dicer*$^{Fl/+}$cre- and *Dgcr8*$^{Fl/+}$*cre*- females, respectively, mice displaying the *Dicer*$^{Fl/\Delta}$ cre+ and *Dgcr8*$^{Fl/\Delta}$ *cre*- genotypes were regarded as being *Dicer*$^{\Delta/\Delta}$ cre+ and *Dgcr8*$^{\Delta/\Delta}$ *cre+* in the targeted cell types (referred to as *Dicer* and *Dgcr8* cKO, hereafter) and used for subsequent analysis along with wildtype *(WT: +/+, cre+ or cre-)* and heterozygous (Δ/+, cre+ or cre-) littermates as controls. This breeding strategy was implemented because it allows for the sequential exposure of the floxed alleles to the recombinase. The breeder animals are essentially heterozygous for the deleted allele, which is then passed on without the need for excision, thus reducing the catalytic burden on CRE protein, to ensure a more thorough excision of the target allele in cKO testis.

Initial analysis reveals no evidence for misexpression of *Cre* in non-targeted tissues (data not shown). Although exhibiting normal mating behavior, *Dicer* cKO and *Dgcr8* cKO mice are infertile as no offspring were recovered from matings to WT (C57BL/6) females over a 7-day period. At day 70pp, cKO mice from both strains showed reduced testis size in spite of being able to grow to normal body sizes and weights (*Dicer*: WT N=2, heterozygote N=4, cKO N=2 Fig 1A,B,C, *Dgcr8*: WT N=2, heterozygote N=1, cKO N=2 Fig 2A,B,C). The *Dicer* cKO testes were 29.6% of the mass of the WT littermate (p=0.0093), while the

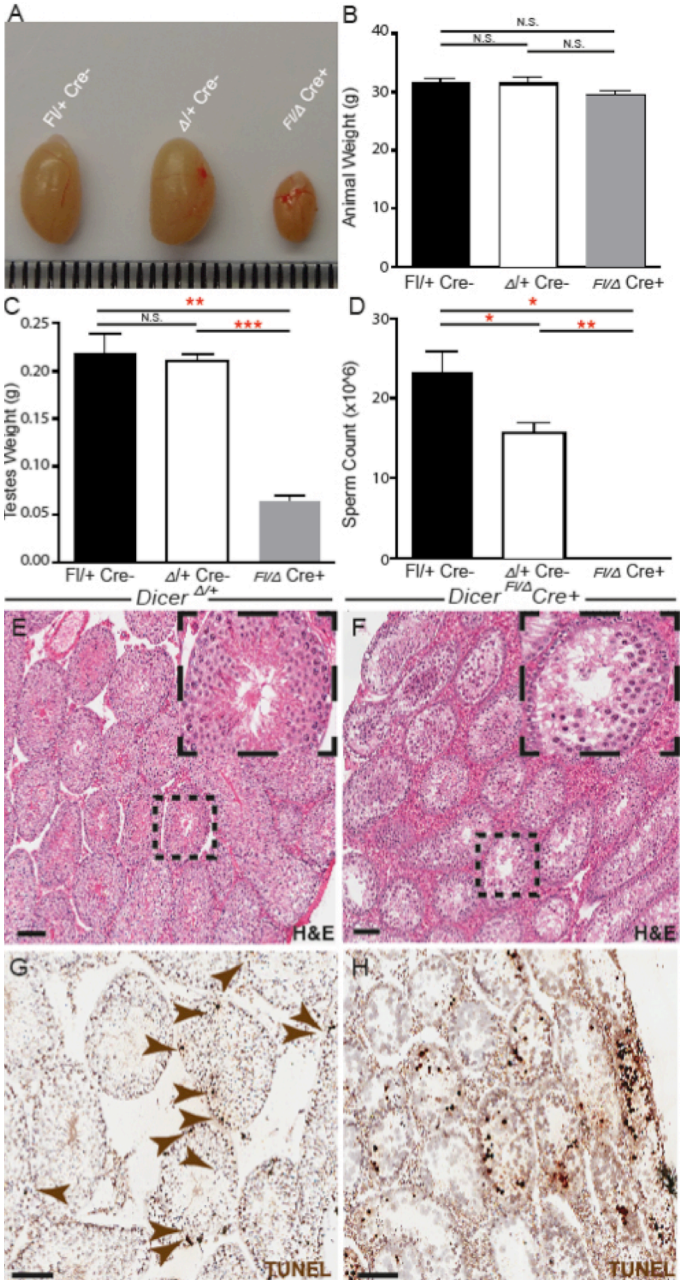


**Figure 1: Phenotypic Analysis of *Dicer* cKO males.** (A,C) Testes from *Dicer* cKO mice (Grey bars, n=2) are reduced in size compared to WT (Black Bars, n=2, **p=0.0093, t test) and heterozygous (White bars, n=2, ***p=<0.0001, t test). WT and heterozygous testes weights are not significantly different (N.S.; p=0.6765, t test). (B) Total animal weights are not significantly different from one another. (D) Caudal epididymal sperm counts shown in millions. Sperm from Dicer cKO mice were not detected while a reduction in heterozygous sperm number was reduced compared to WT (*p=0.038, t test). Error bars SEM. (E and F) Testes sections from Dicer heterozygous (E) and cKO (F) mice with H&E. Scale bars are 100uM. Vacuous tubules are prevalent in the *Dicer* cKO mice (F, inset). (G and H) TUNEL staining of testis sections from HET (G) and cKO (H) mice. Brown arrowheads serve to identifiy apoptotic cells in the heterozygous (G) samples, while positive cells are readily detectable in cKO (H).

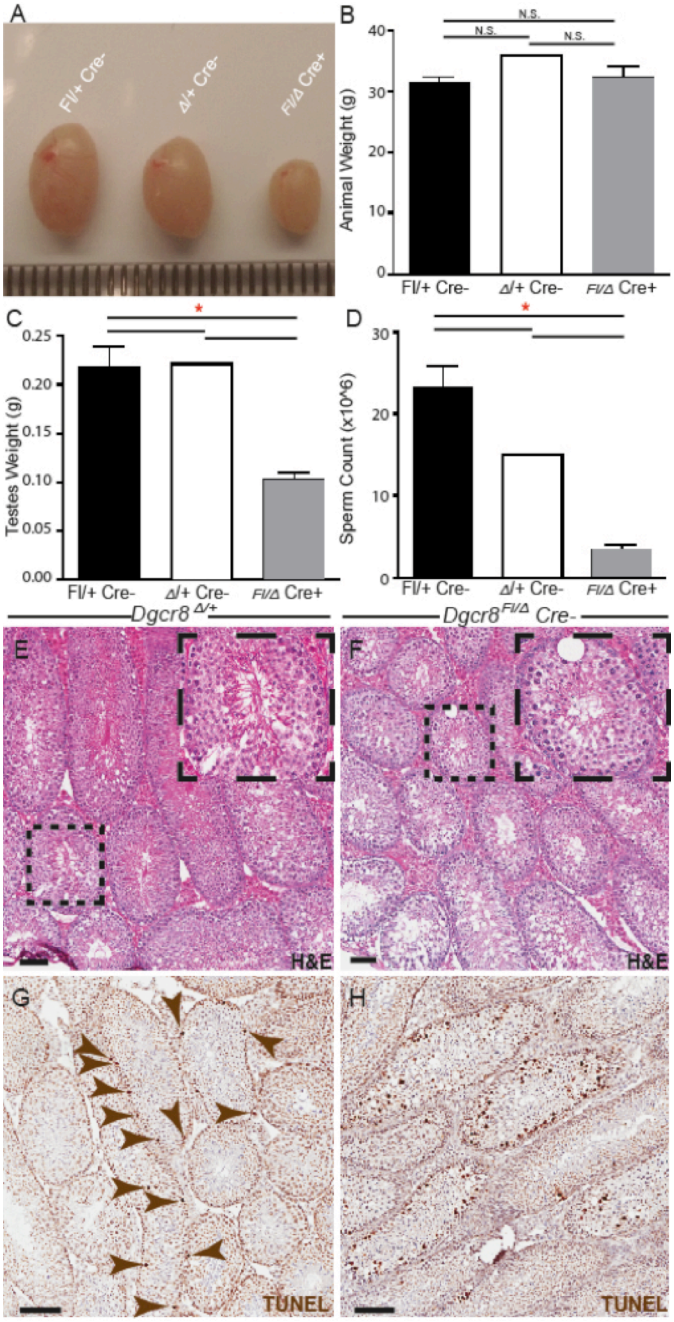


**Figure 2: Phenotypic Analysis of *Dgcr8* cKO males.** (A,C) Testes from *Dgcr8* cKO mice (Grey bars, n=2) are reduced in size compared to WT (Black Bars, n=2, **p=0.0093, t test) and heterozygous (White bars, n=2, ***p=<0.0001, t test). WT and heterozygous testes weights are not significantly different (N.S.; p=0.6765, t test). (B) Total animal weights are not significantly different from one another. (D) Caudal epididymal sperm counts shown in millions. Sperm from Dicer cKO mice were not detected while a reduction in heterozygous sperm number was reduced compared to WT (*p=0.038, t test). Error bars SEM. (E and F) Testes sections from Dicer heterozygous (E) and cKO (F) mice with H&E. Scale bars are 100uM. Vacuous tubules are prevalent in the *Dicer* cKO mice (F, inset). (G and H) TUNEL staining of testis sections from HET (G) and cKO (H) mice. Brown arrowheads serve to identifiy apoptotic cells in the heterozygous (G) samples, while positive cells are readily detectable in cKO (H).

*Dicer*$^{\Delta/+}$*( Dgcr8* heterozygote*)* showed no significant difference when compared to WT (Fig 1C). The *Dgcr8* cKO testes were 47.2% the mass of the WT littermate (p=0.0172), with *Dgcr8*$^{\Delta/+}$*(Dgcr8* heterozygote) littermates showing no difference to WT (Fig 2C).

Mean epididymal spermatozoa counts from both *Dicer* and *Dgcr8* cKOs were reduced when compared with their respective littermates. *Dicer* cKO consistently produced no epididymal spermatozoa, while *Dicer* heterozygotes had a reduction in sperm count, 67.7% compared to WT littermate (Fig 1D). The *Dgcr8* cKO displayed a comparatively less severe drop in sperm number (Fig 2D), with the cKO being able to produce 15.3% of the WT level (p=0.0176, Student's T-test), and *Dgcr8* heterozygotes producing 64.7% the WT level.

Histological examination of testes from both *Dicer* and *Dgcr8* cKOs revealed similar phenotypes in terms of cellular morphology. In both cases, the heterozygous testicular cross sections showed no discernable structural differences when compared to WT littermates, in spite of both having significant drops in sperm count (Figs 1E, 2E). The reduced testes weight in the *Dicer* heterozygote is largely consistent with published results using the same *Ddx4-cre* deletor mouse line, presumably due to defects later in spermiogenesis (Romero et al., 2011). Routine histological analysis of testis morphology in male mice that were heterozygous for the conditional deletion of either *Dgcr8* or *Dicer* revealed no obvious gross abnormalities (Fig 1E, Fig2E). However, both the *Dicer* and *Dgcr8* cKOs display structural defects throughout the mutant seminiferous epithelium. Each example has an increased frequency of vacuous tubules (Fig1F, Fig2F), however this was far more prevalent in the *Dicer* cKO (Fig1F, inset). Additionally, there were no tubules found in the *Dicer* cKO displaying fully formed spermatozoa, although these were readily detectable in the *Dgcr8* cKO

testis sections (Fig 2F, inset). The frequency of apoptotic cells per tubule, as assessed by TUNEL labeling, is also increased in both cKOs, with the *Dicer* cKO displaying a 3.58 fold increase in apoptotic cells per tubules and *Dgcr8* showing a 4.38 fold increase (Fig 3 A: *Dicer* WT mean 0.56, KO mean=2.01 p=0.0061. B: *Dgcr8* WT mean 0.6, KO mean=2.63 p=0.0008, Student's T-test). Taken together, these data show that while the *Dicer* and *Dgcr8* cKO defects are largely similar, there are subtleties in the frequency and severity of abnormalities that clearly distinguish them from one another. Although each mutant is deficient in their miRNA populations, the loss of both miRNA and endo-siRNA results in a more pronounced level of infertility, strongly suggesting that endo-siRNA participate in spermatogenic processes that do not overlap with the responsibilities of miRNAs in spermatogenesis.

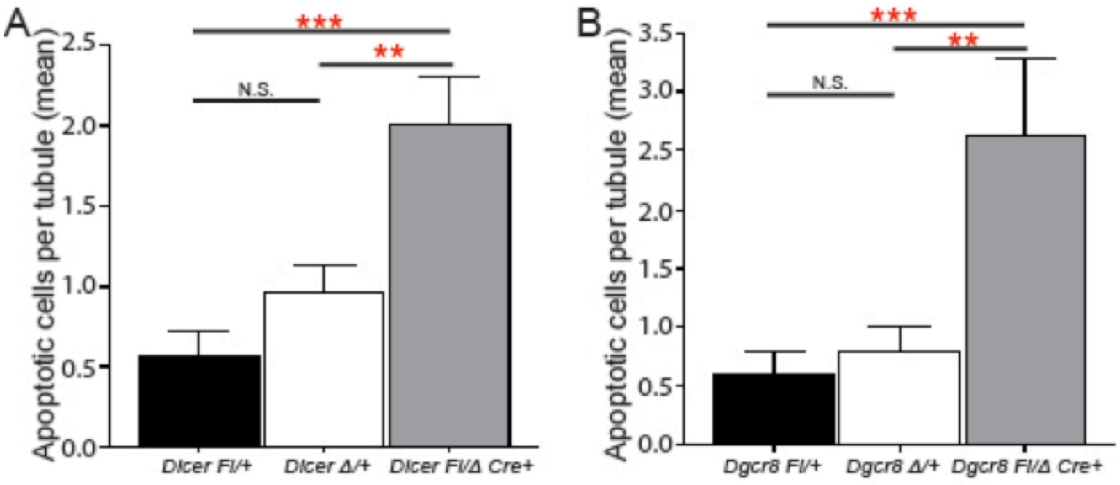


**Figure 3: Quantification of TUNEL Staining from Dicer and Dgcr8 testes sections**. (A) *Dicer* and (B) *Dgcr8* WT (Black Bars), heterozygous (White bars) and cKO (Grey bars). TUNEL positive cells were counted from 100 tubules per section to determine the mean number of apoptotic cells were tubule. In both *Dicer* and *Dgcr8* cKO testes, there were significant increases in apoptotic numbers (n=200, Dicer: 3.58 fold increase **p=0.0061. Dgcr8: 4.38 fold increase ***p=0.0008. t test). Error bars, SEM.

*Loss of DICER or DGCR8 disrupts sex body formation and localization of sex body components*

Our previous studies utilizing *Ago4*-deficient mice demonstrated that miRNAs play a role in proper meiotic silencing through meiotic sex chromosomes inactivation (MSCI) and meiotic silencing of unsynapsed chromosomes (MSUC) (Modzelewski et al., 2012). Therefore, we reasoned that ablation of most miRNAs would have a similar, if not more pronounced cytological effect. At the same time, however, our histological analysis of *Dicer* and *Dgcr8* cKO mutants revealed that loss of both endo-siRNA and miRNA components results in a more severe loss of spermatogenic cells through apoptosis than does loss of miRNAs alone, suggesting contributions from at least two small RNA populations. Thus, we turned our analysis towards determining the consequence of these losses on meiotic prophase I progression.

To evaluate the status of meiotic silencing, antibodies raised against various silencing related proteins were applied to chromosomes spread preparation generated from WT, heterozygous and cKO *Dicer* and *Dgcr8* littermates (Figs 4 and 5). To monitor the progress of prophase I spermatocytes, we immunostained for one of the lateral elements of a meiosis specific structure called the SC, or synaptonemal complex, SYCP3, which localizes between paired chromosomes at sites of synapsis. The kinase ATR phosphorylates its targets in response to DNA damage during meiotic prophase I in mouse spermatogenesis

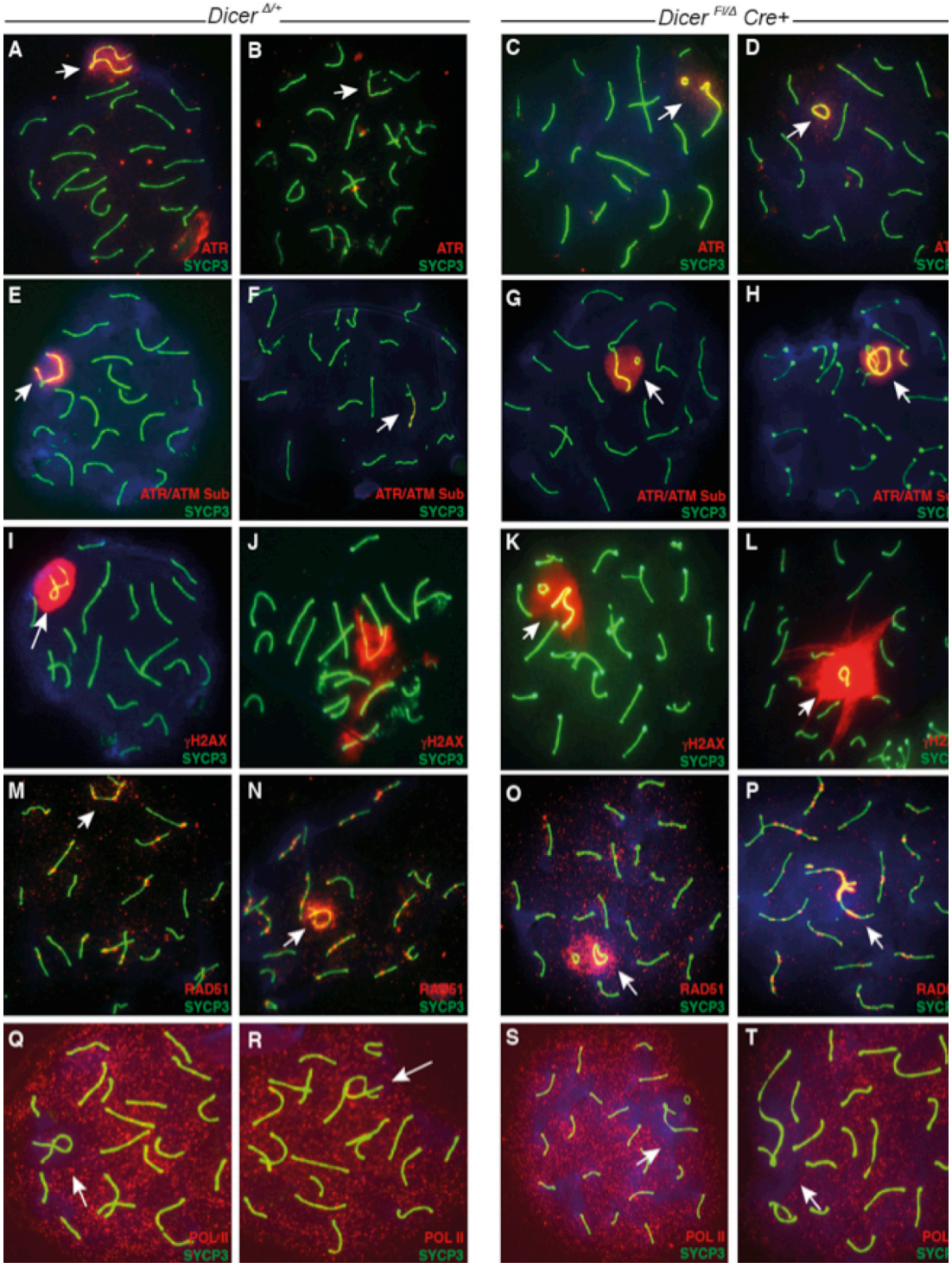


**Figure 4. Loss of DICER disrupts localization of SB associated Proteins, RNAP II and Chromosomal abnormalities at the Sex Chromosomes during Pachynema.** Pachytene staged spermatocytes with XY chromosomes (white arrows) from *Dicer* heterozygous (A,B,E,F,I,J,M,N,Q,R,U,V) and Dicer cKO (C,D,G,H,K,L,O,P,S,T) mice, stained with anti-SYCP3 (green). (A-D) anti-ATR in red. (E-H) anti-ATR/ATM Substrate in red. (I-L) anti-γH2AX in red. (M-P) anti-Rad51 in red. (Q-T) RNA POL II (POL II) in red.

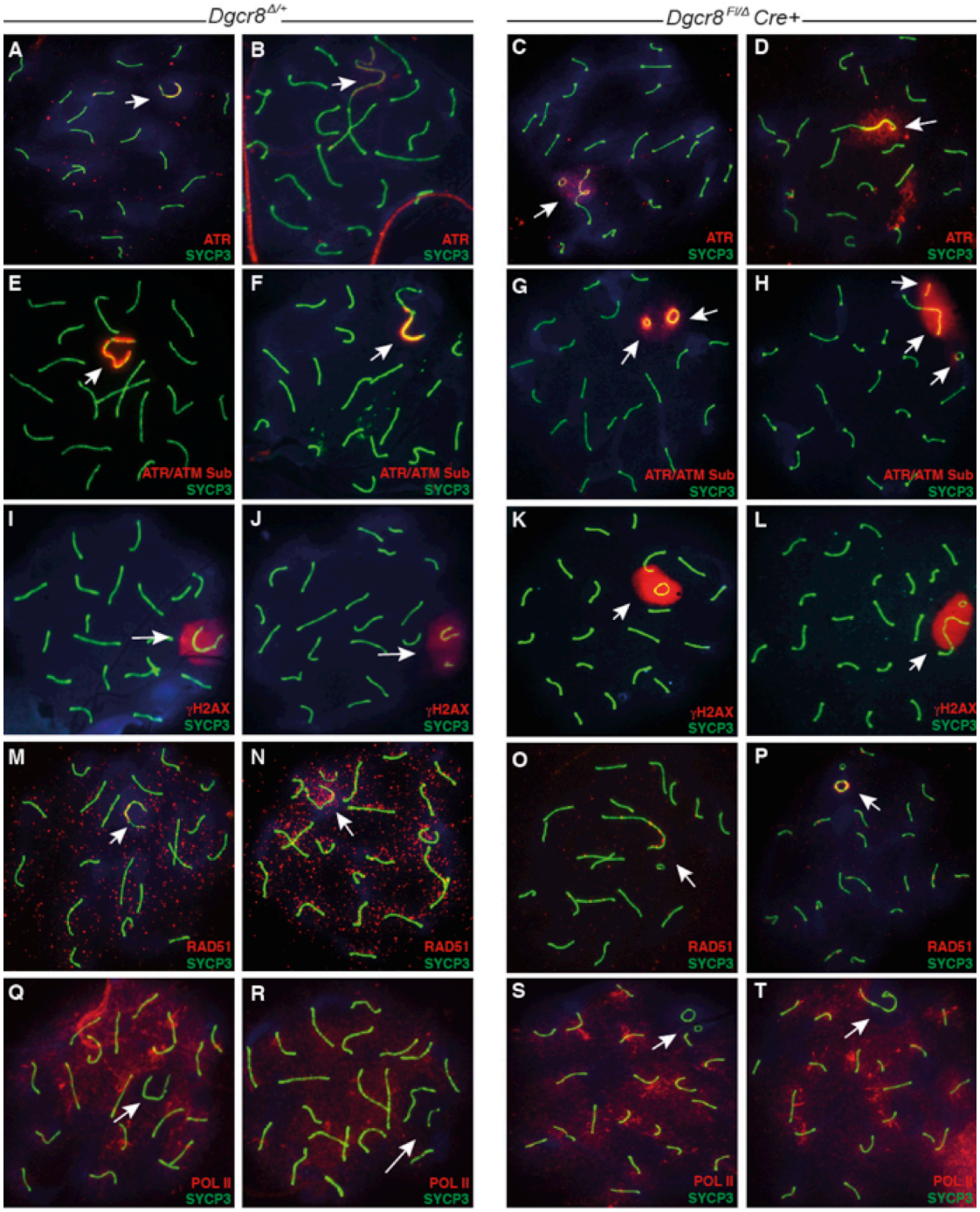


**Figure 5. Loss of DGCR8 disrupts localization of SB associated Proteins, RNAP II and Chromosomal abnormalities at the Sex Chromosomes during Pachynema.** Pachytene staged spermatocytes with XY chromosomes (white arrows) from *Dgcr8* heterozygous (A,B,E,F,I,J,M,N,Q,R,U,V) and *Dgcr8* cKO (C,D,G,H,K,L,O,P,S,T) mice, stained with anti-SYCP3 (green). (A-D) anti-ATR in red. (E-H) anti-ATR/ATM Substrate in red. (I-L) anti-γH2AX in red. (M-P) anti-Rad51 in red. (Q-T) RNA POL II (POL II) in red.

and localizes to the silenced XY domain during the pachytene stage of meiosis (Fig 4A,5A; (Royo et al., 2013). The general targets of ATR can be visualized using an antibody against the phospho-(Ser/Thr)ATM/ATR substrate motif and displays a relatively identical pattern, with the exception of the pseudo autosomal region (PAR) shared between the X and Y, in which the substrate antibody does not localize(Fig 4E,5E. (Weiss et al., 2002)). A more specific target of ATR is γH2AX, a histone variant that associate exclusively to the SB domain during pachytene of normal spermatogenesis (Fig 4I, 5I) and at sites of asynapsis at autosomes that are unable to pair properly.

In *Dicer* and *Dgcr8* WT and heterozygous littermates, ATR, ATR/ATM substrate and γH2AX localizations are largely unperturbed, with the normal appearance at the SB as well as enrichment at the XY chromosome cores, as seen by colocalization of ATR and SYCP3 (*Dicer*: Fig 4A,E,F, *Dgcr8*: Fig 5A,E,F). A subset of *Dicer* and *Dgcr8* heterozygous spermatocytes showed increased levels of SB abnormalities compared to WT (*Dicer*: Fig 4B,F,J,N,R,V. WT 4%, $Dicer^{\Delta/+}$ 9%, *Dgcr8*: Fig 5B,F,J,N,R,. WT 4%, $Dgcr8^{\Delta/+}$ 9%,), including altered sex body morphology and depletion of signal intensity at the SB. These defects were also observed previously in the *Ago4* chromosome spread analysis, although the frequency of the $Ago4^{-/-}$ reached greater than 30% of pachytene spermatocytes (Modzelewski et al., 2012). The few observed *Dgcr8* heterozygous SB defects more closely resemble the cKO abnormalities (discussed in the following section). In contrast, in both the *Dicer* cKO and *Dgcr8* cKO there were very few

phenotypically normal spermatocytes displaying unaltered ATR, ATR/ATM substrate and γH2AX localization. In this small group the X and Y take on their typical appearance and pair with each other at the PAR (Fig 6: "Paired" *Dicer cKO* 8.66%, *Dgcr8* cKO 21.41%). In fact, most pachytene spermatocytes from the cKOs show significantly altered sex chromosome conformations that frequently resulted in depleted levels or mislocalization of ATR and associated substrate localization (*Dicer* cKO: Fig 4C,D, G, H, K, L. *Dgcr8* cKO: Fig 5C,D, G, H, K, L.)

We observed several different abnormal chromosomal configurations in the *Dicer* and *Dgcr8* cKOs, but these occurred at different frequencies in each cKO strain. Typical aberrations included the fusion of either the X or Y chromosome to an autosome, the circulization of the X and Y and failure of the sex chromosomes to pair at the PAR.

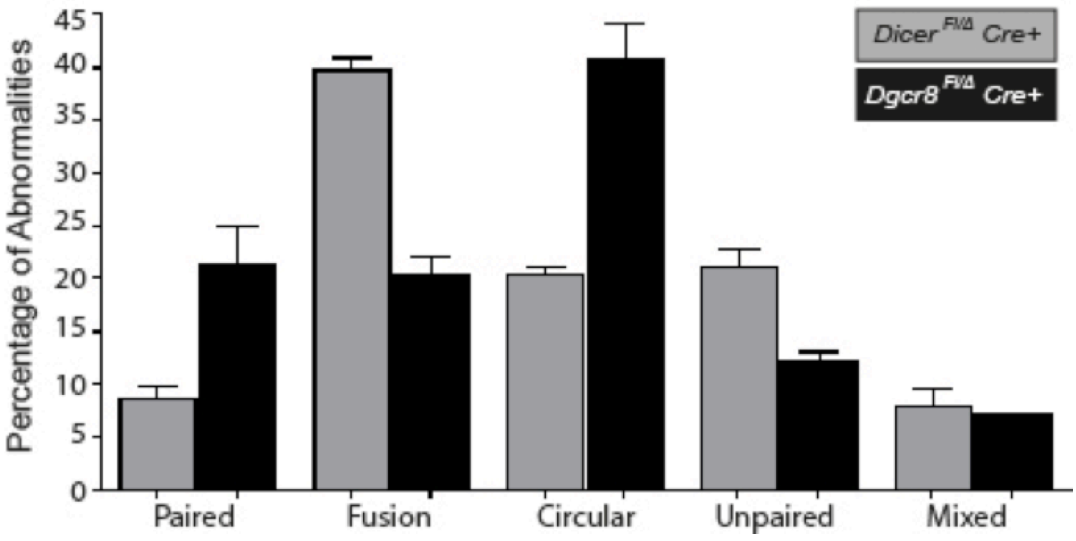


**Figure 6. Losses of Dicer and Dgcr8 have unique frequencies of chromosomal abnormalities.** Pachytene staged spermatocytes from *Dicer* and *Dgcr8* cKOs chromosome spread preparations were assessed for types and frequencies of observed abnormalities. These were distributed into five categories based on X and Y chromosomal structures.

The most abundant of these chromosomal abnormalities in the *Dicer* cKO, and second most abundant in the *Dgcr8* cKO (Fig6 "Fusion" *Dicer* cKO: 39.9%, *Dgcr8* cKO: 20.36%), is the fusion of the sex chromosome telomeres to neighboring autosomal telomeres (*Dicer* cKO: 4C,G,O,P,T,X. *Dgcr8* cKO: Fig5C,D,H,K, L,S). In some instances, the typical staining patterns of ATR, ATR/ATM substrate and γH2AX are largely unaltered in spermatocytes that display sex chromosome abnormalities and for the most part retain their exclusive X and Y chromosome localization patterns and intensity in spite of clear fusions to neighboring autosomes (*Dicer* cKO: 3G. *Dgcr8* cKO: Fig 4D, H, K, L). In various translocation and asynapsis models, the neighboring chromosome that becomes associated with the X or Y is typically engulfed by the silencing machinery and silenced as well (Heard and Turner, 2011). Here, this proper response is bypassed, presumably due to failure to detect the abnormality.

The second most frequent abnormal sex chromosome structure in the *Dicer* cKO, and the most frequent abnormality in the *Dgcr8* cKO (Fig6 "Circular" *Dicer* cKO: 20.51%, *Dgcr8* cKO: 40.72%), is the peculiar circularization of the X and Y-chromosomes (*Dicer* cKO Fig 4C, D, G, H, K. *Dgcr8* cKO Fig5C, G, K). These are present in the *Dgcr8* cKO, albeit at a lower frequency. These defects were observed under all staining conditions and occasionally both the X and Y were found in this configuration (Fig 4S, Fig 5G,O, T). An additional chromosomal abnormality observed was the complete dissociation of the X and Y from one another (Dgcr8: Fig4J,N). Given the low frequency of this type of abnormality compared to the fused and circular chromosomes (Fig6 "Unpaired" *Dicer* cKO:

21.12 %, *Dgcr8* cKO: 12.26%), presence in early pachynema and instances of partial circulization, we believe this is an intermediate stage prior to full circulization of either the X or Y. In support of this, there appears to be a clear preference for each abnormality in the two mutant backgrounds (Fig6 *Dicer*: Fusion, *Dgcr8*: Circular), additionally, in the *Dicer* cKO, there is an increased frequency of unpaired sex chromosomes compared to that seen in the *Dgcr8* cKO, suggesting that in the miRNA deficient cell (*Dgcr8* cKO), the preferred substrate for fusion is the shared telomeres of either the X or Y chromosomes, while in the miRNA and endo-siRNA deficient cell (*Dicer* cKO), the substrate shifts to telomere of the neighboring autosome, leaving a larger proportion of unpaired chromosomes unable to circularize.

These chromosomal abnormalities are not mutually exclusive. In some instances (Fig6 "Mixed" *Dicer* cKO: 7.99 %, *Dgcr8* cKO: 7.1%), spermatocytes display compound abnormalities, the most frequent of which involved a single circulization and non-autonomous fusion event (*Dicer*: Fig4C,O. *Dgcr8*: Fig5C,H,K,S), and suggest that there are parallel, multiple processes that govern chromosome structure in spermatocytes which are altered when the cell is depleted of each small RNA population.

To assess whether or not the loss or *Dicer* or *Dgcr8* impacts the initial events of prophase I, such as recognizing and processing double strand breaks and crossover formation, we investigated the localization of the RecA homolog, RAD51. Early prophase I stages in both *Dicer and Dgcr8 cKOs* show normal localization and distribution of RAD51 foci throughout the chromosomes (data

not shown). The *Dgcr8* cKO pachytene spermatocytes show slight increases in RAD51 foci formation when the X and Y chromosomal structures are abnormal in anyway (Fig5O,P). In contrast, *Dicer* cKO pachytene cells display drastically increased RAD51 localization the XY abnormalities (*Dicer*$^{\Delta/+}$: Fig 4N, cKO: Fig 4P). When both the X and Y chromosomes are circularized in *Dicer* cKO pachytene cells, the localization of RAD51 becomes unique in the sense that it switched from distinct foci along the chromosome cores (Fig4O) to diffuse staining that appears similar to sex body markers such as $\gamma$H2AX (Fig 3S). This is one of the few clear differences observed to visually differentiate the *Dicer* and *Dgcr8* cKO phenotypes, strongly suggesting that the proper localization of RAD51 at this stage of prophase I is in some part dependent on endo-siRNAs and not miRNAs.

To assess any potential issues in transcriptional activity, we investigated the localization of RNA Polymerase II (RNAP II) in the *Dicer* and *Dgcr8 cKO* animals. Normal RNAP II localization is found throughout the pachytene spermatocyte nuclei except for regions of transcriptional inactivity, such centromeres and the SB. This pattern was readily recovered in both *Dicer* and *Dgcr8* heterozygous spermatocytes (Dicer: Fig 4Q. *Dgcr8*: Fig5Q). In few spermatocytes from cKO mutants, RNAP II was found aberrantly localized within the SB domain (*Dicer* 5%: Fig 4R. *Dgcr8* 10%: Fig 5R), suggesting that in these cells, some level of derepression is occurring on the normally silenced X and Y-chromosomes. However, during instances of extreme XY abnormalities, such as X-to-autosome fusion, the *Dicer* cKO and *Dgcr8* cKO pachytene spermatocytes are

still able to retain RNAP II exclusion from the SB, while normal RNAP II staining is seen on the fused autosome (*Dicer* cKO: Fig 4S,T. *Dgcr8* cKO: Fig 5S,T), presumably maintaining the silenced status of the X and Y and the active status of the fused autosome. This observations fits well with the presence of diplotene spermatocytes in both *Dicer* and *Dgcr8* cKOs displaying these same structural defects (Fig 7 A, B), even though such altered spermatocytes would typically be recognized by the pachytene checkpoint and progression would be halted.

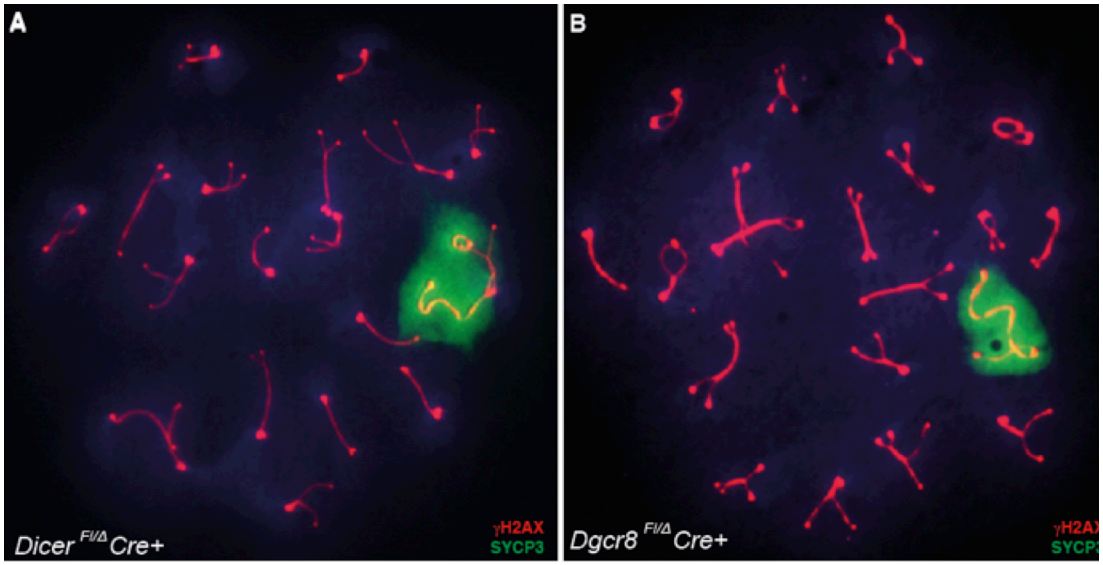


**Figure 7. *Dicer* and *Dgcr8* cKO spermatocytes are able to progress beyond pachytene checkpoint.** Diplotene staged spermatocytes stained with anti-SYCP3 in red and anti-γH2AX in green. (A) *Dicer* cKO spermatocyte with circulization of Y and fusion of X to an autosome during diplonema in which silencing mark γH2AX has spread to entire structure. (B) *Dgcr8* cKO spermatocyte in which X-chromosome is fused to autosome with clear γH2AX localization to entire captured chromosome.

These observations converge on the idea that small RNAs are intricately involved in ensuring proper meiotic progression, and their cumulative losses results in absent checkpoint monitoring. Spermatocytes with compromised sex chromosome integrity can progress well beyond the stages they in which they would normally arrest, demonstrating just how essential these small RNAs are in

not only preventing chromosomal abnormalities, but also precluding their progression in meiosis.

*Dicer and Dgcr8 loss disrupts spreading and proper placement of epigenetic modifications during prophase I*

To better understand the mechanism behind the observed spermatocyte chromosomal abnormalities seen in *Dicer* and *Dgcr8* cKO cells, we investigated the localization of proteins implicated in the recognition, spreading and output of epigenetic modifications in pachytene spermatocytes. These processes were altered in the *Ago4*$^{-/-}$ analysis, implying that small RNAs are also important for the status of epigenetic modifications during meiotic progression (Modzelewski et al., 2012).

The mediator of DNA damage checkpoint 1 (*Mdc1*) is essential for spreading of DNA damage response factors after the initial recognition of asynapsed and damaged chromosome axis by TOPBP1, ATR and γH2AX (Ichijima et al., 2011). *Mdc1* has also been implicated in non-homologous end joining (NHEJ) of dysfunctional telomeres and involves its interaction with both γH2AX and RAD51 in non-meiotic cells (Dimitrova and de Lange, 2006). In WT spermatocytes, MDC1 localization is identical to that of γH2AX. In either *Dicer* or *Dgcr8* heterozygous and cKO spermatocytes, the depletion of MDCI at the SB is observed in a subset of pachytene spermatocytes (*Dicer*: 5%, *Dgcr8*: 10%, Fig8A), while the majority of both *Dicer* and *Dgcr8* heterozygous samples display normal MDC1 accumulation. The *Dicer* and *Dgcr8* cKO samples routinely display unaltered MDC1 localization at the SB when XY abnormalities are present (*Dicer*

Fig 8B, *Dgcr8* Fig 8D). Importantly, it has been reported that the loss of *Mdc1* in spermatocytes results in the association of the X chromosome to autosomes as well as the inability of the X and Y to associate with one another (Ichijima et al., 2011), two phenotypes observed in both the *Dicer* and *Dgcr8* depleted spermatocytes.

The ubiquitin E3 ligase, RNF8 is known to interact with MDC1 and ubiquitinates histone in response to DNA damage, although the purpose of these marks is not known (Lu et al., 2010). RNF8 localizes to the SB in pachynema (Fig 8E). Interestingly, spermatocytes from *Dicer* or *Dgcr8,* heterozygote or cKO, display very minimal SB localization of RNF8 and this is instead replaced by the presence of "flares" along most autosome that originate from the axis and expand out into the chromatin (*Dicer* Fig 8F, *Dgcr8* Fig8G, H) suggesting that proper RNF8 placement is at least partially dependent on small RNAs.

The cyclin-dependent kinase 2 (*Cdk2*) has also been implicated in proper sex chromosome formation along with homologous pairing and recombination in mouse spermatocytes. Interestingly, the loss of Cdk2 results infertility and the drastic increase of non-homologous sysnapsis and eventual arrest at the mid pachytene checkpoint. An additional feature of *Cdk2* loss is the appearance of fusions and ring chromosomes, which are very similar to the abnormalities described here, however published reports of the Cdk2 deficient spermatocytes show that their observed ring structure did not consist of the X or Y. The researchers attributed these abnormalities to a role for Cdk2 in proper telomere maintenance and homeostasis (Ortega et al., 2003), (Viera et al., 2009). In WT

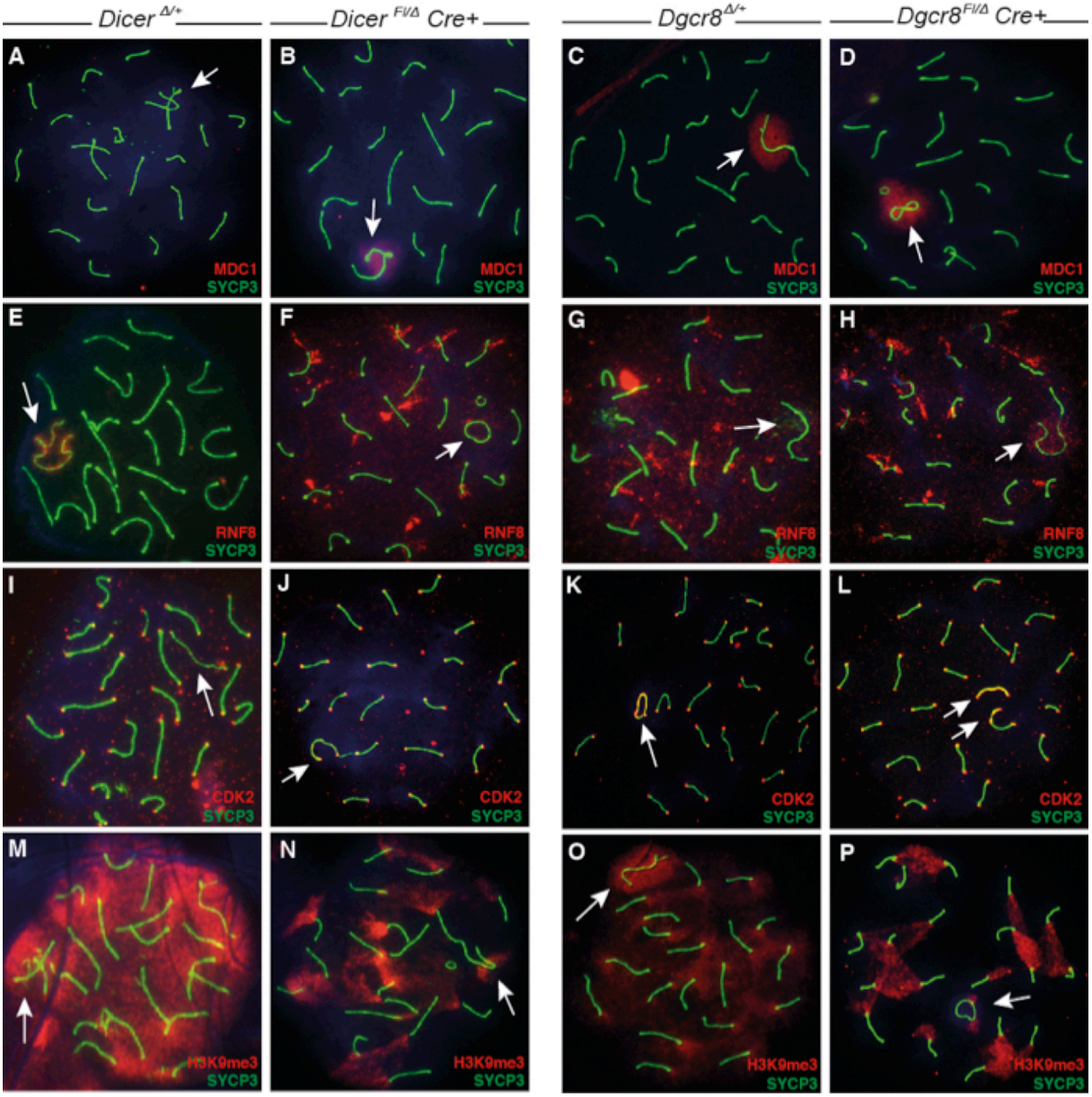


**Figure 8. Loss of DICER and DGCR8 disrupts localization of proteins associated with recognizing, spreading and placement of epigenetic marks in pachytene spermatocyte.** Pachytene staged spermatocytes with XY chromosomes (white arrows) from *Dicer* heterozygous (A,E,I,M,Q,), *Dicer* cKO (B, F, J, N, R), *Dgcr8* heterozygous (C,G,K,O,S) and *Dgcr8* cKO (D,H,L,P,T) mice, stained with anti-SYCP3 (green). (A-D) anti-MDC1 in red. (E-H) anti-RNF8 in red. (I-L) anti-CDK2 in red. (M-P) anti-H3K9me3 in red.

spermatocytes, CDK2 appears normally at telomere and can be seen at recombinations modules (Ashley et al., 2001), and these patterns are observed in the *Dicer* and *Dgcr8* WT, heterozygous and cKO pachytene spermatocyte (Fig 5I,J Fig6I,J). In WT, unaltered spermatocytes and in cKO samples with fused chromosomes, CDK2 localization is barely detectable on the unpaired XY axial regions (Fig 8I,J), however in both *Dicer* and *Dgcr8* cKO spreads, most unpaired and circularized X and Y chromosomes cores display intense CDK2 localization (Fig 8K,L). These results suggest that while autosomal chromosome checkpoints appear largely intact, mechanisms governing the X and Y are perturbed, presumably due to the loss of miRNAs and potentially endo-siRNAs.

Another important aspect of meiotic progression is the proper placement of epigenetic histone modifications. One such modification is Histone 3 Lysine 9 trimethylation (H3K9me3); a mark typically associated with repressed heterochromatin and is primarily restricted to autosomal centromeres and the majority of the SB in WT pachytene spermatocytes (Kim et al., 2007; Tachibana et al., 2007). In *Dicer* and *Dgcr8* heterozygous and KO animals, the mislocalization of H3K9me3 throughout the entire meiotic nuclei is present (Fig8M), however the occurrence of this level of mislocalization is far outnumbered the seemingly unaltered localization in spermatocytes that display the XY chromosomal abnormalities (*Dicer*: Fig 8N. *Dgcr8*: Fig 8O.P). These findings are consistent with previous observations in this analysis, in which the near total ablation of miRNAs and endo-siRNAs results in the generating and masking of chromosomal

abnormalities that would normally be unable to progress beyond the pachytene checkpoint.

## 3.5 Discussion

The aim of the current study was to improve our understanding of how small RNA mediated events participate in and contribute to the process of MSCI. Our studies of *Ago4* mutant animals (presented in Chapter 2) revealed unexpected additional roles for small RNAs in the nuclei during male gametogenesis, specifically in meiotic initiation and in sex body formation during prophase I, leading to loss of meiotic silencing.

The studies reported here demonstrate roles for both miRNA and endo-siRNAs in mammalian spermatogenesis. These data support a model in which small RNAs participate in multiple processes in the developing spermatocyte. As seen previously with the *Ago4*$^{-/-}$ animal, both conditional deletions of *Dicer* and *Dgcr8* in male germ cells result in the altered silence status of the X and Y-chromosomes. Unlike *Ago4*$^{-/-}$, here we report the loss of chromosomal integrity of the X and Y, failure to pair at the PAR, and incorrect telomere maintenance, leading to the fusion of sex chromosomes to autosomes and circularization of the X and Y, suggesting that the role of small RNAs are not limited to initiating and maintaining meiotic silencing as seen by deleting *Ago4*, or perhaps, these roles are in fact related and the loss of a single Argonaute was not enough to reveal additional roles for small RNAs in the spermatocyte nuclei.

In the current study, however, most of the *Dicer* and *Dgcr8* cKO mice displayed seemingly normal sex body protein localization, and presumably repression of the X and Y, in spite of severely altered sex chromosome structural abnormalities. More than likely, given our proposal of functional specificity for

the germ cell Argonautes, the loss of a single Argonaute is not enough to disrupt all the small RNA mediated processes active in spermatocytes, and the remaining three AGOs were not sufficient to fully compensate for *Ago4* loss, implying that either each Argonaute has distinct roles, or that specific small RNAs are involved in distinct functions and associate with individual AGO proteins. Indeed, *Ago2* conditional deletion in primordial germ cells has been reported, but no meiotic defects were detected and therefore a prophase I investigation was never initiated (Hayashi et al., 2008). Although this report used an earlier expressed *Cre* line (e10 vs. e18) and a different breeding strategy, it implies that endo-siRNAs may function to regulate certain processes but defects in these processes may be tolerated in the developing spermatocyte. However a more thorough investigation into *Ago* gene loss is necessary to fully understand the role of miRNA and endo-siRNAs in spermatogenesis. Another approach to understand the functions of miRNA and endo-siRNAs in male meiosis is to remove key components of the small RNA biogenesis pathways, thus removing most of the miRNA and endo-siRNAs, as seen in this report.

Interestingly, the *Dicer* and *Dgcr8* cKO phenotypes are not identical. Both genes are involved in canonical miRNA biogenesis, however only *Dicer* deletion would impact endo-siRNA production. Presumably the only difference between these two animals is the presence of endo-siRNAs, so it is therefore reasonable to predict that the differences in phenotypes observed between *Dicer* and *Dgcr8* in fact reflect the role of endo-siRNAs in spermatogenesis. These results are surprising, given the previously published work on *Dicer* deletion at the same timepoint (Romero et al., 2011), (Liu et al., 2012). One technical difference between this report and those previously published on *Dicer* deletion is the breeding strategy. Previous reports generated testes specific conditional alleles

in *Dicer*$^{Fl/Fl}$ *Ddx4-Cre*+ males, in which the recombinase must excise both alleles in the same genome. The strategy presented here relied on mice inheriting an already excised allele, Dicer$^{\Delta/Fl}$ *Ddx4*-Cre+ males, thus lessening the enzymatic burden on the recombinase to increase excision efficiency. Nevertheless, these studies reported no prophase I defects, but their assessments were limited to the presence or absence of spermatocytes progressing beyond the typical checkpoints activated in response to synaptic or silencing issues. The data presented here shows that while both *Dicer* and *Dgcr8* cKOs show multiple chromosomal abnormalities, they are able to bypass this checkpoint and eventually arrest at later stages. Our data suggest that massive small RNA-related misregulation at prophase I compromise these checkpoints and allow for the progression of highly altered spermatocytes. We believe the previous reports on *Dicer* deletion were unaware of the prophase I defects for this reason.

Although the *Dicer* cKO had comparatively more severe meiotic phenotypes, both *Dicer* and *Dgrc8* conditional deletion mice are infertile and display largely similar abnormalities. In terms of a causal explanation, both mice are lacking in miRNAs during spermatogenesis. Based on the similarities of chromosomal abnormalities, we believe the majority of these defects result from misregulation of miRNAs. The key distinction is the frequency in which these abnormalities occur in either mutant as well as which abnormality is more prevalent. These differences strongly imply that while the role of endo-siRNAs may be overshadowed miRNAs, endo-siRNAs regulate a distinct subset of meiotic processes.

The loss of *Ago4* uncovered just one of the many roles of small RNAs in spermatogenesis, specifically meiotic silencing of sex chromosomes. We predict that similar prophase I phenotypic analyses of individual deletions in the

remaining *Ago* genes would uncover the remaining processes. Deletion of all four Argonautes would most likely recapitulate the *Dicer* cKO phenotype, such that miRNA and endo-siRNAs would be present within the spermatocyte nuclei but not utilized. Indeed, evidence from our lab suggests that small RNAs are not only present in the nucleus, but take on specific localization patterns. These studies are underway in our lab and are aimed at further understanding the overall contribution of small RNA mediated regulation in spermatogenesis.

## 3.6 Acknowledgements

This work was supported by the Vertebrate Genomics Center at Cornell University (VERGE predoctoral award to S.H.) and by funding from the NIH to P.E.C. (HD041012 and GM grant). A.M. was supported by NIH training grants in Genetics and Development (T32GM00761), and in Reproductive Genomics (T32HD052471); S.H. was supported by an NIH training grant in Biochemistry, Molecular and Cellular Biology. The authors acknowledge with gratitude the generosity of Dr. Mary Ann Handel (The Jackson Laboratory) for providing the anti-H1T antibody, Dr. Raimundo Freire (Tenerife, Spain) for providing the anti-MDC1 and RNF8 antibodies. We are grateful to Ian Welsh for technical advice, and to Ewelina Bolcun-Filas, Jen Grenier, Kim Holloway, and Mark Roberson for reading this manuscript and for helpful suggestions. We also thank Kim Holloway for extensive guidance in preparing figures and editorial assistance. We thank Peter L. Borst for assistance in mouse care.

# CHAPTER 4

## Concluding Remarks & Future Endeavors

Small RNA mediated regulation exists in many forms and in virtually every eukaryotic organism studied. RNAi mechanisms have been intensely investigated and, while great advances have been made in the past decade, very little is known about how these systems operate in the mammalian system, particularly *in vivo*. It was originally presumed that RNAi was a solely cytoplasmic phenomenon in the mammalian cell, even though examples of transcriptional gene silencing (i.e. non-cytoplasmic) events had been demonstrated in lower eukaryotes. One of the major findings of the work presented here, therefore, is that not only do RNAi components enter the nuclei of mammalian spermatocytes, but function in ways that are closely related to ancient mechanism found in the distantly related eukaryotes fission yeast, fruit fly and roundworm. In the past few years, evidence emerged that nuclear RNAi components were not just some interesting artifact of largely synthetic cell culture studies, and that during normal cellular processes these components shuttle in and out of the nucleus, and presumably function in some manner (Ahlenstiel et al., 2011; Robb et al., 2005). These discoveries are very recent and emphasize that our current understanding of RNA mediated regulatory events is lacking. In order to better understand the molecular mechanism of RNA mediated regulatory events, an important approach is to use the knowledge from cell culture systems as well as the open mindedness to entertain the possibility that mammals may use similar RNA mediated regulatory mechanisms as the model organisms. It also reasonable to consider that over the course of evolution, the highly specialized aspects of biology could have developed variations of the RNAi core process. The germline is arguably the most

critical system in terms of ensuring the survival of a species, and would therefore benefit from the variety imparted from nearly one billion years of co-evolution with RNAi components. I feel that my research keeps these ideas in mind, and only by thoroughly, and some times obsessively, exploring the extremes; we will be able to better understand every aspect of biology.

The work presented here encompasses two main bodies of work that focus on the role of small RNAs in the male mouse germline. In Chapter 2, I characterized the loss of the small RNA binding protein, AGO4, in the male meiosis. Although this mouse is a complete knockout, resulting in no protein production, it displayed no overt phenotype that we were able to assess on initial inspection. It was difficult to accept that this incredibly ancient and well-conserved protein could be lost or changed without so much a minor phenotype. More so, *Ago4* is most highly expressed in pachytene spermatocytes. It was not until five generations of backcrossing and many routine phenotypical evaluations later that the consequence to *Ago4* loss began to emerge. In spite of no change in body weight, the testes of the mutant mice became progressively smaller than the WT littermates at each successive backcross, and apoptotic cells were more prevalent in the KO at generations beyond P4. This may be due to some background effect, going from the original ES cell 129/BL6 mixed background into the C57BL/6 pure background. However, the possibility of an epigenetic effect manifested over progressive generations cannot be ruled out. To distinguish between these two possibilities, and in collaboration with another lab member, I have initiated an outcrossing study in which the *Ago4* allele is crossed onto different mouse strains, including 129, PWD, and castaneus, each exhibiting different recombination frequencies (Lynn et al., 2002). The hypothesis is that an epigenetic effect would result in the emergence of the $Ago4^{-/-}$ phenotype across

each outcrossed line as the effect of *Ago4* loss accumulated over time. If there were a background effect, the *Ago4*$^{-/-}$ phenotype would never emerge, for example, in the 129 line, the parental ES cell line from which the original chimeric animal donor cells were derived, suggesting that additional factors not present in each strain contribute to the requirement of AGO4.

Given the localization and high level of expression of *Ago4* during pachynema, we had expected more spermatocytes would have been affected than the 30% we observed. This result guided us to look at the remaining Argonuates, as they share a large degree of similarity and conservation. Indeed, the levels of *Ago3* transcripts are significantly increased in the *Ago4*$^{-/-}$ mRNA profile, presumably sharing some functions with AGO4, or more specifically, interacting with a similar group or class of small RNAs that are essential for meiotic progression. Described in Appendix I, I have generated an *Ago314* triple knockout mouse line. This line is currently in the process of breeding to mice that express the appropriate tissue-specific *Cre* recombinases and should be available for analysis later this year. One prediction is that the meiotic phenotype will be assessed at least at the same level as the *Ago4* defect, since *Ago2* will be intact and presumably compensate for the loss of the three non-slicing *Agos* in the miRNA pathway. The compound deletion of all four Argonautes will most likely result in the loss of fertility we set out to generate at the onset of this investigation, perhaps recapitulating the *Dicer* cKO phenotype (Chapter 3)

The full extent of the *Ago4* phenotype did not become clear until a more thorough analysis was done involving cytology and immunofluorescence. In about 30% of all pachytene spermatocytes, the normally silenced sex body took on a dismorphic appearance. The presence of RNA POL II in this normally repressed domain suggested a loss of silencing. We found that the loss of

silencing did not massively derepress the X and Y, but instead released transcripts that are toxic to the spermatocyte.

It was during this part of the analysis that we discovered an additional role for *Ago4* in the male germline. Originally we included day 3pp and day 8pp testes as non-meiotic controls for support cells and since *Ago4* expression was low at this timepoint, we did not expect any appreciable change, but the mRNA-seq profiles were too altered to ignore. We found that the retinoic acid (RA) meiotic induction pathway was prematurely activated in the mutant testes and this resulted in mice entering meiosis 5 days early. The exact mechanism behind RA induced meiotic initiation is not clear, as multiple sources of RA exist in the context of the germline. The analysis presented in chapter 2 briefly touched on the idea of a non-autonomous role for AGO4 in RA signal transduction between germ cells and sertoli cells. Such a process may involve either the transport of small RNAs or an AGO: small RNA complex between cell types. This is a topic that the Grimson lab is now aggressively pursuing by use of massive parallel sequencing on a developmental time course between *Ago4* WT and KO littermates.

Since *Ago4* binds small RNAs, we wanted to see if AGO4 loss was altering their steady state levels by small RNA cloning. Together with Andrew Grimson's lab, we sequenced small RNAs from isolated spermatocytes and found that nearly half of all the miRNAs were missing, and 20% of these losses originated from the X-chromosome. This finding is particularly interesting because of the AGO4 localization and the observation that only miRNA clusters are able to escape the silencing effects of MSCI. We ended the analysis with an additional technique to confirm the small RNA sequencing data set. Using probes specific to the mature miRNAs that changed the most, we found that not only were they indeed missing

in the altered spermatocytes, but also they took on very distinct localization patterns.

This final aspect of the initial AGO4 analysis is the basis of Appendix II and our attempt to uncover the mechanism of silencing at the sex body and potentially throughout male meiosis. Importantly, the novel finding presented thus far is not only the presence of small RNAs and AGO4 in the nucleus, but implied function based on their localization and phenotypes. Others have reported on such finding in the past, but these are presented as more peculiarities and possible cell culture artifacts in their synthetic systems (Morris et al., 2004), (Ting et al., 2005), (Kim, 2006). In contrast, the AGO4 analysis shows a possible small RNA mediated transcriptional regulatory mechanisms in an intact mammalian system.

Appendix II aims to further validate the small RNA cloning results by looking at the abundance and localization of miRNA that originate from both the X chromosome and autosomes. The distinct localization patterns of these miRNAs imply a potential mechanism for how silencing occurs. Since they are lost when AGO4 is missing, it is possible that during this stage of meiosis, they have preferential affinity for individual AGOs. These small RNAs would provide the sequence specificity required to target just the X chromosome during normal meiotic progression. The fact that miRNA clusters can escape silencing provides the target for these miRNAs to bind to. A recent report in *C. elegans* showed that a very similar sequence of events occurs that allows mature Let7d to regulate the processing of its own precursor in the nucleus (Zisoulis et al., 2012). Similarly, AGO4 would then take on a role similar to its fission yeast counterpart in a RITS-LIKE complex and direct local chromatin remodeling events, initiating silencing

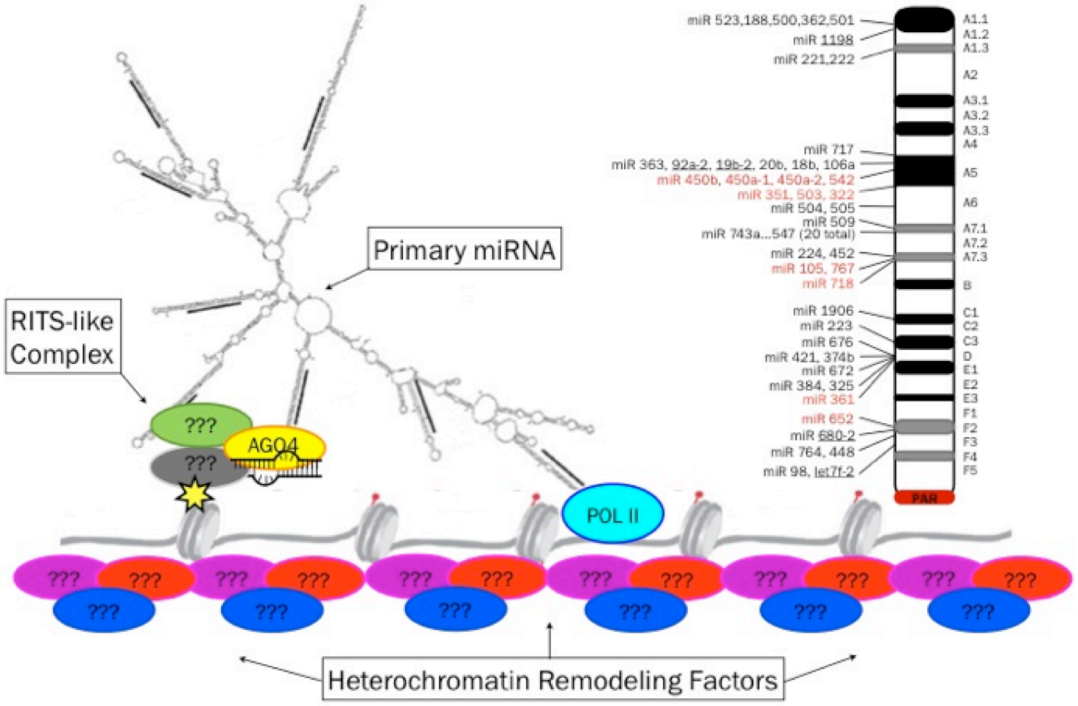


**Figure 1. Model for RITs-LIKE meiotic silencing by AGO4 and miRNAS at the X-Chromosome.**

at the immediate region. The spreading ability of meiotic silencing would then take into effect and maintain proper MSCI (Figure 1).

The work started in appendix III expands on the idea of determining the mechanism of small RNA mediated meiotic silencing. There are quite a few gaps in the logic of the presented model. Most of which rely on figuring out where AGO4 fits into what has already been established as being involved in meiotic silencing. The approach we have decided to take is to use Laser Capture Micro-Dissection (LCMD) to unbiasedly determine what proteins are present in this domain. As of yet, the analysis is focused on C57BL/6 samples, but will eventually move towards understanding what the loss of AGO4 has on the protein population at the sex body, since our research shows that certain sex body components fail to localize in the absence of AGO4. Perhaps even more exciting

than knowing the proteins present at the sex body is to determine if and what RNA species exist there. Given the silenced nature of the X and Y during pachytene, it is expected that we will recover no nascently transcribed RNA. However, with the discovery that the miRNA clusters escape this silencing, it becomes a very promising investigation. The model presented above suggests that the miRNA clusters serve as docking sites for miRNA transcriptional targeting, which serves as a tempting and convenient hypothesis. Although not thoroughly characterized yet, it is thought that a large number of Long Intergenic Non-coding (Linc) RNAs are highly expressed during meiosis. These lincRNAs may instead serve as the docking site or perhaps a more structural role, similar to that seen in X-inactivation in female nuclei. In addition, small RNA cloning will be attempted to determine if any mature miRNAs are present, in support of the miRNA FISH experiments described above. Taken together, the list of proteins, small RNAs and their potential targeting of sequenced RNAs at the sex body would allow us to begin developing a network of participants involved in the novel mechanism of meiotic silencing in the spermatocyte.

Appendix IV expands beyond the scope of the sex body and into the related mechanisms of MSUC. Based on X-Inactivation and MSCI, it is feasible that the X chromosome has some inherit property that makes it the chromosome of choice for silencing. Rather than having multiple silencing reaction centers, the cell may just have one, and the spreading ability of repressive chromatin marks can be used to silence the remaining chromosomes that seldom require such a response. The Ts($17^{16}$)65Dn model was used for this purpose because it involves the translocation of segments from chromosomes 16 and 17. These segments are small and do not seem to hinder the development of the animal. More importantly, the mouse is infertile but progresses to pachynema. For these

reasons, this is an excellent model to study MSUC. Preliminary results support the idea of an X-Inactivation center, as nearly all spermatocyte show the translocation event either within the sex body or directly adjacent to this domain. A pilot study of small RNA sequencing detects massive small RNA population changes in the early spermatocyte fraction, just prior to pachynema. This would coincide with the establishment of silencing in which various regions of the genome are selected for activity or repression.

Chapter 3 takes a step away from the fine focused effort of determining the exact mechanism of meiotic silencing. Instead, we are interested in understanding the effect of global small RNA loss on spermatogenesis. The *Ago4* phenotype displayed losses of small RNAs, but were these causal or consequential for the drop in fertility? There is no doubt that small RNAs are important, but what species of small RNAs and when? To answer these questions we began a parallel investigation into the meiotic phenotypes of *Dicer* and *Dgcr8* loss at e18, a timepoint prior to the initiation of meiosis and should effectively produce germcells devoid of small RNAs. The underlying strategy is to produce samples that have distinct small RNA profiles. The *Dicer* deficient testes would be devoid of canonical miRNAs and presumably all endo-siRNAs, while the *Dgcr8* deficient testes would be lacking only the miRNA population. Inspiration for this research stems from the literature based on similar conditional deletions, which at some times becomes confusing and contradictory. Research from the oocyte describes that in spite of miRNA abundance, their function is suppressed until early embryo development, and it is the endo-siRNAs that are responsible for ensuring proper oogenesis. Preliminary results from this chapter suggest that both populations function in spermatogenesis and have largely non-overlapping responsibilities. The miRNAs appear to be the small RNA species associated with

the majority of meiotic phenotypes, however, removal of only endo-siRNAs at this point is not technically possible, given the overlapping biogenesis pathways. Therefore a thorough investigation into the role of endo-siRNAs cannot yet be made.

Here, I have presented evidence to support a nuclear role for Argonautes and small RNAs in inducing transcriptional gene regulation in the mammalian spermatocyte. The cumulative efforts described here support the existence of a RITS-like mechanisms operating in the meiotic nuclei that is in some ways similar to the RNAi mechanism that exists in various lower eukaryotes. In the past decade, our understanding of how small RNAs functions has been developing and is just now provided the framework to investigate their roles in intact biological systems. There is no doubt that as these types of analyses continue and grow, additional specialized small RNA based mechanisms will emerge. Our concerted efforts work together to better understand the complicated and intricate regulatory networks that exist in every living organism. Once we are able to better grasps the various levels of regulation, we will be better suited to approach every important biological issue.

APPENDIX I

## Generation of Ago3-1-4 Mutant Mice

This work was conducted by Andrew J. Modzelewski in 2009-13 to evaluate relationship between the three non-slicing Argonautes, *Ago1*,3 and 4. This work will eventually be inherited by a new member of the Cohen lab after the primary researcher has begun his Post Doctoral position.

### Summary

During the analysis of the *Ago4*$^{-/-}$ mouse line, it was determined that *Ago3* transcript and protein levels were significantly increased in the testes (Modzelewski et al., 2012). This raised the possibility that the remaining 3 Argonautes (*Ago1,2,3*) may be partially compensating for the loss of *Ago4*. The *Ago2* cKO was generated using a *Tnap*-Cre system that excises at e10 in primordial germ cells. No meiotic phenotype was reported, however an examination of prophase I was not made (Hayashi 2008). A prediction is that although there was no fertility defect reported, a similar or lesser level of disrupted silencing was actually taking place. The *Ago4* phenotype did not fully emerge until at least five backcrosses, and it is unlikely that many groups would carefully monitor a conditional deletion for such an extended period of time. Additionally, the *Ago1,3* total knockout was recently generated (Van Stry et al., 2012). Like *Ago4*, this animal displays no overt phenotype, even though two of the miRNA effectors are deleted. The authors report no fertility defect, but this was assessed only by litter size and not a thorough meiotic phenotypical analysis. However, the expression level of *Ago4* was determined to have increased in

various tissues in the *Ago1*,3 KO, but no mention of testes expression was made. Another prediction is that, like the *Ago4* deletion, there was a spermatogenic defect but was overlooked.

Since *Dicer, Dgcr8* and *Drosha* testes specific deletions all result in spermatogenic arrest; it is therefore reasonable to predict that miRNAs must play some essential role in spermatogenesis. As the only known effectors of miRNA mediated regulation, the Argonautes are most likely involved in essential meiotic processes, but share certain overlapping responsibilities, given the lack of individual knockout infertility. Taken together, it is likely that the deletion of all three non-slicing Argonautes will not produce an infertile animal and will result in spermatogenic defects either similar or more severe than the ones associated with *Ago4* loss, since 75% of the miRNA effectors will be lost.

To this end, an animal lacking the three non-slicing Argonautes is being generated to answer some of the questions and test the predictions presented in this analysis. The highly conserved genes encoding the three non-slicing Argonautes lie in tandem (*Ago3*, then *Ago1* followed by *Ago4*) in a 150kb region on mouse chromosome 4 (Fig1). Using standard mouse mutagenesis techniques, additional features were added to the ES cell lines used to generate the original *Ago4*$^{-/-}$ line. These features consist of a *pgk2-hyg/neo* cassette, flanked by *Frt*-5 sites, (modified so as to not recombine with existing Frt sites), with a single Lox-P immediately 5' to the cassette. This construct was inserted downstream of the final *Ago3* exon and designed to recombine with the existing Lox-P site found in intron 2 of *Ago4*. ES cells were screened via Southern blot using probe sequences

specific to the region immediately upstream of the construct and extending into the antibiotic resistance cassette (Data not shown). Chimera mice were tested by PCR amplification using primers specific to the construct. Germline transmission was confirmed by the same approach (Figure 2). Following FlpE and CRE mediated excision; the entire 150kb region will be deleted, removing all three non-slicing *Ago* genes. In case of embryonic lethality, *Ddx4*-Cre will be used to delete the construct, as the expression is restricted to spermatogonia. If fertile, the mice will be bred to homozygosity to the C57BL/6 background and total knockout will be assessed in terms of any overt phenotype and specifically meiotic phenotypes.

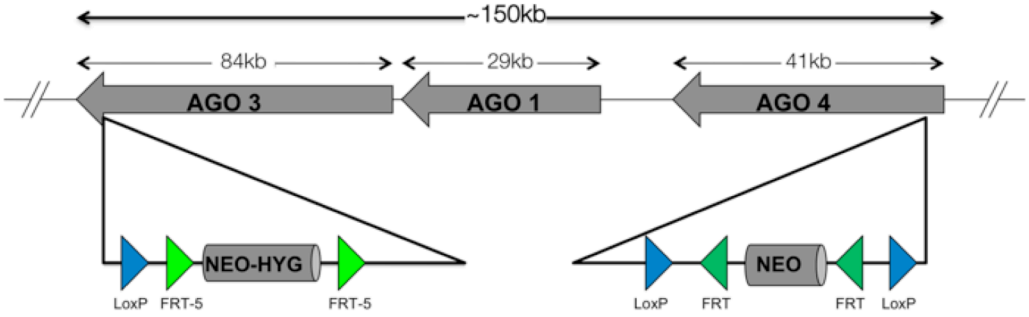


**Figure AI-1: Deletion of *Ago314*.** Ago314 targeting construct describing the genetic approach to guide the excision of all three non-slicing *Ago* genes following cre-mediated excision.

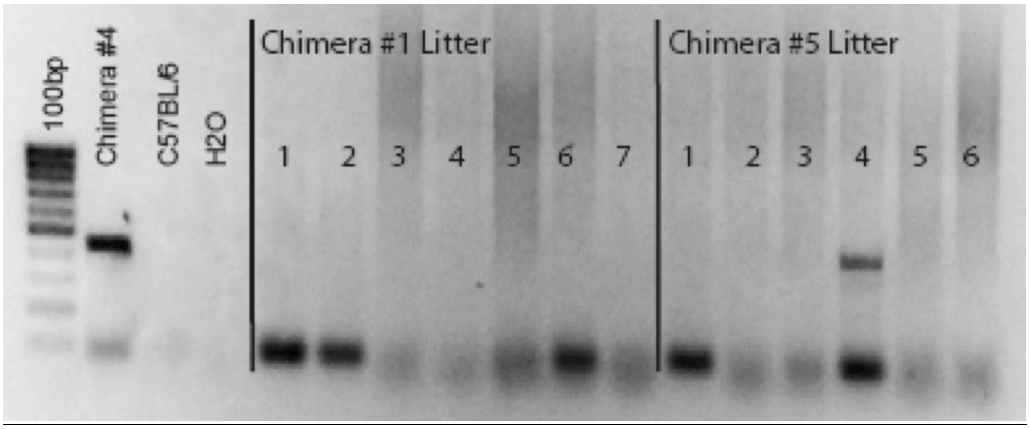


**Figure AI-2: PCR confirmation of germline transmission of A*go314 construct*.** Ago314 construct was probed for using primers specific to a segment starting in the genomic DNA and ending in the Hygromycin cassette. Positive samples are identified by a band at 447bp. Chimera #4 tail DNA was used as a positive control. Samples shown are the offspring of Chimera#1 and #5 matings to C57BL/6 female mice. Offspring # 4 from the Chimera #5 litter is positive for the construct.

**Materials and Methods:**

*Generation of Ago314 mutant mice.*

All mouse studies were conducted with the prior approval of the Cornell Institutional Animal Care and Use Committee. An *Ago314*-targeting construct, engineered using BAC# RP23-451023 as genomic source material, containing a 1.6 kbp 5′ arm from intergenic region immediately following Exon 19 of *Ago3*, a LoxP site, an *Frt5*-flanked *Pgk2-hyg/neo* cassette, 8.7 kbp of *Ago3* from exon 16–19. The targeting construct was electroporated in 129P2 ES cells, previously targeted in the generation of the *Ago4*$^{-/-}$ line (Modzelewski et al., 2012) to utilize the already present second LoxP site found 180 kbp away in intron 2 of *Ago4.* Correctly targeted ES cells were screened by Southern Blot for present of construct, injected into blastocysts and transferred to pseudo pregnant females. Chimeric mice were bred and germline transmission was achieved. Removal of the FRT-5 sites by FLPe transgenic mice produced the floxed allele (no hyg/neo) with LoxP sites flanking the 150 kbp region containing *Ago3,1* and *4*. Removal of the floxed region will be carried out by breeding to Ddx4-cre transgenic mice, thus removing this region at e18 in spermatogonia. The resulting *Ago314*$^{-/-}$ allele (lacking Ago3-1-4) will be bred to homozygosity onto a C57BL/6 background.

**Proposed Studies, Expected Results, and Potential Pitfalls**

Upon completion of both FLPe and CRE recombinase breeding strategies, the *Ago314*$^{-/+}$ mice will be bred onto the C57Bl/6 background line until homozygosity. If the deletion proves to be embryonic lethal, mice will be bred using *Ddx4-Cre* mice to ensure germ cell specific deletion at e10. These mice will be aged to 10 weeks, as was done for the *Ago4*, *Dicer* and *Dgcr8* studies and assessed by routine meiotic phenotypical analysis, such as total weight, testes weight, sperm count, and histological examinations. Based on the Ago4-/- analysis, we expect similar, if not more sever chromosomal abnormalities, specifically at the silenced XY chromosomes during pachynema. To monitor this, chromosome spread preparations from *Ago314*$^{-/-}$ testes and assessed for meiotic phenotypes similar to those observed in *Ago4* (Chapter 2), *Dicer* and *Dgcr8* (Chapter 3) deletion studies.

We predict similar derepression of sex-linked transcript during pachyenema and will therefore isolate distinct spermatocyte pools for subsequent mRNA to determine which regulatory networks are perturbed. The loss of *Ago4* also resulted in disruptions in the steady state levels of both miRNA and endo-siRNAs, therefore small RNA cloning experiments will be made to determine what small RNA small RNA populations is specifically altered by the loss of the three non-slicing Argonautes.

Some complications to this study reflect those encountered during the *Ago4* analysis. The *Ago4* deletion line was backcrossed 5 generations onto the

C57BL/6 genetic background before the meiotic phenotypes manifested enough for detection. Therefore, mice carrying the floxed or deleted allele will be backcrossed for at least 5 generations, with phenotypic analysis done on KO mice at each generation to determine if and when the phenotype emerges.

Another potential outcome is that the deletion of the three non-slicing *Ago* genes is compensated by the presence of *Ago2*, at least to the degree seen in the *Ago4* deletion study. Since Ago2 is embryonic lethal, a conditional allele will be bred into the *Ago314* deletion line to generate animals lacking all four Argo genes, effectively removing the cells ability to use both miRNAs and endo-siRNAs. We suspect this will phenocopy the results of the *Dicer* cKO analysis (Chapter 3), since both deletion strains cannot make use of miRNAs and endo-siRNAs.

APPENDIX II

## Investigating miRNA localization using Locked Nucleic Acid FISH

This work was conducted by Andrew J. Modzelewski in 2012-13 to evaluate the localization of the mature miRNAs that were most differentially expressed between *Ago4*$^{+/+}$ and *Ago4*$^{-/-}$. This work will eventually be added to and submitted for publication to better understand the mechanisms behind small RNA directed meiotic silencing.

### Summary

A critical feature behind the potential involvement of *Ago4* in proper meiotic silencing is its reported function as a small RNA binding protein. Thus far, AGO4 has only been associated with miRNAs. For these reasons, it is essential to determine if and when miRNAs have access to the nuclear compartment in order to gain some insight into the molecular mechanisms behind this RITS-like silencing.

It has been previously reported that both miRNAs and piRNAs localize to regions of the nucleus during spermatogenesis ((Marcon et al., 2008b), (Klattenhoff and Theurkauf, 2008)) and recent studies report the presence of AGO1 and AGO2 within the mammalian nucleus (Ahlenstiel et al., 2011; Robb et al., 2005), however their function in this compartment is still unclear.

Given our previous observation of AGO4 sex body localization, as well as the dramatic loss of small RNAs in the *Ago4*$^{-/-}$ pachytene spermatocyte, we chose to investigate another method to determine if these losses are genuine and if possible, whether they have stage specific or even distinct localization patterns.

In order to accomplish this, we used locked nucleic acid (LNA) probes against various miRNAs of interest. We found that each miRNA present during pachytene of prophase I localizes to the dense body, a region devoid of DNA but shown to encompass both RNA and protein (Takanari et al., 1982). Most probes showed diffuse nuclear staining, however some displayed distinct chromosome core and SE staining patterns, suggesting that they may serve some particular functions at these regions.

**Proposed Studies, Expected Results, and Potential Pitfalls**

The presence of mature small RNAs is not expected in the nuclei of any mammalian cell, however the evidence gathered from the Ago4 analysis (Chapter 2) strongly suggests a TGS role for AGOs and small RNAs in the nuclei. Therefore purpose of these studies is twofold: Purpose one is aimed at confirming the losses of the miRNAs that displayed differential regulation in the cloning experiment (Table 1). The second purpose is to attempt to gather any insight into the function of small RNAs in the nucleus based on potential localization patterns. Both point will be addressed by use of LNA probes specific to mature miRNAs for hybridization on chromosome spreads followed my immunofluorescence.

The following preliminary data shows that mature miRNAs do indeed populate the spermatocyte nuclei and in some cases have distinct localization patterns (Figure 1-5). Comparison between *Ago4*$^{+/+}$ and *Ago4*$^{-/-}$ spermatocyte localization confirms the losses reported in the small RNA cloning datasets. When

the meiotic silencing statuses of pachytene cells are compromised by the loss of AGO4, and presumably the cumulative loss of miRNAs, the nuclei are depleted of the probed miRNA. These results suggest that not only are these small RNA species abundant within the meiotic nuclei, but also function to regulate proper meiotic silencing and potentially other essential processes.

One of the concerns of this experiment is that a quantifiable result cannot be obtained, given the small RNA cloning was generated from a mixture of millions of spermatocytes, the visual inspection of individual chromosome spreads may not fully reflect the small RNA alterations determined from the small RNA cloning experiment. Additionally, given that this analysis is investigating small RNAs in a compartment that they are not normally associated with, it is possible that the probes may be hybridizing to the precursor products that are expected to populate the nucleus. A solution to both of these concerns is to use the LNA probes for Northern blot analysis, as this approach has successfully been used for both quantification purposes as well as inspecting the status of pre-miRNA using RNA derived from a mixture of cells (Kim et al., 2010b).

**Results**:

(Note: miR322 and miR206 localization is published in Modzelewski 2012)

| Seed | Family | Origin | Ago4 +/+ | Ago4 -/- | WT/KO Ratio | Note |
|---|---|---|---|---|---|---|
| GGCUCAG | mmu-mir-24 | Multiple | 11,604 | 1,662 | 6.98 | Moen's Paper, Not X-Linked |
| GAGGUAG | mmu-let-7d | Chromosome 13 | 23,635 | 4,229 | 3.74 | Retinoic Acid Related |
| AGCAGCA | mmu-mir-322 | Chromosome X | 3,283 | 331 | 6.49 | X-Linked, Large Change |
| AAAGACA | mmu-mir-743a | Chromosome X | 26,005 | 6,900 | 2.52 | X- Linked, Small Change |
| GGCAGUG | mmu-mir-34c | Chromosome 9 | 28,575 | 26,870 | 0.82 | No Change |
| GGAAUGU | mmu-mir-206 | Chromosome 1 | 0 | 1 | 0.42 | Not Expressed |

**Table AII-1. Summary of Locked Nucleic Acid miRNA probes.** The seed sequence along with the miRNA family are shown in the first and second columns, respectively. The chromosomal origin of the individual miRNA is shown in the third column. The *Ago4*$^{+/+}$ and *Ago4*$^{-/-}$ expression levels determine from the Modzelewski 2012 publication are shown the fourth and fifth columns, respectively. The *Ago4*$^{+/+}$/*Ago4*$^{-/-}$ expression level ratio is shown in the sixth columns. Notes describing the reason each particular miRNA was chosen are in the seventh column.

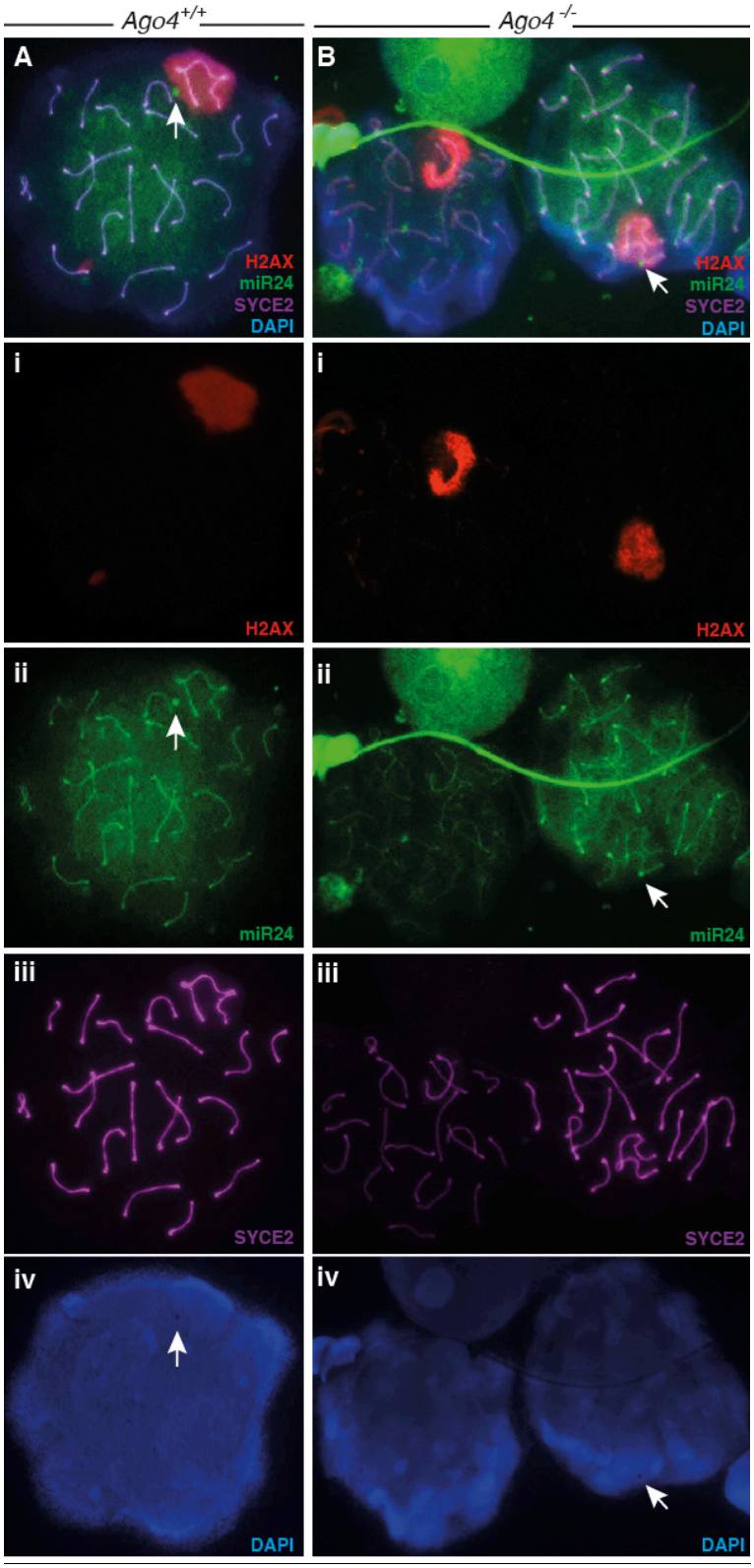


**Figure AII-1: Localization of miR-24**. Pachytene stage spermatocytes from *Ago4*$^{+/+}$ (A) and *Ago4*$^{-/-}$ (B) mice stained with anti-γH2AX (i), miR-24 (ii), anti-SYCE2 (Zan et al.), and DAPI (iv). In WT (Aii), miR-24 signal is found at the dense body (arrow) and SC cores. In *Ago4*$^{-/-}$ (Bii), altered spermatocyte is shown with noticeably reduced miR-24 signal. miR-24 targets are enriched for DNA repair and cell cycle regulatory transcripts.

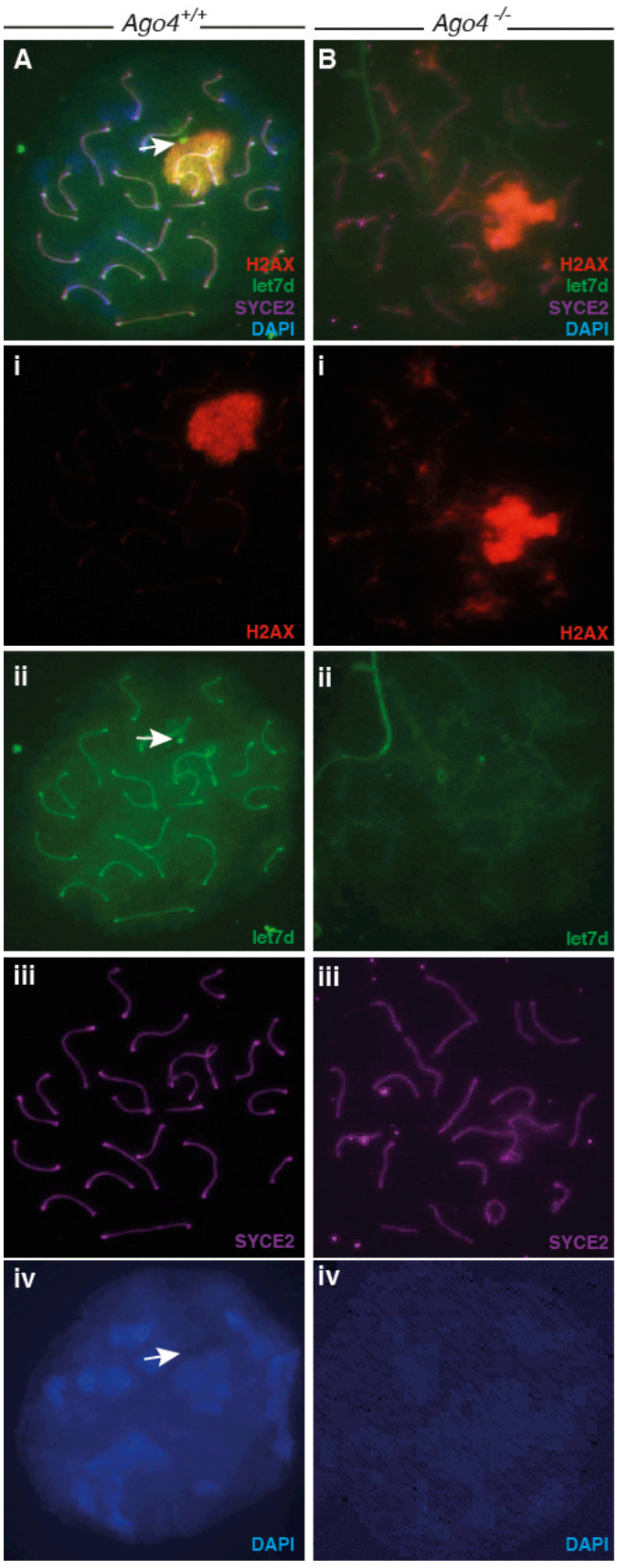


**Figure AII-2: Localization of miR-Let7d**. Pachytene stage spermatocytes from *Ago4*$^{+/+}$ (A) and *Ago4*$^{-/-}$ (B) mice stained with anti-γH2AX (i), let7d (ii), anti-SYCE2 (Zan et al.), and DAPI (iv). In WT (Aii), let7d signal is found at the dense body (arrow) and SC cores. In *Ago4*$^{-/-}$ (Bii), altered spermatocyte is shown with noticeably reduced let7d signal. Let7d is expressed highly in both male and female germ cells and targets *Igf2* (imprinted gene).

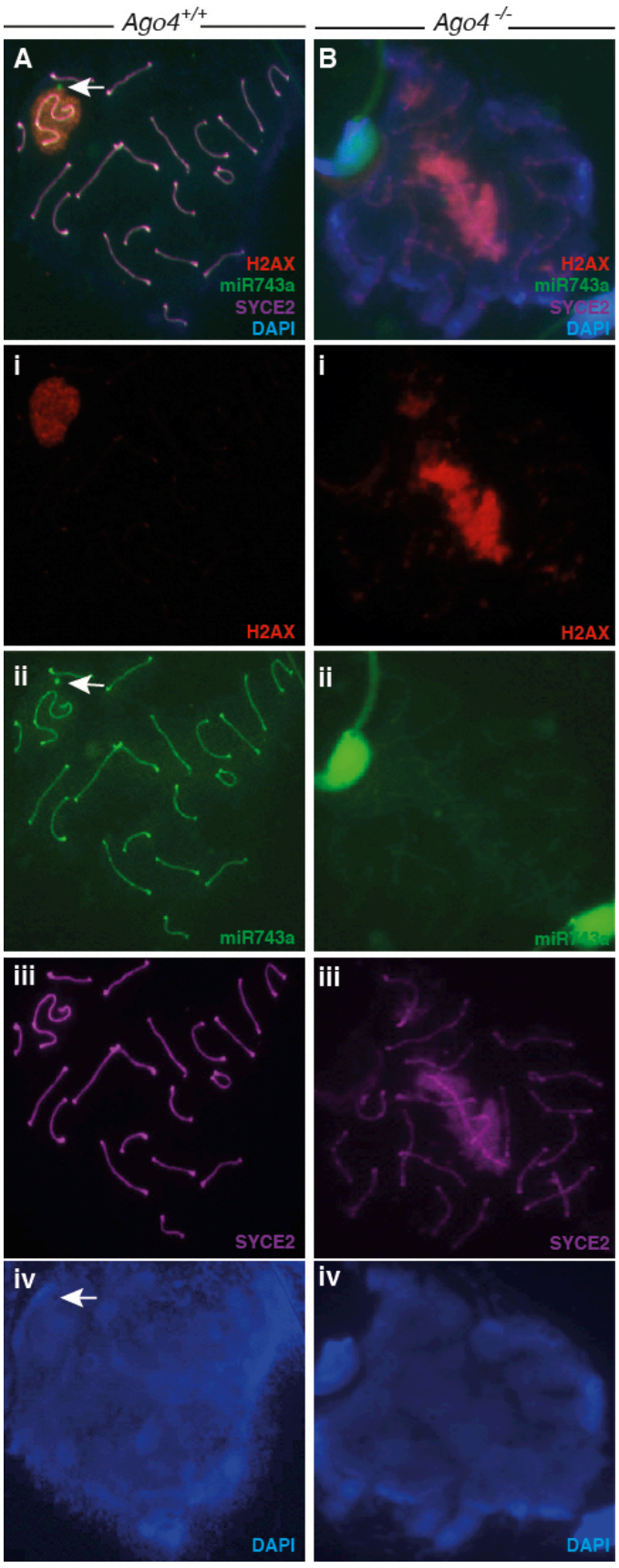


**Figure AII-3: Localization of miR-743a**. Pachytene stage spermatocytes from *Ago4*$^{+/+}$ (A) and *Ago4*$^{-/-}$ (B) mice stained with anti-γH2AX (i), 743a (ii), anti-SYCE2 (Zan et al.), and DAPI (iv). In WT (Aii), 743a signal is found at the dense body (arrow) and SC cores. In *Ago4*$^{-/-}$ (Bii), altered spermatocyte is shown with noticeably reduced 743a signal.

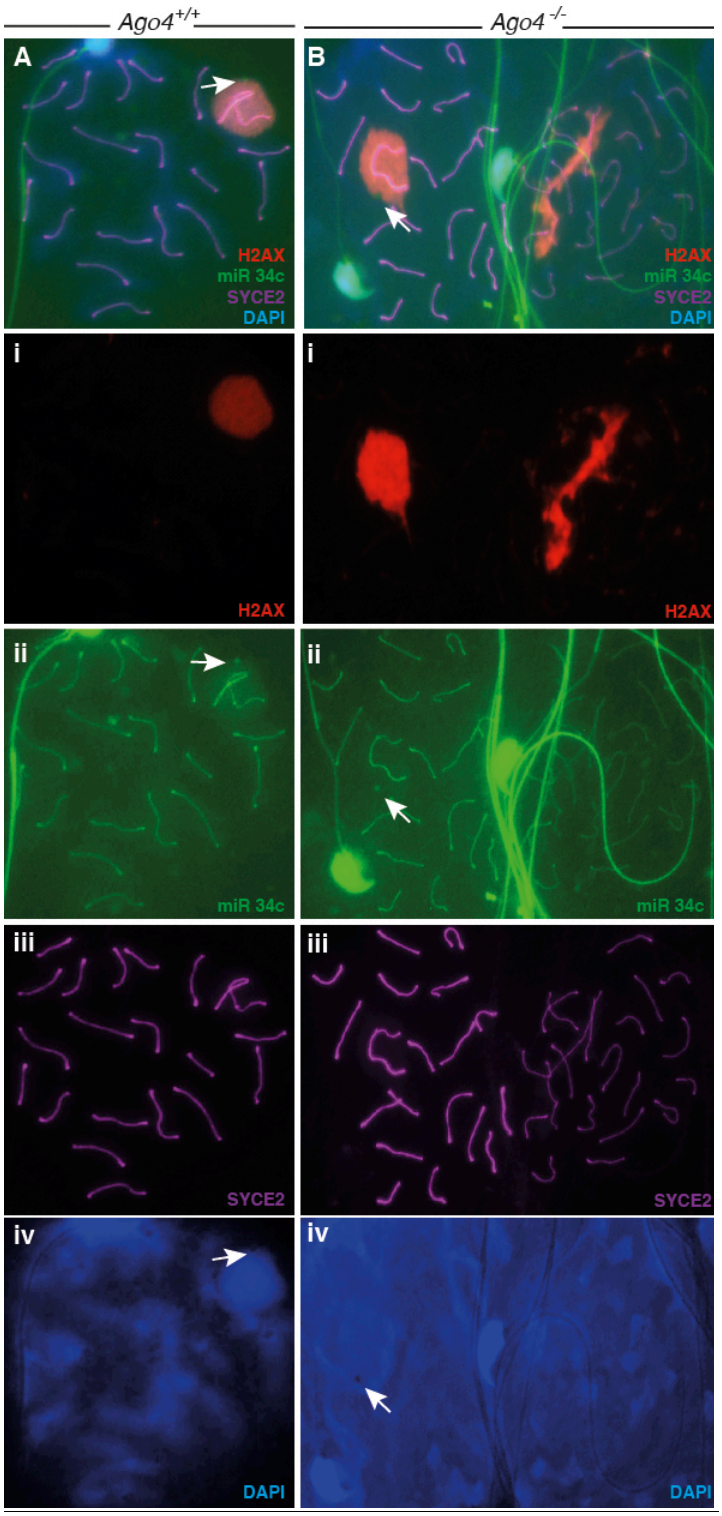


**Figure AII-4: Localization of miR-34c**. Pachytene stage spermatocytes from *Ago4*$^{+/+}$ (A) and *Ago4*$^{-/-}$ (B) mice stained with anti-γH2AX (i), miR-34c (ii), anti-SYCE2 (Zan et al.), and DAPI (iv). In WT (Aii), miR-34c signal is found at the dense body (arrow), sex body and SC cores. In *Ago4*$^{-/-}$ (Bii), altered spermatocyte does not show reduced miR-34c signal. Although miR-34c is highly expressed in pachynema, small RNA cloning did not reveal significant differential expression.

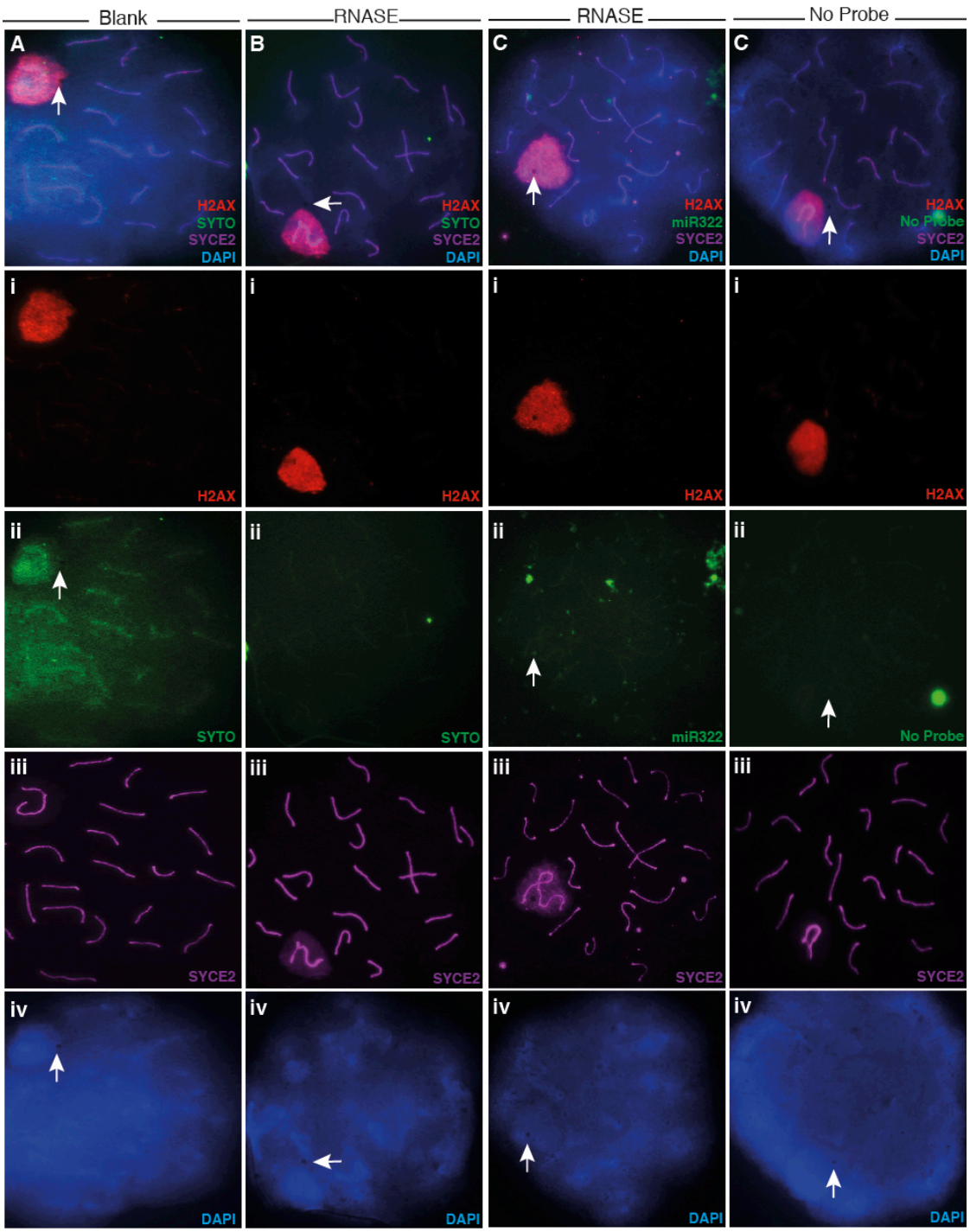


**Figure AII-5: miRNA FISH Controls**. Pachytene stage spermatocytes from *Ago4*$^{+/+}$ mice stained with anti-γH2AX (i), SYTO (Aii,Bii), miR322 (Cii) No Probe (Dii), anti-SYCE2 (Zan et al.), and DAPI (iv). In WT (Aii), SYTO RNA signal is found at the dense body (arrow), sex body and SC cores. When treated with an RNASE cocktail (Bii), SYTO RNA signal is almost completely abolished. When miR-322 is used (Cii) as a probe on slides that were treated with RNASE cocktail, the miR-322 signal is almost completely lost. When no probe is used (Dii), no signal is found.

**Materials and Methods:**

*miRNA Fluorescent In Situ Hybridization and Immunofluorescence.*

Slides were prepared and stained as described above. The following modifications to the previous protocol were implemented to prevent RNA degradation throughout the chromosome spread preparation and immunofluorescence procedures: DEPC (Sigma Aldrich) treated water was used to create each buffer, Hypotonic extraction buffer (HEB) contained 2 mM Ribonucleoside Vanadyl complex (NEB S1402), EDTA was replaced with 125 mM EGTA so as to not dissociate the complex. Primary antibodies and conditions used herein have been described previously (Holloway et al., 2011 ; Holloway et al., 2010; Kolas et al., 2005), except for anti-SYCE2 (from Howard Cooke, Edinburgh, Scotland), which was used at 1:500.

Fluorescein conjugated Locked Nucleic Acid (LNA) probes (Exiqon, Denmark) used to probe for mature miRNA localization are as follows:

miR-24 Exiqon 18121-04 Batch number 214279

/56-FAM/CTGTTCCTGCTGAACTGAGCCA

miR-LET7d Exiqon 38459-04 Batch number 214966

/56-FAM/AACTATGCAACCTACTACCTCT

miR-322* Exiqon 21397-04 Batch number 214963

/56-FAM/TGTTGCAGCGCTTCATGTTT.

miR-743a Exiqon 39656-04 Batch number 214962

/56-FAM/TCTACTCAGCTTGGTGTCTTTC

miR-34c-5p Exiqon 38542-04 Batch number 214964

/56-FAM/GCAATCAGCTAACTACACTGCCT

miR-206 Exiqon 18100-04 Batch number 214965

/56-FAM/CCACACACTTCCTTACATTCCA.

Briefly, after secondary antibody incubation, slides were washed in PBS three times and 40 nM of each probe in hybridization buffer (2x Buffer: 4X SSC, 50% Dextran Sulfate, 2 mg/mL BSA, 2 mM Ribonucleoside Vanadyl complex) were applied to each slide and incubated overnight at the appropriate temperature (Probe RNA Tm – 30$^{o}$C). Probes were first denatured by incubation at 90$^{o}$C for 4 minutes prior to addition to 2X hybridization buffer. Probe and buffer were then pre-incubated at the appropriate incubation temperature for 30 minutes prior to slide application followed by overnight hybridization. Slide were then washed under three stringency conditions:

A: 42$^{o}$C, 50% Deionized formamide, 1X SSC, pH 7.2-7.4, 3 Washes

B: 42$^{o}$C, 2X SSC, pH 7.2-7.4, 3 Washes

C: RT, 4X SSC, 4 mg/mL BSA, 0.1% Tween 20, pH 7.3, 1 Wash

Slides were Washed and mounted with Prolong Gold antifade (Molecular Probes).

APPENDIX III

## Laser Capture Microdissection of Pachytene Stage Sex Bodies

This work was conducted by Modzelewski AJ in 2013 with Connor Roberson and Tyler Maley, in order to determine what proteins and RNAs exist in the sex body domain in an unbiased approach.

### Summary

So far, our knowledge of sex body components relies on both reliable antibodies and viable knockout mice. When an antibody displays distinct SB localization, the next step is to ensure it is no present in spermatocytes deficient for that gene. Assuming the animal can progress into a spermatogenic stage with and SB, then the absence of this pattern is a decent indicator that the gene truly does participate in meiotic silencing. The analysis can be muddled if the knocked out gene actually works upstream of the protein that the antibodies was raised against. This would essentially give a false positive.

A major hallmark of AGO4 involvement in meiotic silencing is the presence of small RNAs in the nucleus. Based on the localization of AGO4 and the results of the miRNA FISH experiments, one prediction is that miRNAs, and perhaps additional small RNAs, would be present at the sex body and possibly in complex with AGO4.

### Proposed Studies, Expected Results, and Potential Pitfalls

One approach to look at both proteins and small RNAs present at the SB is to use laser capture microdissection (LCMD) technology to select individual

repressed SBs from spermatocyte nuclei while leaving the transcriptionally active autosomes. By first staining chromosome spreads with antibodies to reveal the SB, or a DNA dye to contrast between euchromatin and heterochromatin, the SB can then be targeted and collected (Figure 1). This would be followed by both Mass Spectrometry to determine the panel of proteins present at the SB, RNA and small RNA cloning to determine if and what non-coding RNAs are present. The list of proteins would provide candidates that may be involved in small RNA mediated silencing. If RNA is recovered from the SB, this would provide a very informative hint at the mechanism behind small RNA and silencing during mammalian spermatogenesis.

The largest hurdle in this analysis is collecting enough material. Since the X and Y chromosome encompass only 7% of the genome, approximately 14 times the material would be need to be collected. To alleviate this concern, the above-mentioned approach will be adapted for use with a more high-throughput LCMD microscope capable of collecting hundreds of targets, once these targets are selecting using proprietary Zeiss software. This will reduce the time of collection, and more importantly, opportunity of RNAse contamination.

Another pitfall is the possibility that we will not be able to recover any RNA species from these experiments. This is unlikely given the various reports describing the ability of X-linked miRNA clusters escaping MSCI. These nascently transcribed pri-miRNAs will be used to confirm we are able to sequence RNA from these samples.

Additionally, it is possible that we are collecting samples from autosomes. To test for this, chromosome specific primers will be designed and periodically checked from samples collected during these experiments.

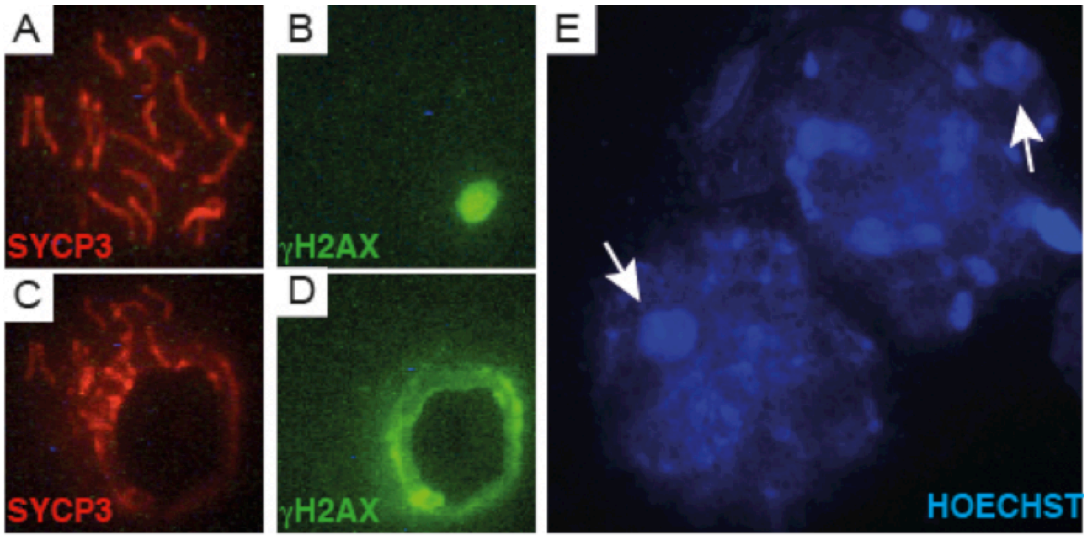


**Figure AIII-1. Laser Capture Microdissection of Pachytene Stage Sex Bodies.** C57BL/6 pachytene staged spermatocytes were processed and spread onto PET membrane LCM slides and stained with anti-SYCP3 in green, anti-γH2AX in red (A, B, C, D) and the DNA dye Hoechst in blue (E).. The LCMD was able to target (A,B) and select (C,D) just SBs while leaving the majority of the nucleus intact. Hoechst was used to contrast heterochromatin from euchromatin. The SB is a highly repressed region of DNA and therefore is easily recognizable using this technique.

## Materials and Methods

*Chromosome spreading and immunofluorescent staining*

Prophase I chromosome spreads and antibody staining were prepared as previously described (Modzelewski 2012). The following modifications to the previous protocol were implemented to prevent RNA degradation throughout the chromosome spread preparation and immunofluorescence procedures: DEPC (Sigma Aldrich) treated water was used to create each buffer, Hypotonic extraction buffer (HEB) contained 2 mM Ribonucleoside Vanadyl complex (NEB

S1402), EDTA was replaced with 125 mM EGTA so as to not dissociate the complex. Primary antibodies and conditions used herein have been described previously (Holloway et al., 2011 ; Holloway et al., 2010; Kolas et al., 2005). Chromosome spreads were prepared on MembraneSlide 1.0 PET (415190-9051-000 Zeiss Germany). Hoecscht staining was prepared by first washing slides in 1x PBS for 5 minutes, followed by incubation in 1ug/mL of Hoescht Dye (H-1398 Molecular Probes Eugene Oregon) in water for 5 minutes. Slides were washed once more in 1x PBS for 5 minutes and allowed to dry. Laser capture microdissection was performed on Leica ASLMD (Leica, Bannackburn Illinois). Total RNA, protein and genomic DNA will extracted from sex bodies using TRIZOL reagent (Invitrogen).

APPENDIX IV

# Cytological and Small RNA Analysis of Chromosome 16:17 Translocation on mouse spermatogenesis.

This work was conducted by Modzelewski, AJ. in 2013 with Stephanie Hilz in the Grimson Lab to investigate the consequence of having two autosomes involved in a translocation event in order to see what affect MSUC activation has on the small RNA population of mouse spermatocytes.

## Summary

In order to further investigate the roles of miRNAs in meiotic silencing, we began investigating what the effect of having a translocation event involving two autosomes would have on the small RNA population of both leptotene/zygotene and pachytene spermatocytes. We hypothesize that this would be a clear activation of the remaining meiotic silencing mechanism that exists in spermatocytes. The first being MSCI, which governs the X and Y-chromosomes, while the second mechanism would be activated by autosome-to-autosome translocations, MSUC, as it monitors the autosomes. We choose Ts($17^{16}$)65Dn mice (chromosome 16-to-17 translocation) which have breakpoints at 84,351,351bp on chromosome 16 and 9,426,822bp on chromosome 17, because they involve two small autosomes, are viable, infertile and have the added interest factor of being a human trisomy 21 mouse model, a segregation error that has relevance to our labs research.

**Proposed Studies, Expected Results, and Potential Pitfalls**

To being understanding what the role of small RNAs in MSUC is, Ts($17^{16}$)65Dn mouse will be used to produce chromosome spreads and probed with antibodies specific to various proteins associated with meiotic silencing to access the silencing status of the translocated chromosomes. This will be followed up with small RNA cloning of RNA extracted from isolated spermatocytes to generate a list of small RNA expression that is perturbed in response to the translocation. If small RNAs are not involved in this specific regulatory mechanism, then we should not expect any changes in the small RNA profile of the Ts($17^{16}$)65Dn samples compared to C57BL/6 isolated spermatocytes.

The analysis is still preliminary at this point but some findings can already be reported on. When viewing chromosome spread preparations from these spermatocytes, it is clear that the silencing machinery recognizes the translocation event (Figure 1). What is also clear is that in nearly all instances of the event, the translocated chromosomes are always either in extremely close proximity to the normally silent SB, or are completely engulfed by the silencing machinery, and in some rare cases, the chromosomal axis are in contact with the X and Y cores. Additionally, spermatocytes were found to progress beyond the pachytene checkpoint and appear to be in diplonema (Fig1D). Although these animals are infertile, such a bypass of the checkpoint machinery has been observed when the silencing of autosome regions that are not critical for the meiotic program are silenced. However, subsequent checkpoints are in place to

recognize and clear these types of errors later in spermatogenesis and spermiogenesis (Heard 2010).

The bioinformatics analysis reports little changes when comparing total RNA extracted from isolated spermatocytes from WT (C57B6) and Ts($17^{16}$)65Dn. However, preliminary results report massive decreases of all small RNA populations between the WT (C57B6) and Ts($17^{16}$)65Dn leptotene/zygotene spermatocytes (Fig 2) . The relevance of this finding is not clear, however as this is just an initial attempt at uncovering the role of small RNAs in MSUC, additional sequencing attempts must be made before any conclusions are drawn.

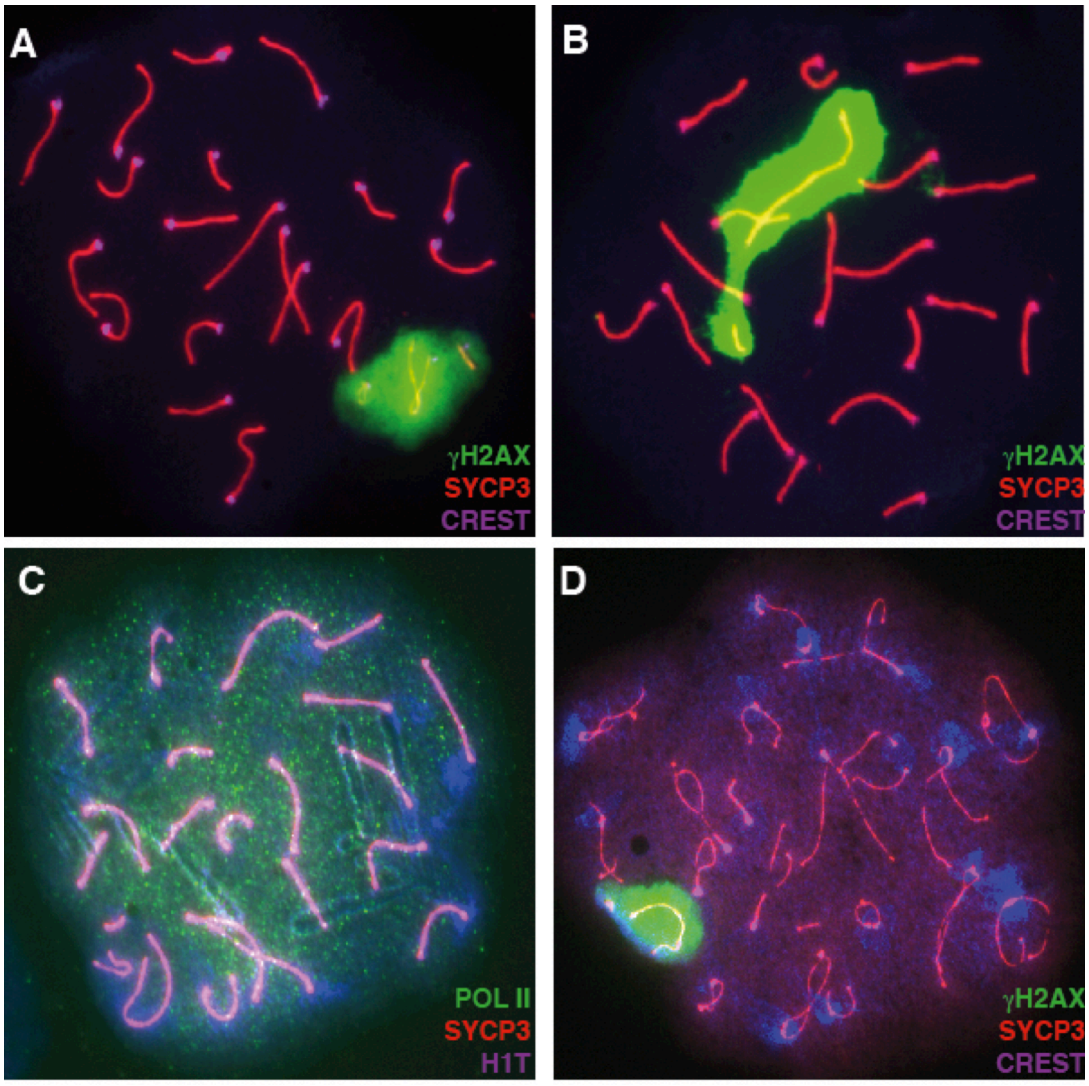


**Figure AIV-1. Cytological analysis of Ts(17$^{16}$)65Dn spermatocytes**. Pachytene (A,B,C) and Diplotene stage spermatocytes from Ts(17$^{16}$)65Dn mice stained with anti-SYCP3 in red (A,B,C,D), anti-γH2AX in green (A,B,D), anti-RNA POL II in green (C), anti-CREST in purple (A,B,D) and anti-H1T in purple (C). In pachytene (A,B,C), the translocation event is recognized by the silencing machinery (A,B) and is encompassed into the SB, in which RNA POL II colocalization is not observed (C), suggesting that these autosomal fragments are transcriptionally repressed. In these cells, diplotene is reached (D), a stage beyond the pachytene checkpoint in which chromosomal abnormalities are usually recognized and meiotic arrest is initiated.

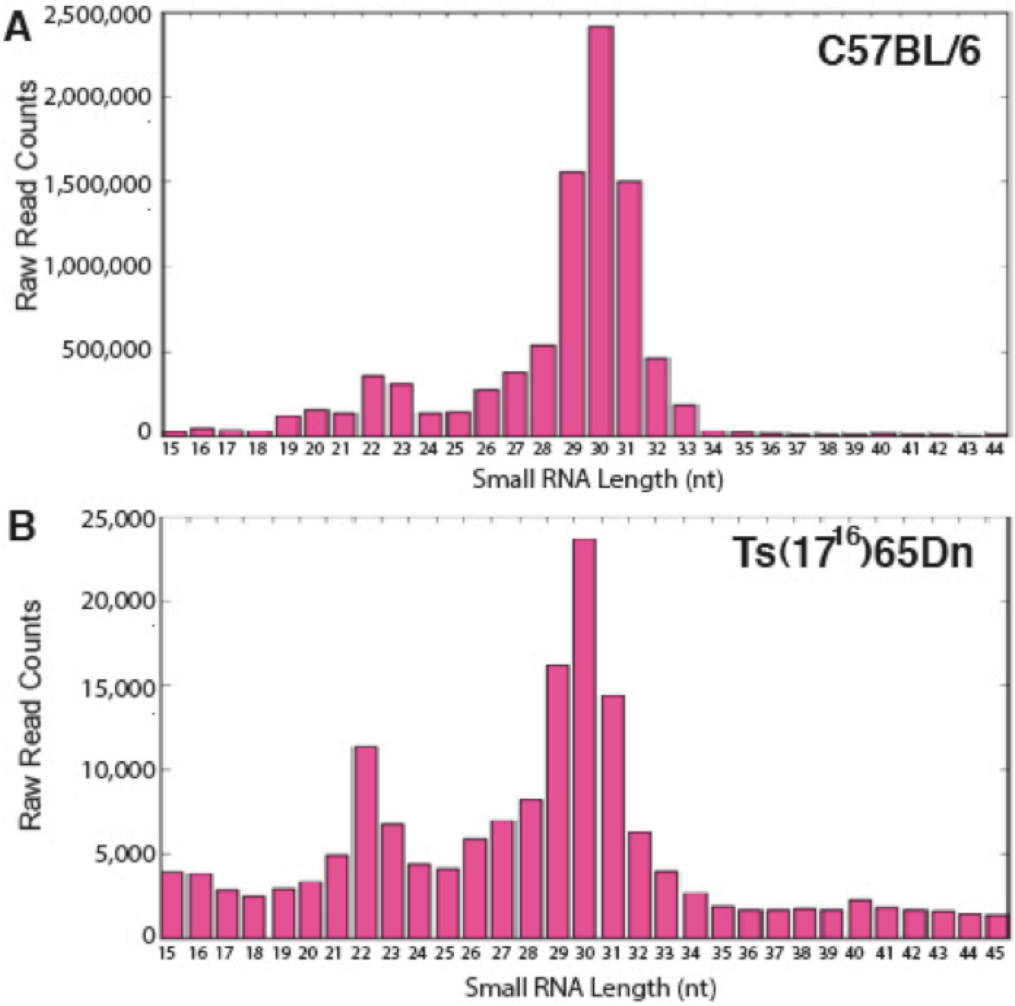


**Figure AIV-2. Small RNA cloning analysis of Ts($17^{16}$)65Dn spermatocytes**. Leptotene/zygotene isolated spermatocytes were sequenced for small RNA populations from WT C57BL/6 (A) and Ts($17^{16}$)65Dn (B) mice. For both (A,B), raw read counts are on the Y axis and small RNA lengths are on the X axis. There is a 100X drop in the level of small RNAs when comparing WT C57BL/6 (A) and Ts($17^{16}$)65Dn (B).

**Materials and Methods:**

*Chromosome spreading and immunofluorescent staining*

Prophase I chromosome spreads and antibody staining were prepared as previously described, (Holloway et al., 2008; Holloway et al., 2011 ; Kolas et al., 2005; Lipkin et al., 2002) (Modzelewski 2012).

*Isolation of mouse spermatogenic cells*

Testes from adult *Ago4*$^{+/+}$ and *Ago4*$^{-/-}$ adult mice (day 70-80 pp) were removed, weighed and decapsulated prior to enrichment of specific spermatogenic cells types using the STA-PUT method based on separation by cell diameter/density at unit gravity (Bellve, 1993). Purity of resulting fractions was determined by microscopy based on cell diameter and morphology. Pachytene cells were at approximately 95% purification with potential contamination from spermatocytes of slightly earlier or later developmental timing.

*Small RNA Cloning and Analysis*

Small RNAs were isolated from total RNA and sequenced as described previously (Modzelewski 2012). High quality reads were then mapped to the mouse genome (mm9) using Bowtie in order to determine their chromosomal origin. We then compared small RNAs from the translocation mouse to replicate wild-type samples in order to ascertain differences in small RNAs.

# REFERENCES


Ahlenstiel, C.L., Lim, H.G., Cooper, D.A., Ishida, T., Kelleher, A.D., and Suzuki, K. (2011). Direct evidence of nuclear Argonaute distribution during transcriptional silencing links the actin cytoskeleton to nuclear RNAi machinery in human cells. Nucleic Acids Research.

Ameyar-Zazoua, M., Rachez, C., Souidi, M., Robin, P., Fritsch, L., Young, R., Morozova, N., Fenouil, R., Descostes, N., Andrau, J.C.*, et al.* (2012). Argonaute proteins couple chromatin silencing to alternative splicing. Nat Struct Mol Biol *19*, 998-1004.

Aravin, A., Gaidatzis, D., Pfeffer, S., Lagos-Quintana, M., Landgraf, P., Iovino, N., Morris, P., Brownstein, M.J., Kuramochi-Miyagawa, S., Nakano, T.*, et al.* (2006). A novel class of small RNAs bind to MILI protein in mouse testes. Nature *442*, 203-207.

Ashley, T., Walpita, D., and de Rooij, D.G. (2001). Localization of two mammalian cyclin dependent kinases during mammalian meiosis. J Cell Sci *114*, 685-693.

Baarends, W.M., and Grootegoed, A. (2003a). Chromatin dynamics in the male meiotic prophase. Cytogenet Genome Res *103*, 225-234.

Baarends, W.M., Wassenaar, E., van der Laan, R., Hoogerbrugge, J., Sleddens-Linkels, E., Hoeijmakers, J.H., de Boer, P., and Grootegoed, J.A. (2005). Silencing of unpaired chromatin and histone H2A ubiquitination in mammalian meiosis. Mol Cell Biol *25*, 1041-1053.

Babiarz, J.E., Ruby, J.G., Wang, Y., Bartel, D.P., and Blelloch, R. (2008). Mouse ES cells express endogenous shRNAs, siRNAs, and other Microprocessor-independent, Dicer-dependent small RNAs. Genes Dev *22*, 2773-2785.

Barchi, M., Mahadevaiah, S., Di Giacomo, M., Baudat, F., de Rooij, D.G., Burgoyne, P.S., Jasin, M., and Keeney, S. (2005). Surveillance of different recombination defects in mouse spermatocytes yields distinct responses despite elimination at an identical developmental stage. Mol Cell Biol *25*, 7203-7215.

Bellani, M.A., Romanienko, P.J., Cairatti, D.A., and Camerini-Otero, R.D. (2005). SPO11 is required for sex-body formation, and Spo11 heterozygosity rescues the prophase arrest of Atm-/- spermatocytes. J Cell Sci *118*, 3233-3245.

Bellve, A.R. (1993). Purification, culture, and fractionation of spermatogenic cells. Methods Enzymol *225*, 84-113.

Bowles, J., and Koopman, P. (2010). Sex determination in mammalian germ cells: extrinsic versus intrinsic factors. Reproduction *139*, 943-958.

Brown, P.W., Hwang, K., Schlegel, P.N., and Morris, P.L. (2008). Small ubiquitin-related modifier (SUMO)-1, SUMO-2/3 and SUMOylation are involved with centromeric heterochromatin of chromosomes 9 and 1 and proteins of the synaptonemal complex during meiosis in men. Human Reproduction *23*, 2850-2857.

Bukhari, S.I., Vasquez-Rifo, A., Gagne, D., Paquet, E.R., Zetka, M., Robert, C., Masson, J.Y., and Simard, M.J. (2012). The microRNA pathway controls germ cell proliferation and differentiation in C. elegans. Cell Res *22*, 1034-1045.

Burgoyne, P.S., Mahadevaiah, S.K., and Turner, J.M. (2009). The consequences of asynapsis for mammalian meiosis. Nat Rev Genet *10*, 207-216.

Burkhart, K.B., Guang, S., Buckley, B.A., Wong, L., Bochner, A.F., and Kennedy, S. (2011). A Pre-mRNA-Associating Factor Links Endogenous siRNAs to Chromatin Regulation. PLoS Genet *7*, e1002249.

Cenik, E.S., and Zamore, P.D. (2011). Argonaute proteins. Curr Biol *21*, R446-449.

Chakravarthy, S., Sternberg, S.H., Kellenberger, C.A., and Doudna, J.A. (2010). Substrate-specific kinetics of Dicer-catalyzed RNA processing. Journal of molecular biology *404*, 392-402.

Chu, D., Ren, S., Hu, S., Wang, W.G., Subramanian, A., Contreras, D., Kanagavel, V., Chung, E., Ko, J., Amirtham Jacob Appadorai, R.S.*, et al.* (2013). Systematic analysis of enhancer and critical cis-acting RNA elements in the protein-encoding region of the hepatitis C virus genome. J Virol *87*, 5678-5696.

Claycomb, J.M., Batista, P.J., Pang, K.M., Gu, W., Vasale, J.J., van Wolfswinkel, J.C., Chaves, D.A., Shirayama, M., Mitani, S., Ketting, R.F.*, et al.* (2009). The Argonaute CSR-1 and its 22G-RNA cofactors are required for holocentric chromosome segregation. Cell *139*, 123-134.

Crackower, M.A., Kolas, N.K., Noguchi, J., Sarao, R., Kikuchi, K., Kaneko, H., Kobayashi, E., Kawai, Y., Kozieradzki, I., Landers, R.*, et al.* (2003). Essential role of Fkbp6 in male fertility and homologous chromosome pairing in meiosis. Science *300*, 1291-1295.

Czech, B., and Hannon, G.J. (2011). Small RNA sorting: matchmaking for Argonautes. Nat Rev Genet *12*, 19-31.

Daniel, K., Lange, J., Hached, K., Fu, J., Anastassiadis, K., Roig, I., Cooke, H.J., Stewart, A.F., Wassmann, K., Jasin, M.*, et al.* (2011). Meiotic homologue alignment

and its quality surveillance are controlled by mouse HORMAD1. Nature cell biology *13*, 599-610.

Dimitrova, N., and de Lange, T. (2006). MDC1 accelerates nonhomologous end-joining of dysfunctional telomeres. Genes Dev *20*, 3238-3243.

Drinnenberg, I.A., Weinberg, D.E., Xie, K.T., Mower, J.P., Wolfe, K.H., Fink, G.R., and Bartel, D.P. (2009). RNAi in budding yeast. Science *326*, 544-550.

Edelmann, W., Cohen, P.E., Kane, M., Lau, K., Morrow, B., Bennett, S., Umar, A., Kunkel, T., Cattoretti, G., Chaganti, R.*, et al.* (1996). Meiotic pachytene arrest in MLH1-deficient mice. Cell *85*, 1125-1134.

Edelmann, W., Cohen, P.E., Kneitz, B., Winand, N., Lia, M., Heyer, J., Kolodner, R., Pollard, J.W., and Kucherlapati, R. (1999). Mammalian MutS homologue 5 is required for chromosome pairing in meiosis. Nat Genet *21*, 123-127.

Fagegaltier, D., Bouge, A.L., Berry, B., Poisot, E., Sismeiro, O., Coppee, J.Y., Theodore, L., Voinnet, O., and Antoniewski, C. (2009). The endogenous siRNA pathway is involved in heterochromatin formation in Drosophila. Proc Natl Acad Sci U S A *106*, 21258-21263.

Faller, M., Matsunaga, M., Yin, S., Loo, J.A., and Guo, F. (2007). Heme is involved in microRNA processing. Nat Struct Mol Biol *14*, 23-29.

Fernandez-Capetillo, O., Mahadevaiah, S.K., Celeste, A., Romanienko, P.J., Camerini-Otero, R.D., Bonner, W.M., Manova, K., Burgoyne, P., and Nussenzweig, A. (2003). H2AX is required for chromatin remodeling and inactivation of sex chromosomes in male mouse meiosis. Dev Cell *4*, 497-508.

Fire, A., Xu, S., Montgomery, M.K., Kostas, S.A., Driver, S.E., and Mello, C.C. (1998). Potent and specific genetic interference by double-stranded RNA in Caenorhabditis elegans. Nature *391*, 806-811.

Gagnon, K.T., and Corey, D.R. (2012). Argonaute and the Nuclear RNAs: New Pathways for RNA-Mediated Control of Gene Expression. Nucleic Acid Ther *22*, 3-16.

Gallardo, T., Shirley, L., John, G.B., and Castrillon, D.H. (2007). Generation of a germ cell-specific mouse transgenic Cre line, Vasa-Cre. Genesis *45*, 413-417.

Gan, H., Lin, X., Zhang, Z., Zhang, W., Liao, S., Wang, L., and Han, C. (2011). piRNA profiling during specific stages of mouse spermatogenesis. Rna *17*, 1191-1203.

Garcia-Lopez, J., and Del Mazo, J. (2012). Expression dynamics of microRNA biogenesis during preimplantation mouse development. Biochim Biophys Acta *1819*, 847-854.

Gely-Pernot, A., Raverdeau, M., Celebi, C., Dennefeld, C., Feret, B., Klopfenstein, M., Yoshida, S., Ghyselinck, N.B., and Mark, M. (2012). Spermatogonia differentiation requires retinoic acid receptor gamma. Endocrinology *153*, 438-449.

Gill, M.E., Hu, Y.C., Lin, Y., and Page, D.C. (2011). Licensing of gametogenesis, dependent on RNA binding protein DAZL, as a gateway to sexual differentiation of fetal germ cells. Proc Natl Acad Sci U S A *108*, 7443-7448.

Girard, A., Sachidanandam, R., Hannon, G.J., and Carmell, M.A. (2006). A germline-specific class of small RNAs binds mammalian Piwi proteins. Nature *442*, 199-202.

Goetz, P., Chandley, A.C., and Speed, R.M. (1984). Morphological and temporal sequence of meiotic prophase development at puberty in the male mouse. Journal of Cell Science *65*, 249-263.

Gonzalez-Gonzalez, E., Lopez-Casas, P.P., and del Mazo, J. (2008a). The expression patterns of genes involved in the RNAi pathways are tissue-dependent and differ in the germ and somatic cells of mouse testis. Biochim Biophys Acta *1779*, 306-311.

Greenlee, A.R., Shiao, M.S., Snyder, E., Buaas, F.W., Gu, T., Stearns, T.M., Sharma, M., Murchison, E.P., Puente, G.C., and Braun, R.E. (2012). Deregulated sex chromosome gene expression with male germ cell-specific loss of Dicer1. PLoS One *7*, e46359.

Griffiths-Jones, S. (2004). The microRNA Registry. Nucleic Acids Research *32*, D109-111.

Griffiths-Jones, S., Grocock, R.J., van Dongen, S., Bateman, A., and Enright, A.J. (2006). miRBase: microRNA sequences, targets and gene nomenclature. Nucleic Acids Research *34*, D140-144.

Griffiths-Jones, S., Saini, H.K., van Dongen, S., and Enright, A.J. (2008). miRBase: tools for microRNA genomics. Nucleic Acids Research *36*, D154-158.

Grimson, A., Srivastava, M., Fahey, B., Woodcroft, B.J., Chiang, H.R., King, N., Degnan, B.M., Rokhsar, D.S., and Bartel, D.P. (2008). Early origins and evolution of microRNAs and Piwi-interacting RNAs in animals. Nature *455*, 1193-1197.

Griswold, M.D., Hogarth, C.A., Bowles, J., and Koopman, P. (2012). Initiating meiosis: the case for retinoic acid. Biol Reprod *86*, 35.

Grivna, S.T., Beyret, E., Wang, Z., and Lin, H. (2006a). A novel class of small RNAs in mouse spermatogenic cells. Genes Dev *20*, 1709-1714.

Han, J., Kim, D., and Morris, K.V. (2007). Promoter-associated RNA is required for RNA-directed transcriptional gene silencing in human cells. Proc Natl Acad Sci U S A *104*, 12422-12427.

Handel, M. (2004). The XY body: a specialized meiotic chromatin domain. Exp Cell Res *296*, 57-63.

Handel, M.A., and Eppig, J.J. (1998). Sexual dimorphism in the regulation of mammalian meiosis. Curr Top Dev Biol *37*, 333-358.

Handel, M.A., Park, C., and Kot, M. (1994). Genetic-Control of Sex-Chromosome Inactivation during Male Meiosis. Cytogenetics and Cell Genetics *66*, 83-88.

Handel, M.A., and Schimenti, J.C. (2010). Genetics of mammalian meiosis: regulation, dynamics and impact on fertility. Nat Rev Genet *11*, 124-136.

Hayashi, K., Chuva de Sousa Lopes, S.M., Kaneda, M., Tang, F., Hajkova, P., Lao, K., O'Carroll, D., Das, P.P., Tarakhovsky, A., Miska, E.A*., et al.* (2008). MicroRNA biogenesis is required for mouse primordial germ cell development and spermatogenesis. PLoS One *3*, e1738.

Heard, E., and Turner, J. (2011). Function of the sex chromosomes in mammalian fertility. Cold Spring Harb Perspect Biol *3*, a002675.

Hogarth, C.A., and Griswold, M.D. (2010). The key role of vitamin A in spermatogenesis. The Journal of clinical investigation *120*, 956-962.

Hogarth, C.A., Mitchell, D., Evanoff, R., Small, C., and Griswold, M. (2011). Identification and expression of potential regulators of the mammalian mitotic-to-meiotic transition. Biol Reprod *84*, 34-42.

Holloway, J.K., Booth, J., Edelmann, W., McGowan, C.H., and Cohen, P.E. (2008). MUS81 generates a subset of MLH1-MLH3-independent crossovers in mammalian meiosis. PLoS Genet *4*, e1000186.

Holloway, J.K., Mohan, S., Balmus, G., Sun, X., Modzelewski, A., Borst, P.L., Freire, R., Weiss, R.S., and Cohen, P.E. (2011 ). Mammalian BTBD12 (SLX4) protects against genomic instability during mammalian spermatogenesis. PLoS Genetics *7*, e1002094.

Holloway, J.K., Morelli, M.A., Borst, P.L., and Cohen, P.E. (2010). Mammalian BLM helicase is critical for integrating multiple pathways of meiotic recombination. J Cell Biol *188*, 779-789.

Huang da, W., Sherman, B.T., and Lempicki, R.A. (2009). Bioinformatics enrichment tools: paths toward the comprehensive functional analysis of large gene lists. Nucleic Acids Research *37*, 1-13.

Ichijima, Y., Ichijima, M., Lou, Z., Nussenzweig, A., Camerini-Otero, R.D., Chen, J., Andreassen, P.R., and Namekawa, S.H. (2011). MDC1 directs chromosome-wide silencing of the sex chromosomes in male germ cells. Genes Dev *25*, 959-971.

Ishizu, H., Nagao, A., and Siomi, H. (2011). Gatekeepers for Piwi-piRNA complexes to enter the nucleus. Curr Opin Genet Dev *21*, 484-490.

Kaneda, M., Tang, F., O'Carroll, D., Lao, K., and Surani, M.A. (2009). Essential role for Argonaute2 protein in mouse oogenesis. Epigenetics Chromatin *2*, 9.

Kim, D.H., Villeneuve, L.M., Morris, K.V., and Rossi, J.J. (2006). Argonaute-1 directs siRNA-mediated transcriptional gene silencing in human cells. Nat Struct Mol Biol *13*, 793-797.

Kim, G.J., Georg, I., Scherthan, H., Merkenschlager, M., Guillou, F., Scherer, G., and Barrionuevo, F. (2010a). Dicer is required for Sertoli cell function and survival. Int J Dev Biol *54*, 867-875.

Kim, S., Namekawa, S.H., Niswander, L.M., Ward, J.O., Lee, J.T., Bardwell, V.J., and Zarkower, D. (2007). A mammal-specific Doublesex homolog associates with male sex chromatin and is required for male meiosis. PLoS Genet *3*, e62.

Kim, S.W., Li, Z., Moore, P.S., Monaghan, A.P., Chang, Y., Nichols, M., and John, B. (2010b). A sensitive non-radioactive northern blot method to detect small RNAs. Nucleic Acids Res *38*, e98.

Kim, V.N. (2006). Small RNAs just got bigger: Piwi-interacting RNAs (piRNAs) in mammalian testes. Genes Dev *20*, 1993-1997.

Kim, V.N., Han, J., and Siomi, M.C. (2009). Biogenesis of small RNAs in animals. Nature reviews Molecular cell biology *10*, 126-139.

Kimble, J., and Crittenden, S.L. (2007). Controls of germline stem cells, entry into meiosis, and the sperm/oocyte decision in Caenorhabditis elegans. Annual review of cell and developmental biology *23*, 405-433.

Klattenhoff, C., and Theurkauf, W. (2008). Biogenesis and germline functions of piRNAs. Development *135*, 3-9.

Klipper-Aurbach, Y., Wasserman, M., Braunspiegel-Weintrob, N., Borstein, D., Peleg, S., Assa, S., Karp, M., Benjamini, Y., Hochberg, Y., and Laron, Z. (1995). Mathematical formulae for the prediction of the residual beta cell function during

the first two years of disease in children and adolescents with insulin-dependent diabetes mellitus. Med Hypotheses *45*, 486-490.

Kneitz, B., Cohen, P.E., Avdievich, E., Zhu, L., Kane, M.F., Hou, H., Jr., Kolodner, R.D., Kucherlapati, R., Pollard, J.W., and Edelmann, W. (2000). MutS homolog 4 localization to meiotic chromosomes is required for chromosome pairing during meiosis in male and female mice. Genes Dev *14*, 1085-1097.

Kolas, N.K., and Cohen, P.E. (2004). Novel and diverse functions of the DNA mismatch repair family in mammalian meiosis and recombination. Cytogenet Genome Res *107*, 216-231.

Kolas, N.K., Svetlanov, A., Lenzi, M.L., Macaluso, F.P., Lipkin, S.M., Liskay, R.M., Greally, J., Edelmann, W., and Cohen, P.E. (2005). Localization of MMR proteins on meiotic chromosomes in mice indicates distinct functions during prophase I. J Cell Biol *171*, 447-458.

Korhonen, H.M., Meikar, O., Yadav, R.P., Papaioannou, M.D., Romero, Y., Da Ros, M., Herrera, P.L., Toppari, J., Nef, S., and Kotaja, N. (2011). Dicer is required for haploid male germ cell differentiation in mice. PLoS One *6*, e24821.

Kozomara, A., and Griffiths-Jones, S. (2011). miRBase: integrating microRNA annotation and deep-sequencing data. Nucleic Acids Res *39*, D152-157.

Kumagai, A., Lee, J., Yoo, H.Y., and Dunphy, W.G. (2006). TopBP1 activates the ATR-ATRIP complex. Cell *124*, 943-955.

Kuramochi-Miyagawa, S., Watanabe, T., Gotoh, K., Takamatsu, K., Chuma, S., Kojima-Kita, K., Shiromoto, Y., Asada, N., Toyoda, A., Fujiyama, A.*, et al.* (2010). MVH in piRNA processing and gene silencing of retrotransposons. Genes Dev *24*, 887-892.

Langmead, B., Trapnell, C., Pop, M., and Salzberg, S.L. (2009). Ultrafast and memory-efficient alignment of short DNA sequences to the human genome. Genome biology *10*, R25.

Lee, R.C., Feinbaum, R.L., and Ambros, V. (1993). The C. elegans heterochronic gene lin-4 encodes small RNAs with antisense complementarity to lin-14. Cell *75*, 843-854.

Lei, L., Jin, S., Gonzalez, G., Behringer, R.R., and Woodruff, T.K. (2010). The regulatory role of Dicer in folliculogenesis in mice. Mol Cell Endocrinol *315*, 63-73.

Lin, H.K., Bergmann, S., and Pandolfi, P.P. (2004). Cytoplasmic PML function in TGF-beta signalling. Nature *431*, 205-211.

Lin, Q., Sirotkin, A., and Skoultchi, A.I. (2000). Normal spermatogenesis in mice lacking the testis-specific linker histone H1t. Mol Cell Biol *20*, 2122-2128.

Lin, Y., Gill, M.E., Koubova, J., and Page, D.C. (2008). Germ cell-intrinsic and -extrinsic factors govern meiotic initiation in mouse embryos. Science *322*, 1685-1687.

Lin, Y., and Page, D.C. (2005). Dazl deficiency leads to embryonic arrest of germ cell development in XY C57BL/6 mice. Developmental Biology *288*, 309-316.

Lipkin, S.M., Moens, P.B., Wang, V., Lenzi, M., Shanmugarajah, D., Gilgeous, A., Thomas, J., Cheng, J., Touchman, J.W., Green, E.D*., et al.* (2002). Meiotic arrest and aneuploidy in MLH3-deficient mice. Nat Genet *31*, 385-390.

Liu, J., Carmell, M.A., Rivas, F.V., Marsden, C.G., Thomson, J.M., Song, J.J., Hammond, S.M., Joshua-Tor, L., and Hannon, G.J. (2004). Argonaute2 is the catalytic engine of mammalian RNAi. Science *305*, 1437-1441.

Liu, X., Jin, D.Y., McManus, M.T., and Mourelatos, Z. (2012). Precursor microRNA-programmed silencing complex assembly pathways in mammals. Mol Cell *46*, 507-517.

Lu, L.Y., Wu, J., Ye, L., Gavrilina, G.B., Saunders, T.L., and Yu, X. (2010). RNF8-dependent histone modifications regulate nucleosome removal during spermatogenesis. Dev Cell *18*, 371-384.

Lund, E., and Dahlberg, J.E. (2006). Substrate selectivity of exportin 5 and Dicer in the biogenesis of microRNAs. Cold Spring Harb Symp Quant Biol *71*, 59-66.

Lynn, A., Koehler, K.E., Judis, L., Chan, E.R., Cherry, J.P., Schwartz, S., Seftel, A., Hunt, P.A., and Hassold, T.J. (2002). Covariation of synaptonemal complex length and mammalian meiotic exchange rates. Science *296*, 2222-2225.

Maine, E.M. (2010). Meiotic silencing in Caenorhabditis elegans. Int Rev Cell Mol Biol *282*, 91-134.

Malone, C.D., Brennecke, J., Dus, M., Stark, A., McCombie, W.R., Sachidanandam, R., and Hannon, G.J. (2009). Specialized piRNA pathways act in germline and somatic tissues of the Drosophila ovary. Cell *137*, 522-535.

Maniataki, E., and Mourelatos, Z. (2005). A human, ATP-independent, RISC assembly machine fueled by pre-miRNA. Genes Dev *19*, 2979-2990.

Marcon, E., Babak, T., Chua, G., Hughes, T., and Moens, P.B. (2008). miRNA and piRNA localization in the male mammalian meiotic nucleus. Chromosome Res *16*, 243-260.

Matranga, C., Tomari, Y., Shin, C., Bartel, D.P., and Zamore, P.D. (2005). Passenger-strand cleavage facilitates assembly of siRNA into Ago2-containing RNAi enzyme complexes. Cell *123*, 607-620.

McPherson, F.J., and Chenoweth, P.J. (2012). Mammalian sexual dimorphism. Anim Reprod Sci *131*, 109-122.

Meister, G. (2013). Argonaute proteins: functional insights and emerging roles. Nat Rev Genet *14*, 447-459.

Meister, G., Landthaler, M., Patkaniowska, A., Dorsett, Y., Teng, G., and Tuschl, T. (2004a). Human Argonaute2 mediates RNA cleavage targeted by miRNAs and siRNAs. Mol Cell *15*, 185-197.

Meister, G., Landthaler, M., Patkaniowska, A., Dorsett, Y., Teng, G., and Tuschl, T. (2004b). Human Argonaute2 mediates RNA cleavage targeted by miRNAs and siRNAs. Mol Cell *15*, 185-197.

Mitchell, P.S., Parkin, R.K., Kroh, E.M., Fritz, B.R., Wyman, S.K., Pogosova-Agadjanyan, E.L., Peterson, A., Noteboom, J., O'Briant, K.C., Allen, A.*, et al.* (2008). Circulating microRNAs as stable blood-based markers for cancer detection. Proc Natl Acad Sci U S A *105*, 10513-10518.

Modzelewski, A.J., Holmes, R.J., Hilz, S., Grimson, A.W., and Cohen, P.E. (2012). AGO4 regulates entry into meiosis and influences silencing of sex chromosomes in the male
mouse germ line. Dev Cell.

Montgomery, M.K., Xu, S., and Fire, A. (1998). RNA as a target of double-stranded RNA-mediated genetic interference in Caenorhabditis elegans. Proc Natl Acad Sci U S A *95*, 15502-15507.

Morelli, M.A., and Cohen, P.E. (2005). Not all germ cells are created equal: aspects of sexual dimorphism in mammalian meiosis. Reproduction *130*, 761-781.

Morris, K.V., Chan, S.W., Jacobsen, S.E., and Looney, D.J. (2004). Small interfering RNA-induced transcriptional gene silencing in human cells. Science *305*, 1289-1292.

Murchison, E.P., Partridge, J.F., Tam, O.H., Cheloufi, S., and Hannon, G.J. (2005). Characterization of Dicer-deficient murine embryonic stem cells. Proc Natl Acad Sci U S A *102*, 12135-12140.

Murchison, E.P., Stein, P., Xuan, Z., Pan, H., Zhang, M.Q., Schultz, R.M., and Hannon, G.J. (2007). Critical roles for Dicer in the female germline. Genes Dev *21*, 682-693.

Nicolosi, R.J., Wilson, T.A., Lawton, C., and Handelman, G.J. (2001). Dietary effects on cardiovascular disease risk factors: beyond saturated fatty acids and cholesterol. J Am Coll Nutr *20*, 421S-427S; discussion 440S-442S.

Niu, Z., Goodyear, S.M., Rao, S., Wu, X., Tobias, J.W., Avarbock, M.R., and Brinster, R.L. (2011). MicroRNA-21 regulates the self-renewal of mouse spermatogonial stem cells. Proceedings of the National Academy of Sciences of the United States of America *108*, 12740-12745.

Ohrt, T., Mutze, J., Staroske, W., Weinmann, L., Hock, J., Crell, K., Meister, G., and Schwille, P. (2008). Fluorescence correlation spectroscopy and fluorescence cross-correlation spectroscopy reveal the cytoplasmic origination of loaded nuclear RISC in vivo in human cells. Nucleic Acids Res *36*, 6439-6449.

Okamura, K., Liu, N., and Lai, E.C. (2009). Distinct mechanisms for microRNA strand selection by Drosophila Argonautes. Molecular Cell *36*, 431-444.

Ortega, S., Prieto, I., Odajima, J., Martin, A., Dubus, P., Sotillo, R., Barbero, J.L., Malumbres, M., and Barbacid, M. (2003). Cyclin-dependent kinase 2 is essential for meiosis but not for mitotic cell division in mice. Nat Genet *35*, 25-31.

Pillai, R.S., and Chuma, S. (2012). piRNAs and their involvement in male germline development in mice. Dev Growth Differ.

Pittman, D.L., Cobb, J., Schimenti, K.J., Wilson, L.A., Cooper, D.M., Brignull, E., Handel, M.A., and Schimenti, J.C. (1998). Meiotic prophase arrest with failure of chromosome synapsis in mice deficient for Dmc1, a germline-specific RecA homolog. Mol Cell *1*, 697-705.

Raju, N.B., Metzenberg, R.L., and Shiu, P.K. (2007). Neurospora spore killers Sk-2 and Sk-3 suppress meiotic silencing by unpaired DNA. Genetics *176*, 43-52.

Ro, S., Park, C., Sanders, K.M., McCarrey, J.R., and Yan, W. (2007). Cloning and expression profiling of testis-expressed microRNAs. Dev Biol *311*, 592-602.

Robb, G.B., Brown, K.M., Khurana, J., and Rana, T.M. (2005). Specific and potent RNAi in the nucleus of human cells. Nat Struct Mol Biol *12*, 133-137.

Roberts, A., Pimentel, H., Trapnell, C., and Pachter, L. (2011). Identification of novel transcripts in annotated genomes using RNA-Seq. Bioinformatics *27*, 2325-2329.

Romero, Y., Meikar, O., Papaioannou, M.D., Conne, B., Grey, C., Weier, M., Pralong, F., De Massy, B., Kaessmann, H., Vassalli, J.D*., et al.* (2011). Dicer1 depletion in male germ cells leads to infertility due to cumulative meiotic and spermiogenic defects. PLoS One *6*, e25241.

Royo, H., Polikiewicz, G., Mahadevaiah, S.K., Prosser, H., Mitchell, M., Bradley, A., de Rooij, D.G., Burgoyne, P.S., and Turner, J.M. (2010). Evidence that meiotic sex chromosome inactivation is essential for male fertility. Curr Biol *20*, 2117-2123.

Royo, H., Prosser, H., Ruzankina, Y., Mahadevaiah, S.K., Cloutier, J.M., Baumann, M., Fukuda, T., Hoog, C., Toth, A., de Rooij, D.G.*, et al.* (2013). ATR acts stage specifically to regulate multiple aspects of mammalian meiotic silencing. Genes Dev *27*, 1484-1494.

Ruby, J.G., Jan, C., Player, C., Axtell, M.J., Lee, W., Nusbaum, C., Ge, H., and Bartel, D.P. (2006). Large-scale sequencing reveals 21U-RNAs and additional microRNAs and endogenous siRNAs in C. elegans. Cell *127*, 1193-1207.

Ruby, J.G., Stark, A., Johnston, W.K., Kellis, M., Bartel, D.P., and Lai, E.C. (2007). Evolution, biogenesis, expression, and target predictions of a substantially expanded set of Drosophila microRNAs. Genome research *17*, 1850-1864.

Sampey, G.C., Guendel, I., Das, R., Jaworski, E., Klase, Z., Narayanan, A., Kehn-Hall, K., and Kashanchi, F. (2012). Transcriptional Gene Silencing (TGS) via the RNAi Machinery in HIV-1 Infections. Biology *1*, 339-369.

Schimenti, J. (2005). Synapsis or silence. Nat Genet *37*, 11-13.

Schwarz, D.S., Hutvagner, G., Du, T., Xu, Z., Aronin, N., and Zamore, P.D. (2003). Asymmetry in the assembly of the RNAi enzyme complex. Cell *115*, 199-208.

Shiu, P.K., Raju, N.B., Zickler, D., and Metzenberg, R.L. (2001). Meiotic silencing by unpaired DNA. Cell *107*, 905-916.

Siomi, M.C., Sato, K., Pezic, D., and Aravin, A.A. (2011). PIWI-interacting small RNAs: the vanguard of genome defence. Nature reviews Molecular cell biology *12*, 246-258.

Song, J.J., Liu, J., Tolia, N.H., Schneiderman, J., Smith, S.K., Martienssen, R.A., Hannon, G.J., and Joshua-Tor, L. (2003). The crystal structure of the Argonaute2 PAZ domain reveals an RNA binding motif in RNAi effector complexes. Nat Struct Biol *10*, 1026-1032.

Song, R., Hennig, G.W., Wu, Q., Jose, C., Zheng, H., and Yan, W. (2011). Male germ cells express abundant endogenous siRNAs. Proc Natl Acad Sci U S A *108*, 13159-13164.

Song, R., Ro, S., Michaels, J.D., Park, C., McCarrey, J.R., and Yan, W. (2009). Many X-linked microRNAs escape meiotic sex chromosome inactivation. Nat Genet *41*, 488-493.

Song, R., Ro, S., and Yan, W. (2010). In situ hybridization detection of microRNAs. Methods Mol Biol *629*, 287-294.

Steiner, F.A., and Plasterk, R.H. (2006). Knocking out the Argonautes. Cell *127*, 667-668.

Su, H., Trombly, M.I., Chen, J., and Wang, X. (2009). Essential and overlapping functions for mammalian Argonautes in microRNA silencing. Genes Dev *23*, 304-317.

Suh, N., Baehner, L., Moltzahn, F., Melton, C., Shenoy, A., Chen, J., and Blelloch, R. (2010). MicroRNA function is globally suppressed in mouse oocytes and early embryos. Curr Biol *20*, 271-277.

Suzuki, A., and Saga, Y. (2008). Nanos2 suppresses meiosis and promotes male germ cell differentiation. Genes & Development *22*, 430-435.

Tachibana, M., Nozaki, M., Takeda, N., and Shinkai, Y. (2007). Functional dynamics of H3K9 methylation during meiotic prophase progression. The EMBO journal *26*, 3346-3359.

Takanari, H., Pathak, S., and Hsu, T.C. (1982). Dense bodies in silver-stained spermatocytes of the Chinese hamster: behavior and cytochemical nature. Chromosoma *86*, 359-373.

Tan, G.S., Garchow, B.G., Liu, X., Yeung, J., Morris, J.P.t., Cuellar, T.L., McManus, M.T., and Kiriakidou, M. (2009). Expanded RNA-binding activities of mammalian Argonaute 2. Nucleic Acids Res *37*, 7533-7545.

Timmons, L., and Fire, A. (1998). Specific interference by ingested dsRNA. Nature *395*, 854.

Ting, A.H., Schuebel, K.E., Herman, J.G., and Baylin, S.B. (2005). Short double-stranded RNA induces transcriptional gene silencing in human cancer cells in the absence of DNA methylation. Nat Genet *37*, 906-910.

Tong, M.H., Mitchell, D., Evanoff, R., and Griswold, M.D. (2011). Expression of Mirlet7 family microRNAs in response to retinoic acid-induced spermatogonial differentiation in mice. Biol Reprod *85*, 189-197.

Trapnell, C., Pachter, L., and Salzberg, S.L. (2009). TopHat: discovering splice junctions with RNA-Seq. Bioinformatics *25*, 1105-1111.

Trapnell, C., Williams, B.A., Pertea, G., Mortazavi, A., Kwan, G., van Baren, M.J., Salzberg, S.L., Wold, B.J., and Pachter, L. (2010). Transcript assembly and

quantification by RNA-Seq reveals unannotated transcripts and isoform switching during cell differentiation. Nature biotechnology *28*, 511-515.

Turner, J.M. (2007). Meiotic sex chromosome inactivation. Development *134*, 1823-1831.

Turner, J.M., Aprelikova, O., Xu, X., Wang, R., Kim, S., Chandramouli, G.V., Barrett, J.C., Burgoyne, P.S., and Deng, C.X. (2004). BRCA1, histone H2AX phosphorylation, and male meiotic sex chromosome inactivation. Curr Biol *14*, 2135-2142.

Turner, J.M., Mahadevaiah, S.K., Fernandez-Capetillo, O., Nussenzweig, A., Xu, X., Deng, C.X., and Burgoyne, P.S. (2005). Silencing of unsynapsed meiotic chromosomes in the mouse. Nat Genet *37*, 41-47.

van Pelt, A.M., and de Rooij, D.G. (1990). Synchronization of the seminiferous epithelium after vitamin A replacement in vitamin A-deficient mice. Biology of Reproduction *43*, 363-367.

Van Stry, M., Oguin, T.H., 3rd, Cheloufi, S., Vogel, P., Watanabe, M., Pillai, M.R., Dash, P., Thomas, P.G., Hannon, G.J., and Bix, M. (2012). Enhanced susceptibility of Ago1/3 double-null mice to influenza A virus infection. J Virol *86*, 4151-4157.

van Wolfswinkel, J.C., and Ketting, R.F. (2010). The role of small non-coding RNAs in genome stability and chromatin organization. J Cell Sci *123*, 1825-1839.

Vaucheret, H., and Chupeau, Y. (2012). Ingested plant miRNAs regulate gene expression in animals. Cell Res *22*, 3-5.

Viera, A., Rufas, J.S., Martinez, I., Barbero, J.L., Ortega, S., and Suja, J.A. (2009). CDK2 is required for proper homologous pairing, recombination and sex-body formation during male mouse meiosis. J Cell Sci *122*, 2149-2159.

Vigodner, M. (2009). Sumoylation precedes accumulation of phosphorylated H2AX on sex chromosomes during their meiotic inactivation. Chromosome Res *17*, 37-45.

Wang, H., Zhang, X., Liu, J., Kiba, T., Woo, J., Ojo, T., Hafner, M., Tuschl, T., Chua, N.H., and Wang, X.J. (2011). Deep sequencing of small RNAs specifically associated with Arabidopsis AGO1 and AGO4 uncovers new AGO functions. Plant J.

Wang, N., and Tilly, J.L. (2010). Epigenetic status determines germ cell meiotic commitment in embryonic and postnatal mammalian gonads. Cell Cycle *9*, 339-349.

Watanabe, T., Takeda, A., Tsukiyama, T., Mise, K., Okuno, T., Sasaki, H., Minami, N., and Imai, H. (2006). Identification and characterization of two novel classes of small RNAs in the mouse germline: retrotransposon-derived siRNAs in oocytes and germline small RNAs in testes. Genes Dev *20*, 1732-1743.

Watanabe, T., Totoki, Y., Sasaki, H., Minami, N., and Imai, H. (2007). Analysis of Small RNA Profiles During Development. Methods in Enzymology *427*, 155-169.

Watanabe, Y. (2011). Overview of plant RNAi. Methods Mol Biol *744*, 1-11.

Weiss, R.S., Matsuoka, S., Elledge, S.J., and Leder, P. (2002). Hus1 acts upstream of chk1 in a mammalian DNA damage response pathway. Curr Biol *12*, 73-77.

Wu, D., Hu, Y., Tong, S., Williams, B.R., Smyth, G.K., and Gantier, M.P. (2013). The use of miRNA microarrays for the analysis of cancer samples with global miRNA decrease. Rna *19*, 876-888.

Wu, Q., Song, R., Ortogero, N., Zheng, H., Evanoff, R., Small, C.L., Griswold, M.D., Namekawa, S.H., Royo, H., Turner, J.M.*, et al.* (2012a). The RNase III enzyme DROSHA is essential for microRNA production and spermatogenesis. J Biol Chem *287*, 25173-25190.

Wu, Q., Song, R., Ortogero, N., Zheng, H., Evanoff, R., Small, C.L., Griswold, M.D., Namekawa, S.H., Royo, H., Turner, J.M.*, et al.* (2012b). The RNase III enzyme DROSHA is essential for microRNA production and spermatogenesis. J Biol Chem.

Yabuta, Y., Kurimoto, K., Ohinata, Y., Seki, Y., and Saitou, M. (2006). Gene expression dynamics during germline specification in mice identified by quantitative single-cell gene expression profiling. Biology of Reproduction *75*, 705-716.

Yadav, R.P., and Kotaja, N. (2013). Small RNAs in spermatogenesis. Mol Cell Endocrinol.

Yang, F., Eckardt, S., Leu, N.A., McLaughlin, K.J., and Wang, P.J. (2008). Mouse TEX15 is essential for DNA double-strand break repair and chromosomal synapsis during male meiosis. The Journal of Cell Biology *180*, 673-679.

Yigit, E., Batista, P.J., Bei, Y., Pang, K.M., Chen, C.C., Tolia, N.H., Joshua-Tor, L., Mitani, S., Simard, M.J., and Mello, C.C. (2006). Analysis of the C. elegans Argonaute family reveals that distinct Argonautes act sequentially during RNAi. Cell *127*, 747-757.

Yoshida, K., Kondoh, G., Matsuda, Y., Habu, T., Nishimune, Y., and Morita, T. (1998). The mouse RecA-like gene Dmc1 is required for homologous chromosome synapsis during meiosis. Mol Cell *1*, 707-718.

Zan, H., Shima, N., Xu, Z., Al-Qahtani, A., Evinger Iii, A.J., Zhong, Y., Schimenti, J.C., and Casali, P. (2005). The translesion DNA polymerase theta plays a dominant role in immunoglobulin gene somatic hypermutation. Embo J *24*, 3757-3769.

Zisoulis, D.G., Kai, Z.S., Chang, R.K., and Pasquinelli, A.E. (2012). Autoregulation of microRNA biogenesis by let-7 and Argonaute. Nature.